Engineering Library

RR

Anal. Ch.

JUL 26 49

Journal of Research

of the National Bureau of Standards

JUNE 1949

VOLUME 42 NUMBER 6

PERIODICALS OF THE NATIONAL BUREAU OF STANDARDS

Journal of Research

The National Bureau of Standards is the principal agency of the Federal Government for fundamental research in physics, chemistry, and engineering. It has the custody of the national standards of physical measurement in terms of which all working standards in research laboratories and industry are calibrated, and carries on necessary research leading to improvement in such standards and methods of measurement. It also has a general responsibility for basic research in physics, chemistry, and engineering, and for development of improved methods for testing materials and equipment. It determines physical constants and properties of materials, tests and calibrates standard measuring apparatus and reference standards, and studies technical processes. The results of the Bureau's research and investigations are published in the JOURNAL OF RESEARCH.

Research Papers

Reprints of individual articles appearing in the JOURNAL OF RESEARCH. They are made available to serve the needs of research workers, technical groups, and others for the separate papers relating to the special subjects in which they are interested.

Technical News Bulletin

Contains short but complete summaries of research, development, and testing in progress at the Bureau, accounts of the Bureau's national and international activities, scientific and technical announcements of new plans and programs, and a list of publications by members of the staff. It is a prompt and reliable source of official information of value to those who desire to keep in touch with the general activities of the Bureau.

Basic Radio Propagation Predictions

The CRPL-D series, Basic Radio Propagation Predictions, is issued as a monthly publication for those concerned with radio communication in determining the best sky-wave frequencies over any path at any time of day for average conditions for the month of prediction, which is made 3 months in advance. Charts of extraordinary-wave critical frequency for the F2 layer, of maximum usable frequency for a transmission distance of 4,000 km, and of percentage of time occurrence for transmission by sporadic E in excess of 15 Mc, for a distance of 2,000 km, are included.

ANNUAL SUBSCRIPTION Send order, with remittance, to Superintendent of Documents, U. S. Government Printing Office, Washington 25, D. C.	United States, Canada, Cuba, Mexico, Newfoundland, Republic of Panama	Other countries
JOURNAL OF RESEARCH of the National Bureau of Standards:		
12 monthly issues (2 volumes), paper covers	$4.50	$5.50
Bound volume (½ year, 1 volume), blue buckram	3.00	3.50
RESEARCH PAPERS	(*)	(*)
TECHNICAL NEWS BULLETIN, 12 monthly issues	1.00	1.35
BASIC RADIO PROPAGATION PREDICTIONS, 12 monthly issues	1.00	1.25

*The prices of the separate Research Papers appearing in this JOURNAL are given in the Contents. If 100 or more copies of any separate are ordered, a discount of 25 percent is allowed. Those who desire copies of separate Research Papers should send their orders and remittances without delay to the Superintendent of Documents, U. S. Government Printing Office, Washington 25, D. C. This will aid him to determine the number of copies to be printed for sale. Research Papers are not printed from electrotypes and usually no more reprints can be had when the first and only printing is exhausted.

The printing of this publication has been approved by the Director of the Bureau of the Budget, April 23, 1947.

U. S. DEPARTMENT OF COMMERCE
Charles Sawyer, Secretary
NATIONAL BUREAU OF STANDARDS
E. U. Condon, Director

JUNE 1949
VOLUME • 42
NUMBER 6

JOURNAL OF RESEARCH

of the

NATIONAL BUREAU OF STANDARDS

Contents

RP		Page
1991	A study of laboratory Bunsen burners for natural gas. John H. Eiseman. (Price 10 cents)	541
1992	Studies on the purification of collagen. James M. Cassel and Joseph R. Kanagy. (Price 10 cents)	557
1993	Flame spectrum of acetylene from 1 to 5 microns. Earle K. Plyler and Curtis J. Humphreys. (Price 10 cents)	567
1994	Viscosity of deuterium oxide and water in the range 5° to 125° C. Robert C. Hardy and Robert L. Cottington. (Price 10 cents)	573
1995	Determination of efficiency of microwave bolometer mounts from impedance data. David M. Kerns. (Price 10 cents	579
1996	Ultraviolet absorption spectra of seven substituted benzenes. Ralph Stair. (Price 10 cents)	587
1997	Acid-base equilibrium constants for the reaction of tribenzylamine with picric acid and with trinitro-*m*-cresol in benzene, from spectrophotometric data. Marion Maclean Davis and E. Anne McDonald. (Price 10 cents)	595
1998	Transmission of reverberant sound through single walls. Albert London. (Price 10 cents)	605
1999	Separation and identification of the major C_7 to C_{10} components of triptene residue. Philip Pomerantz, Thomas W. Mears, and Frank L. Howard. (Price 10 cents)	617
	Index to volume 42 (January to June 1949, Research Papers RP1946 to RP1999).	633

For sale by the Superintendent of Documents, U. S. Government Printing Office, Washington 25, D. C. - Price 60 cents
$4.50 per year on subscription

UNITED STATES GOVERNMENT PRINTING OFFICE, WASHINGTON : 1949

U. S. Department of Commerce
National Bureau of Standards

Research Paper RP1991
Volume 42, June 1949

Part of the Journal of Research of the National Bureau of Standards

A Study of Laboratory Bunsen Burners for Natural Gas

By John H. Eiseman

Sixteen different laboratory-type Bunsen burners, sold as suitable for natural gas, were purchased and their limits of operation determined. Eight of the burners were of the Meker type, and eight were straight-tube burners. The results of the study indicate the need for certain changes in design if satisfactory operating characteristics are to be obtained with natural gas.

A comparison of the dimensions of these burners with the fundamental relations for good burner operation brought out the following three major reasons for their unsatisfactory performance: Too small a port area, improper throat size, and insufficient primary air opening. In addition to these three factors, use of the proper orifice size was also found to be of importance. Two burners, one a straight-tube and the other a Meker type, were modified so that they complied with the requirements as determined by this study. Both burners were found to be greatly improved and were capable of producing a hot, stable flame over a range of gas rates approximately double their former usable rates.

I. Introduction

Although the principle of the Bunsen burner has been known for many years, studies of the elements of design leading to the most effective application of this principle are comparatively recent. In 1921 the Bureau issued Technologic Paper 193 [1],[1] the first American publication on this subject, and for nearly 10 years this was the only authoritative data available on the design of burners of the Bunsen type. Since 1931 additional data have been made available by the American Gas Association Testing Laboratories, the National Bureau of Standards, and others, but even today the literature on burner design is not extensive.

Most of the research work on burners has been done on those used in domestic appliances such as ranges, water heaters, central heating appliances, and space heaters. The manufacturers of these appliances are, in general, utilizing the basic design data now available, but many other types of burners on the market do not conform to the dimensions and proportions essential for the most satisfactory performance. The average laboratory Bunsen burner does not comply with these essential dimensions, and although for many heating operations with certain gases it gives satisfactory performance, there are other laboratory requirements which are not adequately met by these burners, particularly with natural and other slow-burning gases.

In 1947 the gas supplied to Washington, D. C., was changed from a mixed manufactured and natural gas of 600 Btu/ft^3 to a straight natural gas of approximately 1,100 Btu/ft.^{3} Up to this time very little difficulty had been experienced with the various makes of laboratory burners, but since the change-over complaints have been the rule rather than the exception, even though all the burners currently in use were either converted for natural gas or replaced by new burners advertised as natural gas burners.

The average laboratory burner is inexpensive in comparison with most of the domestic or commercial burners. In most laboratories it is not used continuously and many of the heating applications for which it is used do not require any great range of adjustment. In fact in many cases a knowledge of the rate at which heat is delivered is unimportant. If the gas will ignite and continue to burn and not require too long a time to perform the desired heating operation, the burner is satis-

[1] Figures in brackets indicate the literature references at the end of this paper. Additional important papers not cited in the text are also given.

factory. There are other uses, however, where it is necessary to supply gas at a definite and uniform rate with an adjustment that produces a hot stable flame. Most of the trouble experienced in the laboratories at this Bureau has been caused by a flame that is not stable when the rate is adjusted for the delivery of a sufficient number of heat units per hour to raise the material being heated to the desired temperature.

Even if it is known at what rate heat is required, there is little information available that would enable the purchaser to pick out the proper laboratory burner. The catalogs do not usually show the rates for which these laboratory burners are intended, and in some cases where such data are given the burners cannot be used at the indicated rates.

As a result of this lack of information regarding laboratory-type burners and because of failure to obtain satisfactory performance with any of the types on hand, a number of these burners were studied to determine the limits within which they could be used. It was hoped that a correlation of this information with the basic requirements for good burner design would bring out some of the reasons for the poor showing on natural gas and point the way to the changes required for satisfactory operation. Since the composition of the natural gas supply in Washington, D. C., is close to an average of that used in other parts of the country, the results should be equally applicable wherever natural gas is used.

II. Burners Tested

Sixteen different Bunsen-type burners, all advertised as suitable for natural gas, were selected from catalogs and purchased. Of these, eight are straight-tube burners and eight are of the Meker type. These burners are believed to be representative of those most commonly used in laboratory work, and the test results should, therefore, be indicative of the range of operation that can be obtained from laboratory burners in general.

Figure 1 shows the eight Meker burners and figure 2 the eight straight-tube burners tested. These photographs show the variations in size and design of typical laboratory burners. The straight-tube burners are composed of a base into which the orifice is mounted, a straight mixing-tube in which the gas and air are mixed, an opening for the air to enter the mixing tube, and a flame-retainer. The flame-retainer is merely an enlarged annular opening surrounding the main burner port. A small amount of the air-gas mixture is supplied to this annular ring by several small holes connecting it with the main supply in the mixing-tube. The small ring of flame thus formed around the main burner flame permits a greater range of adjustment of the burner without encountering unstable conditions. The orifices used in these burners are either of the fixed or adjustable type. The fixed orifice is, as its name implies, a fixed opening through which the gas passes. Any change in rate (at constant pressure) is made by removing the orifice and inserting one of a different size. The adjustable orifice is usually composed of a cap with a fixed opening and a tapered needle that can be moved in or out of this fixed hole, thereby changing its size.

Like the straight-tube burner, the Meker-type burner has a base, orifice, mixing-tube, air-opening, and burner-head, or port. It differs from the straight-tube burner in that the mixing-tube usually has a constriction, or venturi throat that increases the amount of air drawn into the burner, and the burner-head has a number of small ports in place of the single opening used with the straight-tube burner. The orifice may be either fixed or adjustable. In all of the 16 burners tested it was possible to vary the size of the opening through which room air entered the mixing-tube.

The numbers on the burners in figures 1 and 2 correspond to the burner numbers in table 1. This table gives the type of burner, throat area, port area, and other dimensions of each burner, which will be discussed in connection with the basic design relations in section VIII.

In addition to testing the 16 commercial burners, an experimental burner was designed and built. This burner was used to determine whether certain fundamental relationships that had previously been established with respect to burners of domestic appliances were equally applicable to burners of the laboratory-type.

FIGURE 1. *Laboratory burners tested.*
Meker type.

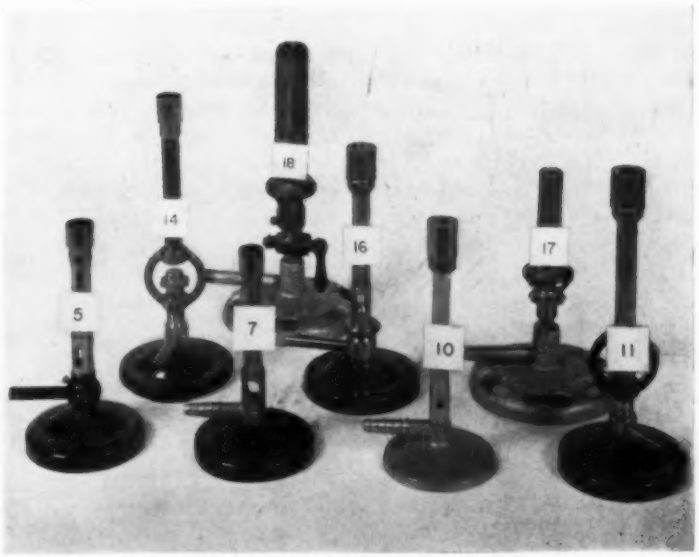

FIGURE 2. *Laboratory burners tested.*
Straight-tube type.

TABLE 1. *List of burners tested, with dimensions of each*

Burner number	Type of burner	Port area	Throat area	Ratio throat / port	Air shutter opening	Ratio air shutter / port area	Number of ports	Diameter of ports	Height of burner	Length of mixing tube	Length of mixing tube and burner head	Orifices used (drill size)
		*in.*²	*in.*²		*in.*²			*in.*	*in.*	*in.*	*in.*	
1	Meker	0.773	0.332	0.429	1.094	1.42	63	0.125	8⅝	4	5	54, 56
2	do	.687	.322	.468	0.402	0.59	56	.125	8	4⅜	5⅜	[a] 46
3	do	.663	.166	.251	.773	1.17	54	.125	7½	3 31/32	4⅛	60
4	do	.589	.174	.295	.646	1.10	48	.125	7¼	3¼	4⅛	56
5	Straight tube with stabilizer top [b] and pilot.	.139	.139	1.000	.414	2.98	1	.420	6	3⅜	3⅜	57, 68
6	Meker	[c] 1.019	.302	0.296	.936	0.92	155	[d] .08	8½	3¾	4 11/32	54, 56
7	Straight tube with flame retainer [b]	0.110	.110	1.000	.163	1.47	1	.375	5½	3½	3½	69
8	Meker	.254	.307	1.207	.807	3.18	121	.052	7	2¾	4 3/16	[e] 54
9	do	1.156	.595	0.514	1.366	1.18	98	.125	10⅝	6⅛	7¼	51
10	Straight tube with flame retainer [b]	0.091	.108	1.184	0.161	1.77	1	.340	6¼	3 11/16	4⅜	52
11	do [b]	.126	.126	1.000	.314	2.49	1	.401	7 11/16	3¾	4½	[a] 43
14	do [b]	.139	.139	1.000	.462	3.33	1	.420	[a] 7¾–8¼	4¾	4¾	[a] 51
15	Meker	.687	.322	0.468	.402	0.59	56	.125	8⅛	4⅜	5⅜	[a] 46
16	Straight tube with flame retainer [b]	.126	.126	1.000	.182	1.44	1	.401	[a] 6⅛–6⅜	3 11/16	4⅜	[a] 51
17	Straight tube	.113	.174	1.537	.308	3.26	[g] 1	[e] .348	[a] 5 13/16–6 13/16	2½	2½	[f] 50
18	do	.296	.363	1.226	.626	2.11	[g] 1	[e] .580	8 5/16	4	4	[f] 45

[a] Adjustable.
[b] Area of stabilizer or flame retainer not included as part of port area.
[c] 42-mm grid.
[d] Square ports.
[e] 12 slots, 0.05 x 0.03 in. each.
[f] Johnson adjustable.
[g] 16 slots, 0.05 x 0.04 in. each.

III. Limits of Operation of a Laboratory Burner

All burners of the Bunsen type are so designed that a portion of the air necessary for complete combustion mixes with the gas before it reaches the burner port, or ports. This "primary air" is injected into the burner by the momentum of the gas flowing from the orifice and enters the burner through the air openings located at the base of the mixing-tube. The additional air required is secured from the atmosphere surrounding the flame and is termed "secondary air." Gas of a definite composition requires a definite volume of air to burn each volume of gas, but the type of flame produced depends upon how much of the total air required is introduced as primary air. A low primary air causes a "lazy" flame, which is not sharply defined. As the primary air is increased the flame becomes smaller in volume and more clearly defined or "harder" in appearance. The same total heat is produced as long as the gas rate remains constant, but the higher the primary air the more concentrated this heat becomes. The usefulness of a burner for many purposes depends on the intensity of the flame, that is on the liberation of much heat in small volume [2]. For any given burner, however, there is a limit above which an increase in primary air causes the flame to become unstable and either lift away from the ports or flash back into the burner, depending upon the gas rate and the composition of the gas used. Natural gas gives very little trouble from flash-back but is particularly susceptible to lifting. Similarly, if the primary air is decreased, a limit is reached below which the color of the tip of the inner cone becomes yellow. This results from the formation of finely divided incandescent particles of solid carbon that are present because the oxygen in the primary mixture is insufficient to carry the oxidation of all the carbon of the hydrocarbons in the fuel gas as far as carbon monoxide. Another limit to satisfactory operation is also encountered in the Meker type of burner where the burner head is composed of a number of closely spaced ports. In this type of construction, no secondary air reaches the vicinity of the inner ports. Secondary combustion is an important factor in preventing the "lifting" of the primary flame. As the primary air is reduced on

a burner of this type, a point is reached at which the inner cones begin to lift off the individual small ports and merge into larger and longer inner cones. A flame of this kind is much less effective for most purposes for which the Meker burner is used. This condition will be referred to in what follows as a smothering limit and is reached on the Meker-type burner at higher primary air rates than the yellow tip limit. Lifting, flash-back, yellow-tip, and smothering of the flames are all conditions that prevent the proper application of heat. Lifting, flash-back, and smothering may result in the escape of unburned gas and carbon monoxide, whereas a yellow-tip condition causes a carbon deposit on the material being heated, and may also be accompanied by incomplete combustion. All four of these conditions result in a loss of heat. It therefore follows that a satisfactory laboratory burner is one that is capable of operating within these limits over the entire range of gas rates required.

IV. Method Used for Determining Limits of Burner Operation

In order to determine the conditions under which the limits of operation are found, each burner was installed so that both the gas rate and the supply of primary air could be varied as desired, and the rates of flow of each could be accurately determined. Figure 3 shows the apparatus used for these tests.[2] With a burner installed in such an apparatus and burning gas at a constant rate, the primary air was increased until the flames either lifted from the ports or flashed back into the burner. When this condition was obtained, the proportion of air in the primary mixture was determined. The primary air was next decreased until yellow appeared in the flame, and the proportion of air in the primary mixture was again determined. When testing each of the Meker burners another setting of primary air was made, so that the inner flame cones were no longer stable on the individual ports and were beginning to merge and elongate. The ratio of primary air to gas where this condition was obtained was also determined. The gas-rate was then changed and the same procedure repeated. This process was continued until a series of tests had been made that covered the desired range of gas rates or until the points obtained indicated that other rates could not be used because they fell outside the limits of operation. The results obtained were plotted, using as the coordinates, "gas rate: thousands of Btu per hour" and "primary air: percentage of the total air required."

Figure 4 represents the position of the boundaries of the regions in which lifting, smothering, and yellow-tips were obtained with Burner 1, a Meker-type burner. The small circles with short lines pointing upward represent conditions under

[2] A detailed description of this apparatus is given in the appendix of [3].

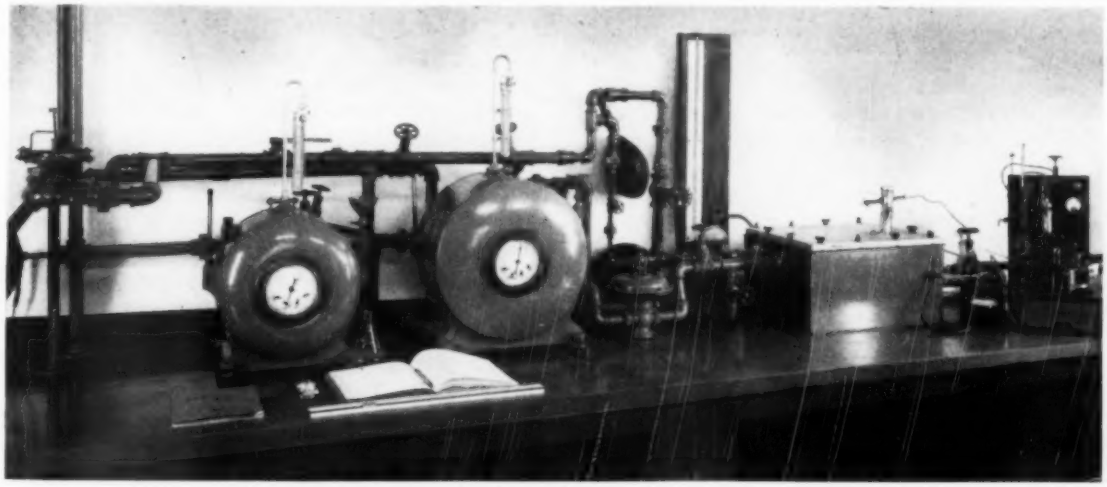

FIGURE 3. *Apparatus used to study the performance of gas burners.*

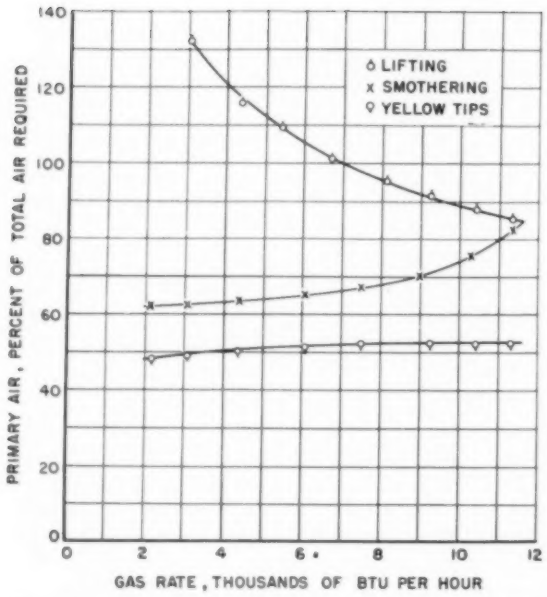

FIGURE 4. *Boundaries of the regions in which lifting, smothering, and yellow-tips occur with burner 1.*

which the flames were observed to lift; those with the short lines pointing downward represent conditions under which yellow-tips first appeared in the flames; and the crosses represent conditions under which smothering of the inner flames occurred. As mentioned previously, flash-back is not usually encountered with the average burner with natural gas and was not found to be a limiting condition with any of the laboratory burners tested.

Any adjustment of primary air which falls above the lifting curve or below the smothering curve will produce an unstable or unsuitable flame, whereas any air adjustment that falls below the yellow tip curve will produce carbon and be otherwise unstatisfactory.

With the Meker-type burner it is therefore necessary to adjust the burner so that the primary air setting falls between the lifting and smothering curves. In the case of a single-port burner, there is no smothering limit so that the adjustment is made between the lifting and yellow-tip limits. It will be observed that the lifting curve and the smothering curve obtained with burner 1 intersect at a gas rate of 11,600 Btu/hr. This rate is, therefore, the maximum that could be used without encountering one of these limits. A rate somewhat less than 11,600 would have to be used in order to obtain a primary air setting that would produce a stable flame.

Having located the position of the limits of operation of a burner, the next step is to determine how much of this stable range can actually be utilized when the burner is operated normally.

V. Normal Air Injection

In the determination of the limits of operation the orifice used was unimportant, because the primary air was forced into the burner. It was merely necessary to use a size that would allow the gas to pass at the desired rate under the range of gas pressures available. However, when an appliance is installed for use, the primary air is drawn into the burner by the energy of the gas stream issuing from the orifice, and the amount thus injected depends in part upon the size of the orifice. When using any given rate of gas supply the amount of air injected increases as the size of the orifice is decreased, higher pressures being necessary, however, to maintain the given rate. For the greatest range of usable gas rates it was therefore necessary to determine the largest orifice that could be used with each burner and still obtain an air injection that would produce a stable flame. For this determination the burner was connected to a source of gas supply only, the air-mixer being left open to the air of the room. When an air shutter was provided, it was set in its wide open position. If the burner was supplied with an adjustable orifice, it was set by means of the needle so that the maximum gas rate possible was obtained without encountering any of the limiting conditions. This setting was made at the highest gas line pressure available, which in these tests was 6 in. of water pressure. If the burner was supplied with a fixed orifice, several different sizes were tried until the one was found that would allow the highest gas rate with a stable flame. Once this condition was found, the proportion of air in the primary mixture within the burner head and the gas rate were determined. Without any further change in orifice adjustment, other points on the normal injection were found by varying the line pressure. These points were then added to the plot showing the limiting curves.

VI. Results Obtained with Meker-Type Burners

Figure 5 shows the complete results obtained on burner 1. The limiting curves showing the position of lifting, smothering, and yellow-tips are the same as given on figure 4, but two normal air injection curves have been added. One of these was obtained with an orifice of No. 54 drill size (0.0023-in.^{2} area) and the other with a No. 56 (0.0017-in.^{2} area). The normal air injection obtained with the No. 54 orifice is below the smothering curve at all rates. A No. 54 orifice is therefore too large to give a stable flame with this burner. The curve obtained with the No. 56 orifice is above the smothering curve at all pressures and its use results in a stable flame. A No. 55 orifice (curve not shown) gave results intermediate between the No. 54 and No. 56, but the injection was below the smothering curve at the 6-in. pressure. It is therefore apparent that a No. 56 orifice is the largest size that can be used with this burner, and since the maximum line pressure available in our laboratory is 6 in. of water, it is not possible to obtain a stable flame above a rate of 7,500 Btu./hr. This condition is typical of all burners of the Meker type tested.

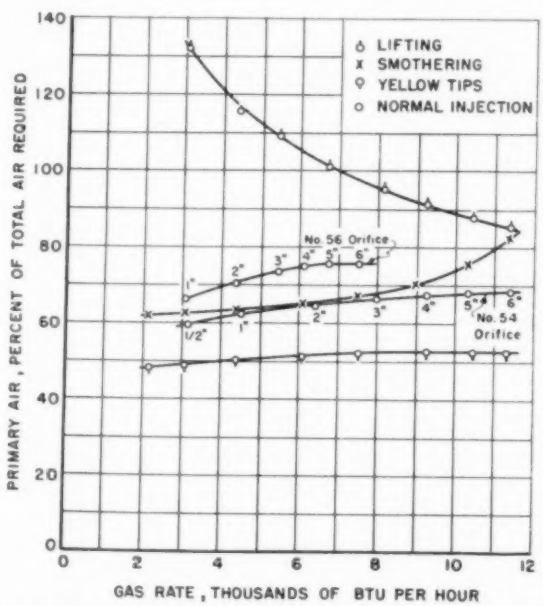

FIGURE 5. *Combined curves showing the limits of operation and normal air injection with Meker burner 1.*

Considering only the lifting and smothering limits, it should be possible to use this burner at gas rates up to 11,000 Btu/hr. (maximum stable gas rate 11,600), but to do so would require a primary air injection of between 80 and 86 percent. To obtain such an air entrainment would require the use of a No. 58 orifice, and with this smaller size the 6-in. pressure available would deliver only about 6,200 Btu/hr. This burner would have to be modified so that higher air injections are possible with a No. 54 orifice, or pressures up to 13 in. of water would be needed to use this burner with the No. 56 orifice at a rate of 11,000 Btu/hr.

Curves similar to those shown in figure 5 were determined and plotted for each of the seven other Meker-type burners. From these curves the maximum stable gas rate determined by the limiting curves only and the maximum stable gas rate obtainable under normal operating conditions were determined in the manner just described and are shown in table 2.

TABLE 2. *Comparison of maximum theoretical gas rate and highest stable rates obtainable with the Meker burners*

Burner number	Maximum stable gas rate determined by limiting curves	Maximum stable gas rate obtainable under normal operating conditions
	Btu/hr	*Btu/hr*
1	11,600	7,300
2	6,500	3,880
3	10,300	5,680
4	11,000	7,350
6	12,000	8,200
8	6,850	4,930
9	29,000	16,150
15	17,500	7,000

In each case the maximum stable gas rate as determined by normal operation is much less than the rate that could be obtained, provided it was possible to obtain higher air injections with an orifice capable of passing these higher rates.

Except for burner 9, which is considerably larger than any of the other burners, the highest usable gas rate is 8,200 Btu/hr. This rate is sufficient for many heating operations but is not high enough for all. We believe these burners should be capable of giving stable flames up to at least 10,000 Btu/hr in order to cover the range of Btu rates required for normal laboratory work.

834349—49—2

VII. Results Obtained with Straight-Tube Burners

The burners shown in figure 2 are all classed as straight-tube burners. Limiting curves were obtained with each of these burners in a manner similar to that used for the eight Meker types, except that with these burners there is no smothering limit. Figure 6 shows the position of the lifting and yellow-tip limits and the normal air injection with burner 5. This burner has a fixed

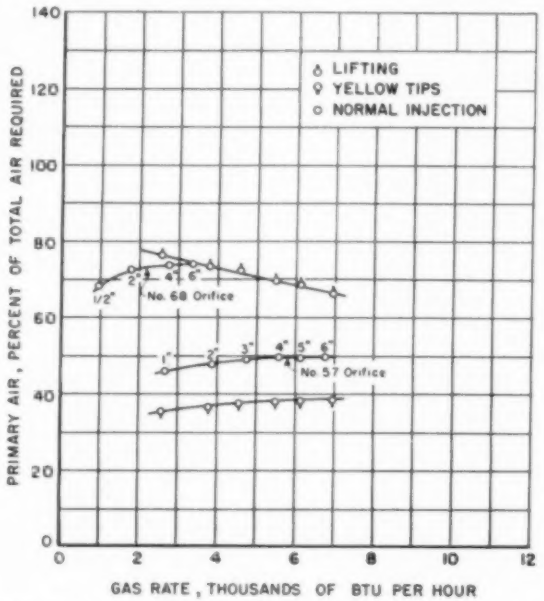

FIGURE 6. *Combined curves showing the limits of operation and normal air injection with stright-tube burner 5.*

orifice of a No. 57 drill size (0.00145-in.^{2} area). The highest gas rate that is possible with this orifice and the maximum 6-in. line pressure is 6,720 Btu/hr, and the air injection obtained was 50 percent of the total air required for complete combustion. The flame produced was stable and fell within the limits of lifting and yellow tips but was soft in appearance and was suitable for few heating applications.

On most domestic appliances it is rarely desirable to produce very high temperatures of the objects heated, and the intensity of the flame is usually unimportant. Any condition of operation that results in complete combustion between the limits of lifting and yellow-tips is nearly equally satisfactory. In contrast, since laboratory burners are used for igniting crucibles and other purposes for which intense flames are needed to produce high temperatures, the highest percentage of primary air practicable without causing lifting is desired. At least 70 percent of primary air should be obtainable. In order to obtain such an air entrainment with this burner, it was necessary to reduce the size of the orifice to a No. 68 drill. This resulted in an air injection of 74 percent but reduced the maximum gas rate obtainable at the 6-in. pressure to 3,360 Btu/hr. We believe it would be desirable for burners of this type to be capable of producing a hard well-defined flame at rates up to at least 5,000 Btu/hr. A study of figure 6 indicates that a rate of 5,000 Btu/hr, with a 70-percent air injection would be a stable setting, since this adjustment falls below the lifting curve. Actually the maximum rate at a 70-percent air injection would be the intersection of the 70-percent air line with the lifting curve that occurs with this burner at a rate of 5,300 Btu/hr. The air injecting power of this burner is not sufficient, however, to obtain a 70-percent injection with an orifice capable of giving a rate of 5,300 Btu/hr with the 6-in. gas pressure available. It is evident that this burner needs some modification in order to accomplish such a result with natural gas.

Table 3 shows the maximum stable rate for each of the straight-tube burners tested. This rate was determined from the curves obtained with each burner by noting the intersection of the 70-percent air line with the lifting curve. The highest rate obtainable with each burner when operated normally is also shown. This was

TABLE 3. *Comparison of maximum theoretical gas rate and highest stable rates obtainable with the straight-tube burners*

Burner number	Maximum stable gas rate determined by intersection of lifting curve and 70-percent air line	Maximum stable gas rate obtainable under normal operating conditions with 70-percent air injection
	Btu/hr	*Btu/hr*
5	5,300	3,360
7	7,500	2,448
10	4,450	2,066
11	13,900	1,680
14	23,000	4,000
16	5,100	1,586
17	7,900	4,331
18	12,500	10,667

obtained by determining the gas rate delivered at a 6-in. pressure when using an orifice that would give at least a 70-percent air injection.

This table shows that all of the burners with the exception of 18 give usable rates below 5,000 Btu/hr on natural gas. Burner 18 is a larger burner than the others, and according to the data in the manufacturer's catalog should be capable of operating at a rate of 13,000 Btu/hr.

This shows that the average straight-tube burner, like the Meker burner, must be redesigned if a range of usable rates higher than can now be obtained is required.

VIII. Basic Data for Burner Design

Research conducted on domestic atmospheric burners has shown that if optimum performance of the burner is to be obtained certain dimensional relationships must be adhered to.

Those factors that are of importance to the operation of a laboratory burner are discussed below.

1. *Port area.*—Previous work has shown that there is a definite relation between the port area and the maximum rate at which gas can be burned. It is also known that the maximum rate per square inch of port area is different for gases of different composition. For example, the port area required to burn natural gas at a definite Btu rate is greater than for manufactured gas because of the greater tendency of the natural gas flames to lift. Consequently, if the same burner were used on both gases without any change of port area, it would not be possible to obtain a stable flame with natural gas at as high a Btu rate as could be obtained with one of the manufactured gases. This variation in rate for equal flame stability is indicated by the following figures, which were determined in studies of range burners.

TABLE 4. *Maximum Btu per square inch of port area for gases of different composition*

Data determined on gas range burners. All determined at 70-percent air injection

Type of gas	Maximum rate per square inch of port area
	Btu/hr
Natural	10,000
Manufactured	19,000
Liquefied petroleum	12,000

However, port area and gas composition are not the only factors that determine the position of the limiting curves of a burner. Two burners may have the same total port area but one may have a single opening, as is the case with a straight-tube burner; the other may have a number of smaller ports. These two burners would not have the same limits of operation and would therefore not be likely to have the same limit of usable gas rate. The heat transfer from the burner tube to the gas mixture, the uniformity of mixing of the air and gas within the burner, and the spacing of the ports are also conditions that influence the position of the limits of operation. All of the range burners used in determining the maximum rates given above were similar in design, whereas the 16 laboratory burners used in this study have wide differences in their construction. Because of this variation in design there is no certainty that the same relation between port area and rate would be obtained as with the range burners nor that the various laboratory burners would all give the same result. One of the Meker burners was supplied with three heads of different size, having port areas of 0.54, 1.02, and 2.07 in.^{2} respectively. Limiting curves were determined for each of these burner heads, and the maximum

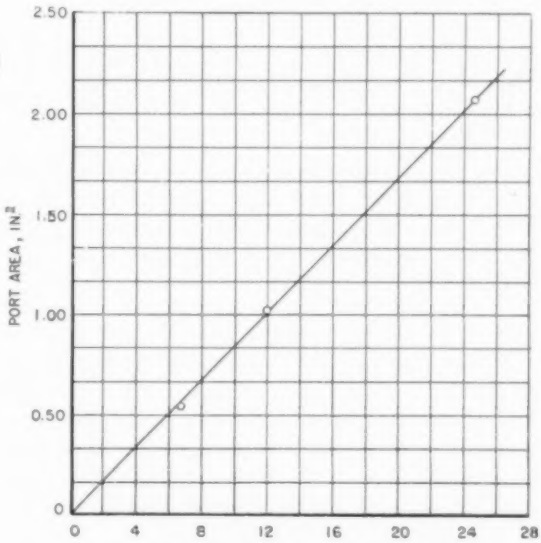

FIGURE 7. *Variation in maximum stable gas rate with change in port area.*

Curve determined with burner 6.

stable rates were determined for each by the intersection of the lifting and smothering curves. These three rates were then plotted against the corresponding port area and give the curve shown in figure 7. This curve gives a straight-line relationship between the port area and the maximum stable rate and indicates that this burner should be capable of burning 12,000 Btu/hr per square inch of port area. Assuming that data of a similar nature, if it could have been determined on the other Meker burners, would have also given straight lines, the results on the other seven burners were calculated to a basis of 1 in.^{2} of port area with the results shown in table 5. It is evident that the maximum rates calculated for these burners, all based on 1 in.^{2} of port area, show considerable variation.

TABLE 5. *Maximum theoretical gas rate per 1 square inch of port area*

Data calculated for eight Meker burners

Burner number	Computed maximum stable gas rate per sq in of port area
	Btu/hr
1	15,000
2	9,450
3	15,850
4	18,700
6	11,800
8	27,000
9	25,100
15	25,500

If the relationship shown above is also applicable to the laboratory burner, then the Meker burner should have a 1-in.^{2} port area for the rate of 10,000 Btu/hr previously assumed to be necessary, and the straight-tube burners should have a port area not less than ½ in.^{2} in order to produce 5,000 Btu/hr.

None of the burners tested could be used at rates as high as the limit set by lifting and smothering. On the average, the maximum usable gas rates with the eight Meker burners were limited by poor air injection to about 60 percent of the maximum rate as determined by the limiting curves. This is because normal operation depends on factors in the design of the burner that do not enter into the determination of the limiting curves. Such conditions as the shape of the mixing-tube, the type and position of the orifice, and the provision for entrance of primary air all affect the air injection that can be obtained and therefore have a part in determining the maximum usable gas rate.

An average of the results shown in table 5, exclusive of burner 9, gives a rate of 17,614 Btu/hr. Sixty percent of this is a rate of 10,568 Btu/hr. It therefore seems reasonable to assume that a Meker burner properly proportioned should be capable of burning gas at the rate of at least 10,000 Btu/hr per square inch of port area.

Treating the data obtained on the straight-tube burners in a somewhat similar manner, the results indicate that a burner having a port area of 0.1 in.^{2} should allow a rate of 3,350 Btu/hr. In order to burn gas at a rate of 5,000 Btu/hr it would be necessary to use a port area of 0.15 in.^{2} or a tube of at least 7/16-in. inside diameter. Only one of the eight straight-tube burners has a port area as large as this. Burner 18 has a port area of 0.296 in.^{2} and should be capable of burning gas at a rate of approximately 10,000 Btu/hr if figured on this same basis. The maximum usable rate with burner 18 was 10,667 Btu/hr.

2. *Throat area.*—In order to obtain maximum air injection with a Meker-type burner it is necessary to constrict the mixing-tube at a point just beyond that at which the primary air enters. This constriction, or venturi, increases the velocity of the gas-air mixture passing this point, which in turn increases the suction that draws air into the burner at the primary air openings. It has been determined that a ratio between this throat area and the port area of 40 percent gives the highest air entrainment. This ratio is not too critical but should be held between 35 and 45 percent. Since this relationship was determined on work with domestic burners, it seemed desirable to verify it for a laboratory-type burner. For this work a straight tube was obtained that would fit the burner top having a port area of 2.07 in.^{2} The lower end of this tube was made to fit one of the burner bases and provided with sufficient primary air openings so that when the air shutter was wide open there was ample area for the entrance of air. Five brass inserts with throat areas of 20, 30, 40, 60, and 83 percent of the port area were made so that they could be inserted into the straight mixing-tube. This experimental burner and four of the five inserts are shown in figure 8. The air injected with each of these five inserts was determined at a 6-in. line

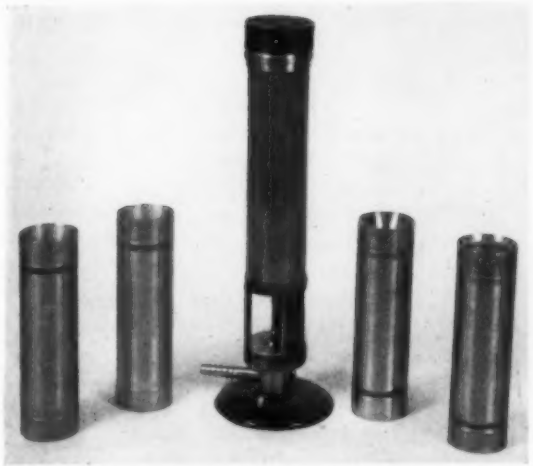

FIGURE 8. *Experimental burner used for checking fundamental relations on laboratory type burners.*

pressure for each of five different sized orifices. Two series of tests were made; one with the gas burning or the burner hot, and one with the gas unlighted or the burner at room temperature. The room-temperature tests had the advantage of being able to cover a greater range of gas rates without being limited by lifting and flash back. The air injection obtained with the burner cold was higher than when the burner was hot, but both series indicated that with a burner of the Meker type the 40-percent throat gives the highest air injection. The results determined with the burner at room temperature are shown in figure 9. These curves also verify the previous findings that small variations from a 40-percent ratio of throat to port area have a small effect upon the air injected, although the change in air injection becomes more pronounced as the gas rate is decreased.

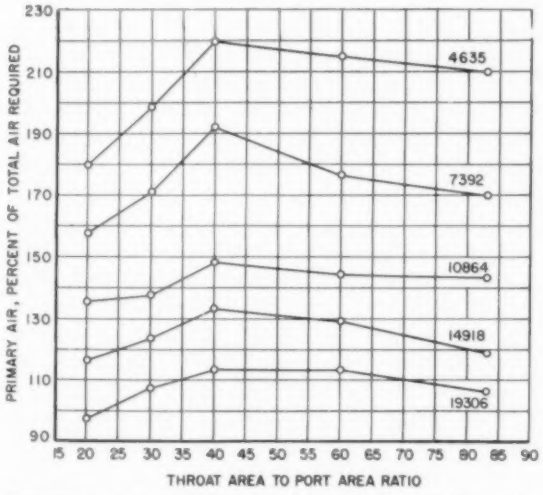

FIGURE 9. *Comparison of air injected with various ratios between throat and port area.*
Numbers on curves indicate Btu/hr.

For the Meker-type burner it therefore follows that the throat area should be approximately 40 percent of the port area in order to obtain the highest air injection with whatever orifice size is used. That this optimum relationship is not followed in all of these burners is apparent from the following table.

TABLE 6. *Ratio between throat and port area for 8 Meker burners tested*

Burner number	Throat area as percentage of port area
1	42.9
2	46.8
3	25.1
4	29.5
6	29.6
8	120.7
9	51.4
15	46.8

The straight-tube burners have no venturi throat and studies of air entrainment in straight tubes [4] have shown that for this type of burner a venturi does not increase the amount of air entrained.

3. *Primary air opening.*—Work conducted by the American Gas Association Testing Laboratories on the amount of opening that should be provided for the admittance of primary air resulted in the conclusion that the minimum opening should be 1.25 times the total port area for burners that would operate normally at less than 70-percent air entrainment. For primary air injection greater than 70 percent, an opening of 2.25 times the total port area is recommended. It seemed desirable to verify these results on the laboratory-type burner. For this purpose the experimental burner with the 40-percent throat was used. Gas at 6-in. pressure was supplied to the burner at a constant rate through one of a series of fixed orifices, and air injection tests were made at various known primary air openings

starting with the air shutter wide open and decreasing this opening by small increments until a definite decrease in air injection was observed. Similar tests were made at other gas rates by substituting other orifices until a sufficient range of rates was covered. These results are shown in figure 10, in which the primary air injected is

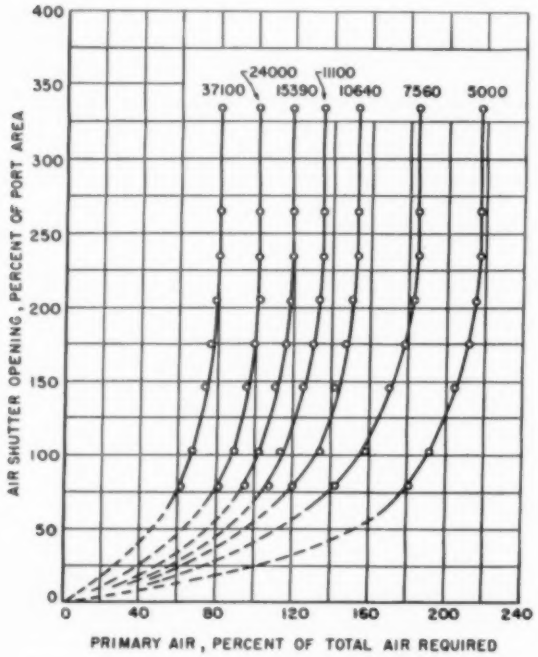

FIGURE 10. *Effect of air shutter opening on primary air injected.*

Numbers on curves indicate Btu/hr.

plotted against the air-shutter opening in percentage of port area. These data verify the American Gas Association figure and indicate that the primary air opening should be at least 2.25 times the port area. Any decrease below 2.25 reduces the maximum air that can be injected by the burner regardless of the gas rate used. Table 7 shows the ratio between the primary air opening and the port area for the 16 burners tested.

Only five of these burners have a sufficient opening for primary air if we consider a ratio of 2.25 as the minimum that should be provided. In fact, the lack of adequate air opening alone is sufficient to account for the poor showing of some of these burners.

4. *Distance between throat and gas orifice.*—

TABLE 7. *Ratio between the primary air opening and the port area for the 16 burners tested*

Burner number	Ratio: $\frac{\text{primary air opening}}{\text{port area}}$
1	1.42
2	0.59
3	1.17
4	1.10
5	2.98
6	0.92
7	1.47
8	3.18
9	1.18
10	1.77
11	2.49
14	3.33
15	0.59
16	1.44
17	3.26
18	2.11

Studies by the gas utilization laboratory at this Bureau and other investigators show that it is necessary to place the orifice at a correct distance from the throat of the burner if optimum air injection is to be obtained. A decrease in air entrainment results if the orifice is either too far away or too close to the throat. The present studies indicate that the best results are obtained if the orifice is located about two throat-diameters away from the throat. Results observed by other laboratories show optimum conditions to be obtained between 0.5 and 2.0 throat-diameters away, depending upon the size of the throat used. For laboratory-type burners the distance should be kept between 1.0 and 2.5 throat-diameters. It is also necessary to have the orifice properly centered with respect to the mixing-tube. If the stream of gas is directed toward the walls rather than the center of the mixing-tube, the air entrainment is greatly reduced. Proper centering and also proper drilling of the orifice are therefore essential. Of equal importance, in this connection, is the travel of the needle in an adjustable orifice. It should be accurately centered with respect to the orifice from the fully open to the completely closed position.

5. *Length and shape of the mixing-tube.*—When a gas under pressure issues from an orifice, the momentum of the gas causes the surrounding air to be set in motion in the direction of the gas stream. Because of the velocity of this gas stream, eddy currents are set up in the surrounding air. The principal function of the mixing-tube is to complete the mixing process as rapidly as possible,

permit the turbulence to die out, and to supply the burner ports with a uniform mixture of air and gas. The length and taper of the mixer beyond the throat should be such that the air-gas mixture expands gradually without sharp changes in diameter or direction that would maintain or produce turbulence until the "velocity head" at the throat has been largely converted into a "pressure head." The length of the mixing-tube should be at least six times the throat-diameter. The outlet from the throat should increase gradually, and the inlet for primary air should be such that the change in direction of flow of primary air is as gradual as possible. The best results are also obtained if the inside of the burner is smooth. Sharp changes in direction and roughness increase resistance to flow and result in a lower injection of primary air. Additional length of the mixing-tube beyond six throat-diameters may be used, but the resistance to flow also increases as the length increases; and this will cause a reduction in primary injection if carried too far.

6. *Burner temperature.*—A cool burner has a higher air injection than a hot one, other things remaining equal. It is therefore advantageous to build the burner so that the heat is dissipated to the room rather than to the mixture of air and gas passing through the burner. A burner having a head temperature of 500° F has an air injection from 2 to 8 percent less than that of the same burner operated at room temperature. It has been shown that temperature causes a greater reduction in primary air injection in burners having long- or small-diameter mixing-tubes than in those having greater diameters or shorter tube lengths. It is also desirable to keep the weight of the metal used at a minimum.

It is believed the use of radiating fins on the Meker-type burners would tend to reduce the over-all temperature and thus increase the air entrained. On these burners, when adjusted for a sharp intense flame, the hottest part of the flame is very close to the metal of the burner head and results in a greater heating of the burner than is the case with the single-port burners.

IX. Results Obtained With Two Burners Modified to Comply With Basic Data

To verify the accuracy of the relationships that appear to be required for the satisfactory operation of a laboratory burner, 2 of the 16 burners were rebuilt to comply with these dimensions.

The port area of burner 16, a straight-tube burner, was increased from 0.13 to 0.15 in.^{2} by drilling out the mixing-tube and flame retainer. The primary air opening was increased from 0.1816 to 0.3375 in.^{2} (2.25 times the port area), and the orifice cap was plugged and redrilled with a No. 62 drill. When the burner was received from the manufacturer the orifice cap was drilled with a No. 51 drill, which delivered entirely too much gas when wide open. A No. 62 drill passes 5,000 Btu/hr at a 6-in. pressure without the use of the needle. This results in a much higher air injection than was possible with the No. 51 orifice and still permits the needle to be used to obtain lower rates of gas flow.

The effect of these changes on the limits of operation and normal air injection is illustrated in figure 11. The curves marked by circles show

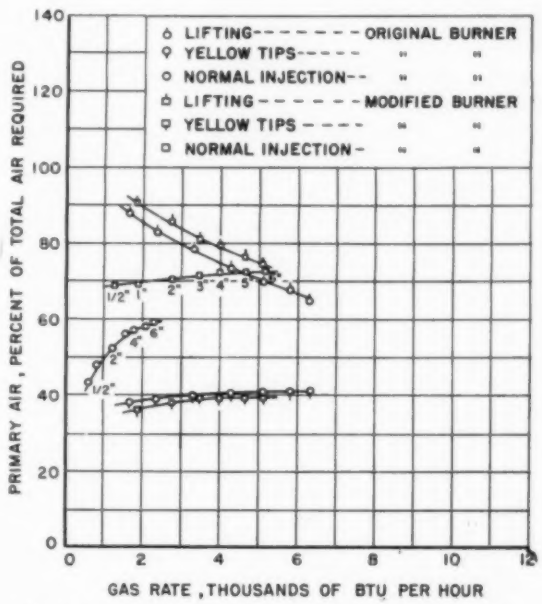

FIGURE 11. *Effect on normal operation of rebuilding burner 16 to comply with basic requirements.*

the normal air injection and limits of operation that were obtained with the burner as received. The highest rate that could be obtained and still inject sufficient air to give a reasonably hard flame was 2,260 Btu/hr. Even with this rate the highest air entrainment was only 59 percent,

which is on the soft side. In order to obtain a 70-percent air entrainment it was necessary to reduce the rate to 1,586 Btu/hr. It will be seen from the shape of this curve that the air entrained is reduced with each change of pressure below 6 in.

The curves marked with a square show the results obtained after the changes described above were made. With these modifications it is possible to obtain a primary air injection of more than 70 percent at any pressure above 1 in. of water, and the maximum gas rate is increased to 5,160 Btu/hr. It will also be observed that changes in pressure have little effect upon the air injection; the curve remains practically horizontal until pressures below 3 in. are used. Increasing the port area also improves the burner from the standpoint of both lifting and yellow tips as can be seen from the position of the two lifting and yellow-tip curves. It is therefore apparent that changing this burner so that the basic requirements are met not only improves the air injection but also increases the range of air entrainment within which the burner can operate without encountering a limiting condition. The modified burner can be satisfactorily operated at more than double the former usable gas rate. This is also illustrated in figure 12, which shows the comparison between the flame produced on the modified burner and that obtained on a duplicate burner used as received from the manufacturer. Both burners are adjusted so that gas is being burned at a rate of 5,000 Btu/hr. The flame on the modified burner is well aerated and hard in appearance while the flame on the burner on the left is soft in appearance and is not suitable for any operation where the application of intense heat is required.

Burner 6, a Meker type, was also changed so that its dimensions corresponded with the basic requirements. In this case the port area was not changed since it was already 1 in.^{2} The throat of this burner was too small, however, being only 29.6 percent of the port area, and the primary air opening was only 0.92 instead of 2.25 in.^{2} A new mixing-tube with a 40-percent throat and an air opening of 2.25 in.^{2} was made. A No. 55 fixed orifice, the size to pass 10,000 Btu/hr at a 6-in. line pressure, was used. The results before and after these changes are shown in figure 13. The position of the limiting curves would remain the same, because no change was made that would affect either lifting, smothering, or the appearance of yellow-tips. The normal air-injection curve marked by circles was obtained with the burner as received and indicates that a No. 56 orifice is the largest size that can be used and still have a normal air injection that is in the stable region. The highest rate that could therefore be used with

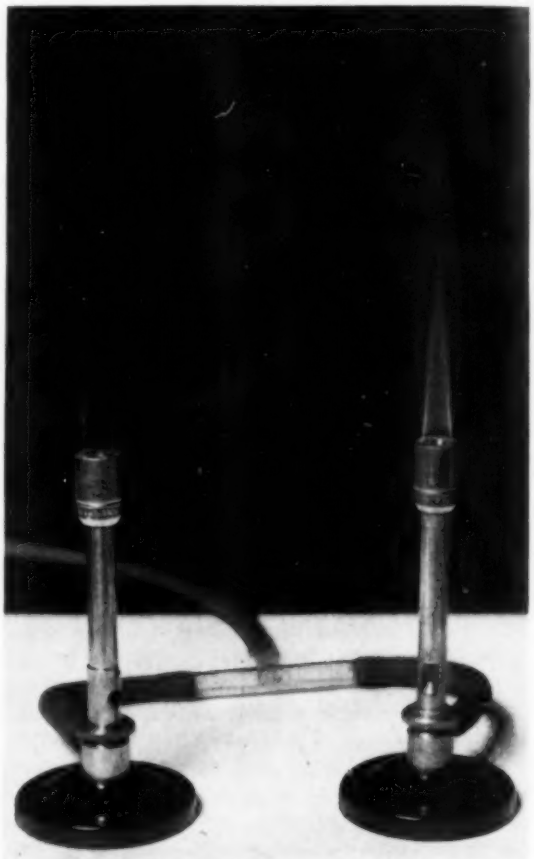

FIGURE 12. *Comparison of flames produced by two similar burners, one as received and the other modified to meet basic requirements.*

this burner was 8,200 Btu/hr. The normal injection curve marked by squares shows the normal air injection obtained with a No. 55 orifice after the changes were made. This is a larger orifice and delivers 10,000 Btu/hr at a pressure of 6 in. It will also be observed that the air entrainment is higher than was obtained with the smaller orifice before the modifications were made. The flame produced is stable at all pressures, and the burner

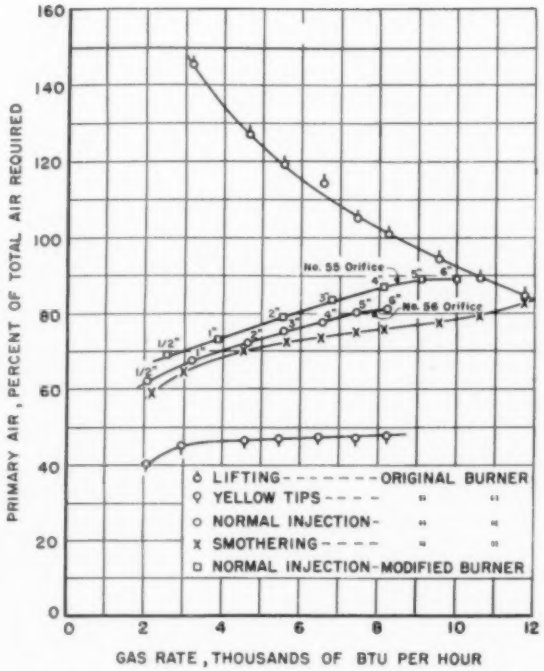
PRIMARY AIR, PERCENT OF TOTAL AIR REQUIRED
GAS RATE, THOUSANDS OF BTU PER HOUR
No. 55 Orifice
No. 56 Orifice
LIFTING - - - - - - - ORIGINAL BURNER
YELLOW TIPS - - - - "
NORMAL INJECTION- "
SMOTHERING - - - - "
NORMAL INJECTION-MODIFIED BURNER

FIGURE 13. *Effect on normal operation of rebuilding burner 6 to comply with basic requirements.*

is now usable at a gas rate 22 percent above its former maximum.

This modified burner was also compared with a similar unmodified burner using propane as the fuel gas. Both burners were adjusted for the highest stable rate at a pressure of 11 in. of water.

The largest orifice that could be used with the unmodified burner was a No. 63, which gave 9,870 Btu/hr.

The modified burner having the proper throat size and primary air opening was capable of producing a stable flame with a No. 59 orifice, which delivers gas at the rate of 13,000 Btu/hr.

X. Summary

Sixteen laboratory burners were included in this investigation, eight of the Meker and eight of the straight-tube type. Each burner was tested, and the limits within which it could be satisfactorily used were determined.

The average Meker burner could not be used at a rate above 6,363 Btu/hr on the natural gas distributed in Washington, D. C., whereas the average usable rate with the straight-tube burners was only 2,781 Btu/hr. A survey of the various heating operations for which a laboratory burner is used indicated that the Meker-type burner should be capable of producing a hot stable flame up to 10,000 Btu/hr, and the straight-tube burners should be usable at rates up to 5,000 Btu/hr.

A comparison of the dimensions of these 16 burners with the fundamental relations for good burner operation brings out three major reasons for their unsatisfactory operation on natural gas.

(1) *Too small a port area.*—A Meker burner should have at least 1 in.^{2} of free port area in order to deliver as much as 10,000 Btu/hr. A study of table 2 indicates that only two of the eight Meker burners tested were as large as 1 in.^{2} From the results obtained on the straight-tube burners a port area of at least 0.15 in.^{2} should be used if rates up to 5,000 Btu/hr are desired. Only one of the straight-tube burners had a port as large as 0.15 in.^{2}

(2) *Improper throat size.*—Results both from this study and those conducted by other investigators show the need of a throat having an area equal to 40 percent of the port area, if optimum air entrainment is to be obtained with a Meker-type burner. Most of these burners were unable to inject enough air to give a satisfactory flame with an orifice of adequate capacity. As shown by table 6, only three of the Meker burners had throats close enough to the 40-percent requirement to approach optimum conditions.

(3) *Insufficient primary air opening.*—Figure 10 illustrates the need for an air opening equal to at least 2.25 times the port area in order to insure a sufficient opening for the entrance of primary air. A burner may be designed with sufficient port area and the proper venturi throat to inject a high percentage of primary air but be prevented from doing so because of too small an opening for the air to enter the mixing tube. Of the 16 burners tested, only 5 had a ratio of air shutter opening to port area as large as 2.25.

In addition to the three factors given above, use of the proper orifice size is equally important. Some of the burners were equipped with adjustable orifices, which when used with the needle backed out gave entirely too high a gas rate for proper operation. By using the needle the rate could be reduced to the desired amount, but so much of the orifice was blocked by the needle

when this condition was obtained that the air injection was impaired. It is much better to use an orifice size that will give the maximum rate desired when used in its wide open position and use the needle only to reduce the rate below this maximum. This will insure the maximum air entrainment from the standpoint of orifice size because the smaller the orifice the higher the percentage of air entrained. If a fixed orifice is used, it is obvious that the size should be the proper one for the maximum rate desired. In addition to the need for more care in the size of the orifices supplied with these burners, more attention should also be given to their assembly. The orifice should be centered with respect to the mixing tube and drilled so that the gas emerges in a vertical stream. The adjustable needles should also be accurately centered with respect to the orifice and stay centered as they are turned from one position to another.

The distance between the throat and the gas orifice, the length and shape of the mixing tube, and the temperature of the burner are all factors that affect the operation of a burner and should be given some consideration.

Two burners, one a straight-tube and the other a Meker type, were modified so that they complied with the basic requirements that appeared to be necessary from the results of our studies. These modified burners were retested and found to be greatly improved, both were capable of satisfactory operation over the range of gas rates desired.

It is believed that the use of these basic data by the manufacturers of laboratory burners would greatly improve this type of appliance and eliminate the dissatisfaction which is now so evident where natural gas is distributed. A burner properly designed for natural gas should also give satisfactory performance with liquefied petroleum gases by merely substituting the proper orifice size.

IX. References

[1] W. M. Berry, I. V. Brumbaugh, G. F. Moulton, and G. B. Shawn, Design of atomspheric gas burners, Techn. Pap. BS **15,** (1921) T193.

[2] F. A. Smith, Problems of stationary flames, Chem. Rev. **21,** No. 3 (Dec. 1937).

[3] J. H. Eiseman, E. R. Weaver, and F. A. Smith, Method of determining most favorable design of gas burners, BS J. Research **8,** 669 (1932) RP446.

[4] G. von Elbe and J. Brumer, Ind. Eng. Chem. **40,** 1123 (June 1948).

Additional References Not Cited in Text

F. Wills, Design of gas burners by the use of fundamental flow formulas, Western Gas **7,** 87 to 99 (Aug. 1931); correction **7,** 34 (Nov. 1931); (Pacific Coast Gas Assoc. Proc. **22,** 1931).

J. H. Eiseman and F. A. Smith, Effect of the depth of drilled ports on the limits of operation of domestic gas burners, J. Research NBS **18,** 485 (1937) RP988.

Flow of gas through orifices on domestic appliances, Bul. No. 1 (Am. Gas Assoc. Testing Lab.).

E. Buckingham and J. D. Edwards, Efflux of gases through small orifices, BS Sci. Pap. **15,** 573 (1920) S359.

E. R. Weaver, J. H. Eiseman, and F. A. Smith, Gas burner design, Am. Gas J. **134,** 54 to 56 (May 1931); **135,** 35 to 38 (June 1931).

A. S. Leonard and E. D. Howe, Characteristics of natural gas flames, Proc. Pacific Coast Gas Assoc. **26** (1935).

Research in fundamentals of atmospheric gas burner design, Bul. No. 10 (Am. Gas Assoc. Testing Lab., 1940).

Washington, November 23, 1948.

U. S. Department of Commerce
National Bureau of Standards

Research Paper RP1992
Volume 42, June 1949

Part of the Journal of Research of the National Bureau of Standards

Studies on the Purification of Collagen

By James M. Cassel and Joseph R. Kanagy

Several methods of purifying collagen were studied. The effects of particular treatments on collagen were followed by nitrogen determinations, by electrometric titration analyses, and by electrophoretic measurements.

Treatment of the raw material with trypsin, as in the conventional method for the preparation of collagen, results in changes that lead to a degradation of the collagen in subsequent extractions. Treatment with dilute salt solution followed by trypsin produces a material of comparatively low isoelectic point (pH 5.5). Apparently soaking in dilute salt solution is not detrimental to collagen, and it is recommended that this type of extraction be substituted for the extraction with trypsin.

A technique for removing all but a negligible part of the mineral content from collagen is described, and a procedure is recommended for use in the preparation of ash-free gelatin.

A specification is proposed for purified collagen: (1) The water extract shall have a pH range of 6.0 to 7.0; (2) the isoelectric point (determined electrophoretically) shall be between pH 6.0 and 7.5; (3) the material shall have an ash content of less than 0.1 percent, total nitrogen content of 17.8 to 18.1 percent, and an amide nitrogen content (determined by hydrolyzing for 20 hours in 0.1 *N* hydrochloric acid at 90° C) of at least 3.8 percent, expressed as percentage of total nitrogen.

I. Introduction

As a preliminary to proposed work on the chemistry of collagen, it is considered necessary to reexamine the methods that have been used in the past for the preparation of a purified material. The ultimate objective of a process for the purification of collagen is the production of a pure, uniform, readily reproducible material in virtually the same physical and chemical state in which it exists in the raw hide.

The chief source of collagen is raw cattle hides. Coexistent with the collagen in the hide are small quantities of extraneous materials as outlined in figure 1. The problem is to effect a separation of these materials with the least possible alteration of the chemical structure of the collagen.

In 1936 Highberger [1] [1] proposed a method of purification that has been generally used in this country. The method includes tryptic digestion of fresh corium under carefully controlled conditions, removal of fats with organic solvents, extraction with half-saturated calcium hydroxide solution, and deliming with acetic acid.

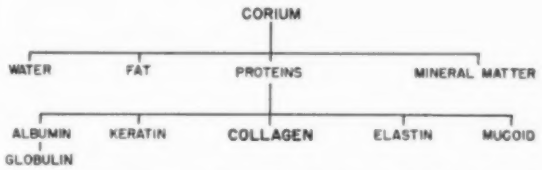

FIGURE 1. *Outline of the materials coexistent with collagen in the hide corium.*

The use of trypsin has been the subject of much discussion. The work of Thomas and Seymour-Jones [2] and that of Merrill and Fleming [3] showed that hide powder, obtained from cowhide that was strongly limed for dehairing purposes, was digested by trypsin. However, Marriott [4] showed that collagen-containing material could be extracted with a trypsin solution under carefully controlled conditions with practically no adverse

[1] Figures in brackets indicate the literature references at the end of this paper.

effect on the collagen if the collagen-containing material had not been previously subjected to the action of reagents likely to cause some alteration. Recently it has been reported that British investigators [5] have elected to omit the trypsin treatment and the extraction with half-saturated calcium hydroxide solution.

The present research was designed primarily to determine the effect on collagen of the various reagents used during its purification, and special effort was made to ascertain the effect of trypsin. The studies included determinations of amide nitrogen, soluble nitrogen, and total nitrogen, electrometric titration analyses, and electrophoretic measurements.

II. Experimental Material

The collagen used in this work was prepared in the leather laboratory of this Bureau from steer hide obtained from the Beltsville Agricultural Research Station. The hair was closely clipped within an hour or two after the animal's death. The hide was cut into strips 4 by 60 in., parallel to the backbone and portioned into four groups for the separate purification methods.

The preliminary treatments of purification varied between groups and are given in figure 2.

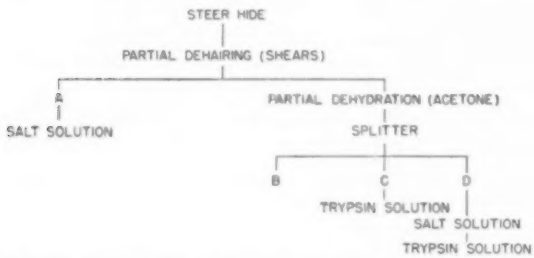

FIGURE 2. *Schematic diagram of the initial steps of the purification methods.*

After this preliminary treatment, all portions were subjected to the following treatment: Acetone, alcohol, lime solution, acetic acid, water, alcohol, and ethyl ether.

One portion (A) was placed immediately in a 5-percent sodium chloride solution, which had been chilled to about 6° C. The salt liquor was drained off daily, and fresh solution was added. After a month of such treatment, during which time the temperature of the salt solution was maintained at 6° C, the epidermal layer could be scraped off with a knife. The fatty layer was removed by the splitting machine. Extraction with trypsin was not included in the preliminary treatment of this portion of the hide.

The remaining three portions (B, C, and D) of the hide were partially dehydrated by treatment in acetone overnight to facilitate splitting off the epidermal and fatty layers in the splitting machine. Batch B received no other preliminary treatment. Batch C was treated with trypsin according to the method suggested by Highberger [1]. The third portion of this subdivision of the hide, D, was subjected to an extraction with dilute salt solution in a manner similar to that described for batch A and was then treated with trypsin.

The principal steps of the purification scheme were the same for all batches of material and included the following treatments: acetone and alcohol extraction to remove fats; extraction with lime solution to remove mucoid protein; treatment with acetic acid to delime; washing with water; and dehydrating first in alcohol and finally in ethyl ether.

Collagen from a second steer hide was purified according to the method suggested by Highberger [1]. Specimens from each step of the process were used for electrophoretic measurements so that changes in the surface characteristics of the collagen caused by each treatment could be determined.

Two samples of hide collagen that had been prepared by the method of Highberger [1] several years previous to this work were also tested. In addition, two sample that had been prepared at Cincinnati University 8 years ago were compared with the collagen prepared in these experiments. One of the samples had been treated with trypsin solution, and the other had been treated with trypsin solution and lime solution.

Small portions of collagen were prepared from the bone and tendon of a steer by the method of Beek [6]. The process included the necessary acid extraction to remove the calcium phosphate from the bone. The treatment with trypsin was omitted in the preparation of one sample of the bone collagen.

The hide powder used in this work was the ALCA Standard Official Hide Powder Lot No. 21.

III. Methods and Results

Several methods of analysis were used to follow the specific effect on collagen of the various purification procedures. These methods included determinations of nitrogen, and of acid- and base-combining capacities, and electrophoretic measurements.

1. Treatment With Trypsin Solution

The extent of the action of the trypsin solution on collagen was estimated from the amo' nts of nitrogenous material dissolved. In each treatment 4 ml of a 1-percent trypsin solution was added per gram of moist corium. The corium covered with this solution was incubated at a temperature of 35° C for 20 hours. The supernatant liquid was then drawn off and 200-ml aliquots were retained for Kjeldahl nitrogen determinations. After rinsing the corium in distilled water, the process was repeated a second and third time.

The nitrogenous material in solution following each trypsin extraction is composed of that introduced by the water solubilization of albumins, globulins, and to some extent mucoid, and that produced by the action of the enzyme on the collagen material. This latter portion is, for the most part, the result of the specific solubility effect of trypsin on elastin [7]. The results are shown in figure 3. The ordinate of the figure represents the loss in nitrogen per 50 g of collagen for each extraction. The points along the abscissa represent the successive treatments of 20 hr each. In all except one instance the curves level off toward a small constant value after three extractions. The tendency for these nitrogen values to approach a constant is in agreement with the results obtained by Highberger [1] that the maximum effect of trypsin on elastin takes place during the first three extractions. The results with bone collagen indicate that degradation of the collagen becomes significant after the third extraction with trypsin. Apparently the acid treatment included in the preliminary steps of the purification of the bone collagen has made the material more susceptible to reaction with trypsin.

Highberger showed that when trypsin is deactivated the main portion of soluble nitrogenous material in the first two extractions does not arise from enzyme activity but is due to the presence of soluble protein. This would probably account

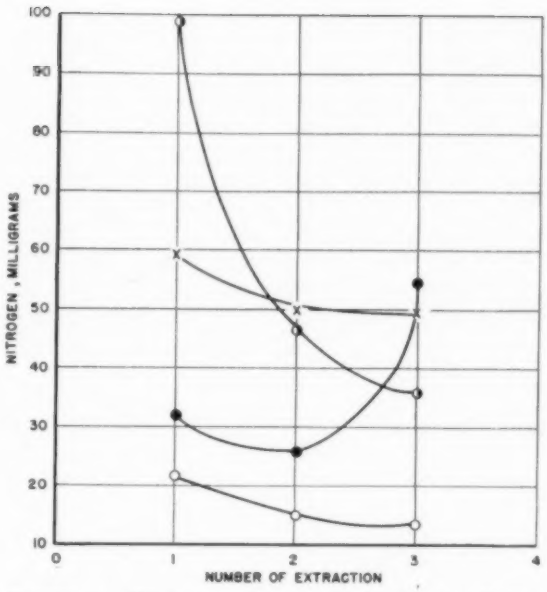

FIGURE 3. *Effect of preliminary treatment of collagen-containing materials on the nitrogenous compounds solubilized in subsequent trypsin extractions.*

The nitrogen values are per 50 g of collagen. ◑, Hide collagen (C), no previous treatment; ○, hide collagen (D), salt treated; ×, tendon collagen, washed in water; ●, bone collagen, acid treated.

for the comparatively high nitrogen result for the portion of corium C, on the first of the three extractions with trypsin. (See fig. 3.) Batch C had received no washing prior to the treatment with trypsin, whereas the other samples had been washed in aqueous solutions that solubilized some of the nitrogen-containing material.

2. Treatment with Calcium Hydroxide Solution

The extent of the action of half-saturated lime solution on collagen was followed by a series of tests similar to those used for studying the effect of trypsin. In each treatment 10 ml of the calcium hydroxide solution was added per gram of moist corium. The corium-lime solution mixture was agitated on a shaker at room temperature for 1 hr. The supernatant liquid was then drained off and 200-ml aliquots were retained for the Kjeldahl nitrogen determinations. The process was repeated a second and third time.

The purpose of this treatment is to remove the mucoid protein. McLaughlin and Theis [8] found 0.45 percent (calculated on dry basis) of this material in the corium of steer hide. This substance,

which contains about 2.4 percent of sulfur and 12.4 percent of nitrogen, exhibits properties of a carbohydrate as well as those of a protein.

The absolute values for the soluble nitrogenous materials given in figure 4 are not important, but the relative values for different collagens seem to have some significance. The four highest nitrogen values in the first extraction period are from those collagens that had been treated with trypsin. In the sample of bone collagen treated with trypsin, the soluble nitrogenous material from the first calcium hydroxide extraction was four times greater than that found in the sample of bone collagen not treated with trypsin.

A similar comparison can be made of two hide collagen samples, the purification of which included a treatment with dilute salt solution. The ratio of the nitrogen content of the exhaust liquors from the initial lime extraction of the sample treated with trypsin and salt solution and that treated with trypsin alone is 3:1. A comparison of the hide collagen samples that had no salt treatment and differed only in the trypsin treatment shows the same trend. The exhaust liquor from the first lime extraction of the sample previously treated with trypsin has one and a half times the nitrogen content of the exhaust liquor from the sample that had not been treated with trypsin. Apparently the treatment with trypsin changes the materials in some manner so that they are more easily degraded in subsequent treatment with lime water.

It should be pointed out that the material least affected by this lime extraction is the collagen which was leached in the 5-percent sodium chloride solution and which was not treated with trypsin.

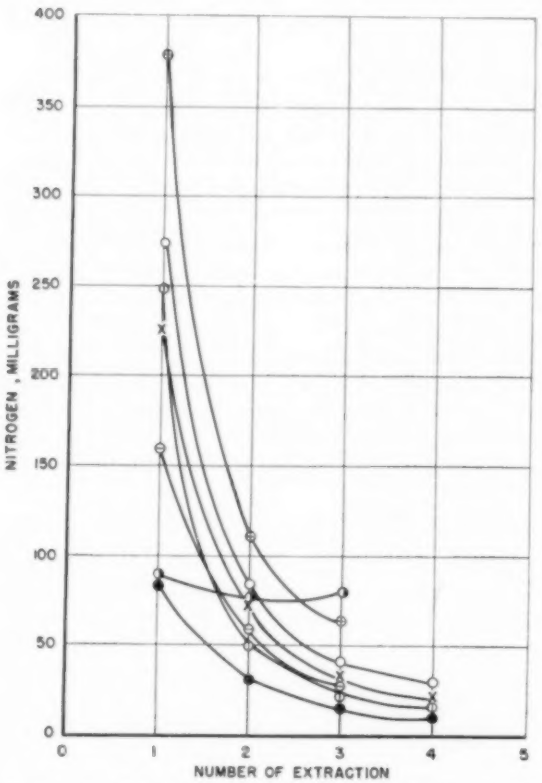

FIGURE 4. *Effect of previous treatment of collagen-containing materials on the nitrogenous compounds solubilized in subsequent calcium hydroxide extractions.*

The nitrogen values are per 100 g of collagen. ⊖, Hide collagen, no previous treatment; ○, hide collagen, treated with salt and trypsin; ⊕, hide collagen, treated with trypsin; ●, hide collagen, treated with salt; ×, tendon collagen, treated with trypsin; ⊕, bone collagen, treated with acid and trypsin; ◑, bone collagen, treated with acid.

3. Determination of Total Nitrogen and Amide Nitrogen

Total nitrogen in the collagen samples was determined by the standard Kjeldahl method. The amide nitrogen contents of the collagens were determined by hydrolyzing in 0.6 *N* sulfuric acid for 3 weeks at 60° C and in 0.1 *N* hydrochloric acid for 20 hrs at 90° C. In both methods the solutions were neutralized and ammonia distilled over in the presence of an excess of magnesium oxide. As the amount of ammonia obtained varies with the conditions of hydrolysis and distillation [9], the results have no absolute significance. However, the relative differences between the results obtained from different samples under the same conditions of hydrolysis and distillation give a measure of the effects of the purification treatments on the amide nitrogen content.

In table 1 the amide values of columns 4 and 5 are for hydrolyses carried out at 60° and 90° C, respectively. By either method it is apparent that the amide value for the hide collagen that was extracted in the dilute salt solution and then treated with trypsin is approximately 0.25 percent lower than that for the other three hide collagens. The other hide collagens have approximately the same concentration of amide nitrogen. These results indicate that the trypsin treatment, when not preceded by soaking in dilute salt

solution, did not attack the amide linkage. However, the combination of the action of the dilute salt solution and the trypsin appears to have lowered the amide nitrogen.

TABLE 1. *Effect of various treatments on nitrogen values of collagen*

Sample	Source	Treatment	Amide nitrogen as percentage of total nitrogen hydrolyzed at—		Total nitrogen
			60° C	90° C	
					Percent
1	Hide	Blank	3.55	4.27	17.75
2	do	Trypsin	3.54	4.34	17.81
3	do	Salt solution	3.50	4.23	17.89
4	do	Salt solution, trypsin.	3.25	4.04	17.87
5	Bone	Acid	2.36	2.99	17.76
6	do	Acid, trypsin	2.22	2.94	18.00
7	Hide powder	Lime, trypsin	2.15	2.46	17.41

Table 1 shows that the amide nitrogen content of the hide collagen samples is considerably higher than that of the bone collagen or hide powder. The bone collagen was subjected to a long acid hydrolysis, and the hide powder to a severe liming process. In either treatment amide bonds would have been attacked and the nitrogen contents lowered.

The nitrogen content of collagen (expressed as total nitrogen) does not seem to be definitely related to the method of preparation. Although the bone collagen sample treated with trypsin had about 1.2 percent less amide nitrogen than the hide collagens, its total nitrogen content was was greatest of the group. In neither the bone collagen nor the hide powder was the loss in amide nitrogen apparent in total nitrogen content. This might be due to removal, during purification of collagen, of proteins with comparatively low nitrogen contents, a process which would, in effect, increase the percentage of nitrogen in the final product.

4. Determinations of Acid and Base Combining Capacities

Combination of acid and base with the several collagen preparations was determined in potassium chloride solutions of constant ionic strength. The volume and normality of potassium chloride were varied with each acid or base concentration to maintain an ionic strength of 0.1. To 1 g of protein in a glass-stoppered bottle was added 100 ml of a solution having a known concentration of acid or base and a known concentration of potassium chloride. The equilibrium pH was determined with a glass electrode after 24 hr. For each bottle containing collagen, a bottle was prepared containing only the 100 ml of the aqueous medium, and then the acid or base bound by the protein was determined by difference. Since large changes in acid (base) content produce only small changes in the pH of extremely acid (basic) solutions, the maximum acid (base) binding values are subject to error.

The titration results are shown in figure 5. Maximum acid-binding values lie between 0.84 milliequivalent per gram for hide powder and 0.89 milliequivalent per gram for the collagen that had been treated with dilute salt solution but not with trypsin.

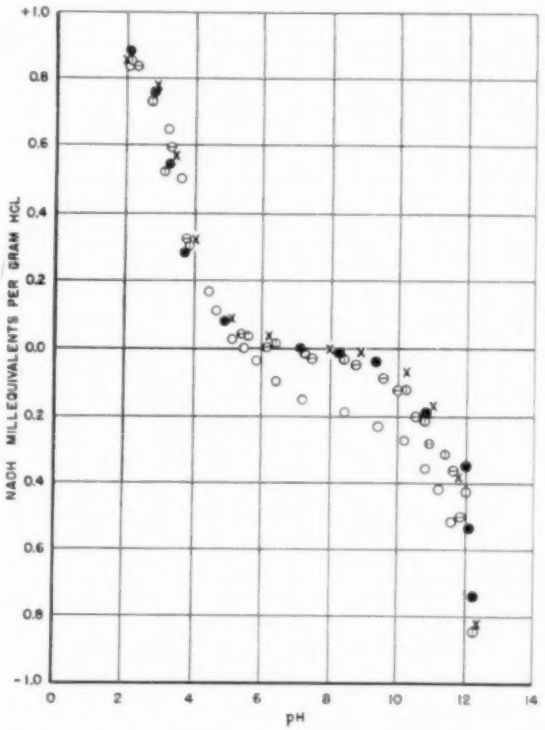

FIGURE 5. *Comparison of the acid-base titration curves of the various hide collagens and hide powder.*

○, Commercial hide powder; ⊖, collagen, trypsin and salt extracted; ⊕, collagen, no salt or trypsin treatment; ×, collagen, extracted with trypsin; ●, collagen, extracted with salt.

The collagen curves show a decided similarity regardless of method of preparation. The material that had been exposed to dilute salt solution and then to trypsin tended to have a more acidic nature than the other hide collagens. This is evidenced by its isoionic point of pH 6.2. The isoionic point is defined as the point at which dissociable groups of a substance combine equally and only with the hydrogen and hydroxyl ions [10]. Within the pH range 5.0 to 12.0 the curve for the hide powder indicates much greater base binding than that exhibited by any of the collagens. Between pH 7.0 to 9.0 this average difference is 0.17 milliequivalents. This may be accounted for by the difference in the average amide nitrogen content of the collagen samples and that of hide powder (0.16 milliequivalents).

5. Electrophoretic Analysis

The Abramson horizontal, microelectrophoresis cell that was used to make the mobility measurements is adequately described by Moyer [11]. A practical application of the cell in the investigation of wool protein is given by Harris [12]. The microscope was used with an 8-mm objective and a 20× eyepiece. The buffer mixtures were as follows: pH 2.4 to 3.6, potassium chloride-hydrochloric acid; pH 4.0 to 5.6, sodium acetate-acetic acid; pH 6.0 to 7.8 disodium phosphate-dihydrogen phosphate; pH 8.0 to 9.2, boric acid-borax, pH 10.0 sodium hydroxide-boric acid-potassium chloride. The ionic strength of all buffers was 0.005. The pH values were measured with glass electrodes and referred to 0.05 *M* potassium acid phthalate (pH 4.01), and to 0.01 *M* borax (pH 9.18). The specific resistance of solutions introduced into the cell was determined with a pipette conductivity cell and a conductivity bridge [11]. Two or three groups of measurements, each consisting of at least 10 measurements of the velocity of the particles, were made at each selected pH. When mobilities were very low, the velocity of the particles was measured in layers adjacent to the stationary layer, and mobility was evaluated by graphical integration of the curve obtained by plotting velocity against depth [13]. Sufficiently stable suspensions for the measurements were prepared with a Waring Blendor.

The mobility measurements were made in a room at approximately 23° C. All values were corrected to 25° C by applying a factor of 2 percent per degree [11].

As a check on the electrophoretic technique to be used, determinations were made of the mobilities of collagen previously prepared at this Bureau and of that sent to the Bureau from the University of Cincinnati. The results of these measurements are shown in figure 6. The isoelectric points determined by this work agree very well with those found by Beek and Sookne [14] and by Highberger [15] on these same materials.

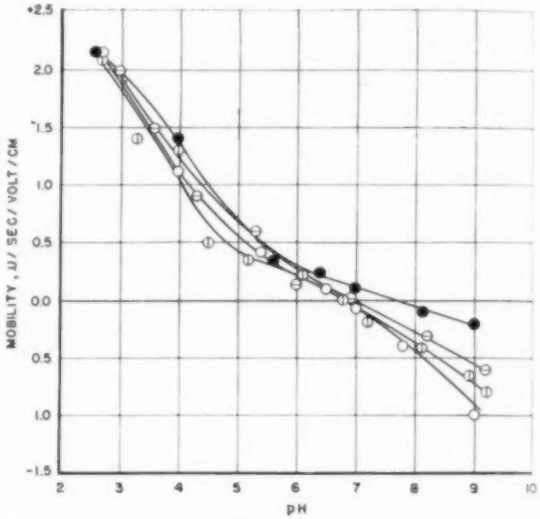

FIGURE 6. *Comparison of the* pH-*mobility curves for some hide collagens in storage for several years.*

⊖, Purified in the leather laboratory of this Bureau, Highberger procedure; ⊕, purified in the leather laboratory of this Bureau, Highberger procedure; ●, purified in another laboratory, Highberger procedure; ○, purified in another laboratory, Highberger method with elimination of lime treatment.

In figure 7 the mobility-pH curves are plotted for the hide collagen samples prepared in a manner discussed previously in the text. The isoelectric point (pH 5.5) of the material extracted with dilute salt solution and trypsin is lowest of this group.

The very close agreement in isoelectric point (6.4, 6.5, 6.4) of the other hide collagen preparations indicates that either trypsin or dilute salt solution, if used alone, will not seriously alter the surface characteristics of the product. However, a combination of these two extractions in preparation of collagen has produced a more acidic surface than would seem desirable in undegraded material.

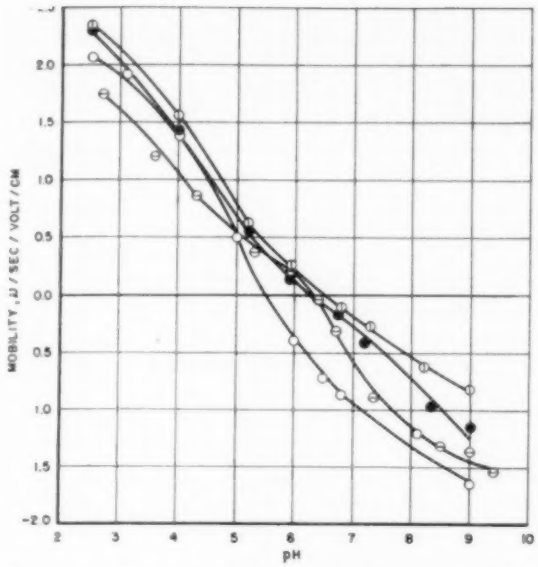

FIGURE 7. *Effect of method of purification on* pH-*mobility curve of collagen.*

○, Extracted with salt and trypsin; ⊕, extracted with trypsin; ●, extracted with salt; ⊖, no extraction with salt or trypsin.

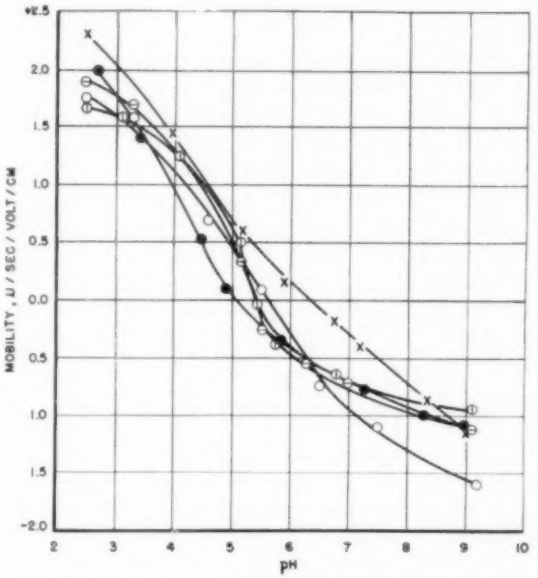

FIGURE 8. *Comparison of the* pH-*mobility curves of hide collagen with those of hide powder, bone, and tendon collagen.*

○, Tendon collagen; ⊕, bone collagen, treated with trypsin; ⊖, bone collagen; ●, hide powder; ×, hide collagen.

The curves in figure 8 show the mobilities as a function of pH for collagen from hide, tendon, and bone, and for hide powder. The hide collagen is isoelectric about one pH unit higher than the other collagens. This is probably due to the drastic hydrolysis to which these materials were subjected during purification. Beek and Sookne [14] have suggested that the decrease in amide nitrogen content is accompanied by an increase in the number of free carboxyl groups, the net result of which is to shift the isoelectric point to a more acid region. The results obtained with the two bone collagen samples, one of which was treated with trypsin, are similar. Since the materials are isoelectric at the same pH value, the extraction with trypsin would seem to have had little effect on the characteristics of the collagen. However, results discussed earlier in this paper [2] indicate that trypsin has a deterimental effect on bone collagen previously subjected to prolonged treatment with acid. It can only be assumed that any degradation that occurs during the extraction with trypsin has no effect on the surface charge of the finished product.

Figure 9 shows the mobility curves of specimens of collagen taken from the material at certain steps of one of the purification processes. (See sec. II.) The isoelectric point of the raw, unpurified collagen is pH 5.8. Extraction with trypsin has not shifted the isoelectric point but has made the material more reactive, as evidenced by the

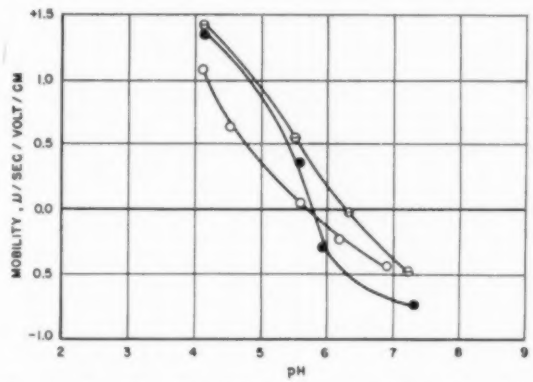

FIGURE 9. *The* pH-*mobility curves of collagen determined at various stages of the purification process.*

○, Raw collagen; ●, collagen treated with trypsin; ⊖, collagen subjected to complete purification.

[2] See discussion of nitrogen analyses made on trypsin extracts.

steeper slope of the curve on either side of the isoelectric point. The effect of the calcium hydroxide treatment has been to raise the isoelectric point. This shift in isoelectric point to a more alkaline region is the same sort of change shown in figure 6 when the unlimed material was isoelectric at pH 6.9, the limed material at 7.7. This shift may be accounted for by either of two reasons. If the mucoid removed by this extraction with half-saturated solution of lime is isoelectric at a pH lower than collagen, then its removal would raise the isoelectric point of the purified collagen product. Hesselvik [16] has made electrophoretic measurements on a number of mucoid samples and has shown that the isoelectric points of the materials varied from pH 3.0 to 4.5.

A second explanation, and one the authors believe to be nearer correct, is that some combination between carboxyl groups of the collagen and calcium atoms occurs during the lime extraction. Any tendency to inactivate the carboxyl groups would raise the isoelectric point. Presumably if all the calcium picked up by the collagen were not washed out in deashing the product, the isoelectric point of the product would be changed toward a more alkaline pH.

IV. Amide Nitrogen Content and Isoelectric Point

Previous investigators [14] have indicated that the isoelectric point and amide nitrogen content of collagen were related. In table 2 the amide content and isoelectric point are listed for several collagen samples. The two collagens of lowest amide nitrogen content have the lowest isoelectric points. However, one sample having about 1 percent greater amide nitrogen has an isoelectric point in the same region. There appears to be no correlation between the isoelectric point and amide nitrogen values of the first five samples. Apparently whereas a low amide content indicates a low isoelectric point, there must be other factors that also have an influence on the location of the isoelectric point.

TABLE 2. *Correlation of nitrogen values with isoelectric points*

Sample	Source	Amide nitrogen	Total nitrogen	Isoelectric point
		Percent	*Percent*	
1	Steer hide	3.93	17.84	7.7
2	do	4.14	17.97	7.0
3	do	3.83	17.38	6.9
4	do	4.34	17.81	6.5
5	do	4.27	17.75	6.4
6	do	4.01	17.71	5.5
7	Bone	2.94	18.00	5.4
8	Hide powder	2.46	17.41	5.1

The total nitrogen contents of the preparations appear to bear no direct relation to their isoelectric points. This same result with wool was noted by Harris [12] in 1932, who found that a difference of 1 percent in nitrogen content did not result in different isoelectric points.

V. Preparation of Ash-Free Collagen

It is desirable for research purposes that purified collagen be as free of mineral matter as possible. The average ash content of the materials prepared during this study was 0.06 percent. Since it is preferable in many instances to use a product with even less ash content, a method was sought that could remove the bulk of the retained mineral matter. The collagen was leached in frequent changes of distilled water kept at 6° C. The bulk of the leach water was ejected by pressing at 5,000 lb/in.^{2} in a Carver press. The conductivity and pH were determined for each extract. The product was considered as free of mineral matter as this technique would permit when after 4 days of contact with distilled water the conductivity of the extract was 5×10^{-6} mho and the pH was 6.5 (conductivity of distilled water 1.5×10^{-6} mho, pH 5.6 to 6.0). Spectrographic analysis of the dried collagen revealed 50 parts per million of copper and of iron, 20 parts of lead and of calcium, and 10 parts of tin and of chromium.

A procedure of the type outlined above would yield a collagen from which ash-free gelatin might be derived for dielectric and other fundamental studies.

VI. Specifications for Purified Collagen

It is believed that a specification for purified collagen might be of value in furthering fundamental research on collagen. It must be stressed that these proposed requirements only satisfy minimum standards and considerable tolerance is intended. The pH and ash content of a product are easily determined. With a minimum of effort the ash content can be kept below 0.1 percent and the pH between 6.0 to 7.0. The isoelectric point

of a purified collagen should not be less than pH 6.0 as isoelectric values below this indicate degradation, and not more than 7.5 since higher values indicate combined metals or degradation [17]. Total nitrogen content of the product should be between 17.8 and 18.1 percent. Amide nitrogen, expressed as percentage of total nitrogen and determined by hydrolyzing for 20 hr in 0.1 *N* hydrochloric acid, should not be less than 3.8 percent.

VII. Conclusion

Even though the surface characteristics of collagen (as determined by electrophoretic measurements) do not seem to be impaired by an extraction with trypsin, there is strong evidence that trypsin modified the material in such a manner that subsequent treatments result in degradation of the product. The large differences observed in the values for the soluble nitrogenous material in the lime extractions for the trypsin- and non-trypsin-treated collagens are evidence of this degradation. It was found also that in preparing bone collagen the nitrogen content of a third trypsin extract was double that of the first, and this increase in nitrogen could only arise by degradation of the material.

Although the dilute salt solution in combination with the trypsin has been shown to be detrimental to collagen, no evidence was observed that the use of the 5-percent sodium chloride solution alone was harmful. In view of the fact that the main portion of elastin is removed mechanically by splitting off the grain layer [18, 19] and since the salt solution removes the bulk of extraneous material without damage to the collagen, it is recommended that soaking in salt solution be used in preference to treatment with trypsin in the purification of collagen. Since it has been observed that a material extracted with dilute salt solution has not been degraded by a subsequent lime extraction, the use of a half-saturated calcium hydroxide solution would then be justified to remove the mucoid.

VIII. References

[1] J. H. Highberger, J. Am. Leather Chem. Assoc. **31,** 93 (1936).

[2] A. W. Thomas and F. L. Seymour-Jones, J. Am. Chem. Soc. **45,** 1515 (1923).

[3] H. B. Merrill and J. W. Fleming, J. Am. Leather Chem. Assoc. **22,** 139 (1927).

[4] R. H. Marriott, J. Intern. Soc. Leather Trades Chem. **16,** 6 (1932).

[5] E. R. Theis. Personal communication.

[6] J. Beek, Jr., J. Am. Leather Chem. Assoc. **33,** 621 (1938); J. Research NBS **21,** 117 (1938) RP1119

[7] R. H. Bogue, The chemistry and technology of gelatin and glue (McGraw Hill Book Co., Inc., New York, N. Y., 1922).

[8] G. D. McLaughlin and E. R. Theis, J. Am. Leather Chem. Assoc. **19,** 428 (1924).

[9] A. Shore, H. Wilson, G. Stueck, J. Biol. Chem. **112,** 407 (1935).

[10] S. P. L. Sørenson, K. Linderstørm-Lang, and E. Lund, J. Gen. Physiol. **8,** 543 (1927).

[11] L. S. Moyer, J. Bact. **31,** 531 (1936).

[12] M. Harris, J. Research NBS **8,** 779 (1932) RP451.

[13] H. A. Abramson, Electrokinetic phenomena (The Chemical Catlog Co., New York, N. Y., 1934).

[14] J. Beek and A. M. Sookne, J. Am. Leather Chem. Assoc. **34,** 641 (1939); J. Research NBS **23,** 271 (1939) RP1230.

[15] J. H. Highberger, J. Am. Chem. Soc. **61,** 2202 (1939)

[16] L. Z. Hesselvik, Physiol. Chem. **254,** 144 (1938).

[17] J. M. Cassel and J. R. Kanagy, National Bureau of Standards publication pending.

[18] H. G. Turley, J. Am. Leather Chem. Assoc. **21,** 117 (1926).

[19] G. D. McLaughlin and F. O'Flaherty, J. Am. Leather Chem. Assoc. **21,** 338 (1926).

Washington, December 9, 1948.

U. S. Department of Commerce
National Bureau of Standards

Research Paper RP1993
Volume 42, June 1949

Part of the Journal of Research of the National Bureau of Standards

Flame Spectrum of Acetylene from 1 to 5 Microns[1]

By Earle K. Plyler and Curtis J. Humphreys

The spectrum of an oxyacetylene flame obtained with a welding torch has been observed and measured by using a Perkin-Elmer spectrometer, with a LiF prism. Bands were observed at 1.2, 1.3, 1.52, 1.85, 2.0, 2.3, 2.48, and 2.8 μ, which agree in position and general appearance with bands originating in the methane flame, except for newly observed bands at 1.5 and 2.3 μ. The 1.5-μ band probably represents the $\nu_1+\nu_3$ combination in the C_2H_2 molecule, and the 2.3-μ band is probably the R-branch of the 2 ν_1 band of CO, the P-branch being overlapped by the R-branch of the 2.7-μ H_2O band.

The band at 2.8 μ shows fine structure on the long wavelength side consisting of 29 lines between 2.8 and 3.6 μ, when a flame of reduced oxygen content is used. With a hot flame obtained with the maximum amount of oxygen, this number is reduced to 10 in the region from 3.1 to 3.7 μ, some of which show good agreement with calculated values for the 2→1 band of OH. On the long wavelength side of the intense CO_2 emission band at 4.45 μ, 27 rotational lines have been observed, some of which agree closely with the rotational absorption lines of the CO fundamental. This structure was also observed in the methane-oxygen flame.

Evidence for the validity of the interpretations of certain features of these bands as originating in OH and CO is critically examined, and it is concluded that further observations with the higher resolution provided by a grating spectrometer, will be required to establish the certain identification of the spectra of OH and CO in the flame.

I. Introduction

Recent spectrometric studies [1, 2][2] of the Bunsen flame and torch flames of natural gas and oxygen mixtures have revealed a considerable amount of structure, not previously observed, in the infrared emission bands. The water vapor and carbon dioxide bands account for nearly all of the emitted energy. There are however a number of other possible features of such flame spectra, interest in which has to a great extent prompted the present series of investigations. These features include bands originating in other combustion products, and in the thermally excited gas molecules previous to combustion. Vibrational-rotational bands of OH appear with increasing intensity as the flame temperature is raised. In the region from 2.8 to 3.7 μ there is observed a series of rotational lines that are produced by OH and H_2O. The relative intensities of these two groups are a function of flame temperature and the chemical composition of the burning substances.

In addition to the bands originating in CO_2, H_2O, and OH, there are bands of low intensity that are attributed to methane, the principal constituent of the natural gas used in the earlier experiments, which is that supplied in the local area for household and commercial use. These bands are detected only when observations are made on the cone of the flame, the under surface of which is the only region where appreciable numbers of thermally excited molecules of unburned gas might be expected to be found.

The study covered by this report was undertaken with a threefold purpose: to determine if the OH rotational components are more intense for C_2H_2 than for CH_4 in combustion; to ascertain in the case of acetylene whether a sufficient

[1] Part of the subject matter of this paper was presented at the Detroit meeting of the Optical Society of America, Oct. 21 to 23, 1948.

[2] Figures in brackets indicate the literature references at the end of this paper.

amount of CO was in the flame as an intermediate combustion product to permit observation of the characteristic infrared bands, under the most favorable conditions of combustion; and, if possible, to observe the infrared emission bands of the C_2H_2 molecule.

The emission flame spectra of any of the simple hydrocarbons, either saturated or unsaturated, when mixed with air or oxygen, are closely similar in the general features of the energy distribution pattern. It is possible, however, to produce marked changes in the structure of such spectra by varying these conditions, as for instance by increasing the proportion of oxygen in the mixture, which has the effect of elevating the flame temperature as long as the fuel mixture remains on the rich side. The energy pattern is also highly dependent on the region of the flame from which the energy is directed into the spectrometer. The hottest part of the flame, in general, is that just above the tip of the cone, whereas the cone itself is cooler and may emit considerable amounts of radiant energy from unburned molecules of gas.

II. Experimental Procedure

This investigation of the acetylene-oxygen flame was confined to the spectral region from 1 to 5 μ. A Perkin-Elmer infrared spectrometer, fitted with a LiF prism, was used as the dispersing instrument. The only modification of the spectrometer was the removal of the cover of the source box and rotation of the plane mirror to permit location of the flame source at a convenient point without removing or disturbing the globar source unit. A continuous record of the spectrum was obtained by employing the amplifying and recording equipment described in an earlier publication [3]. An industrial oxy-acetylene welding outfit, kindly placed at our disposal by this Bureau's welding shop, was used to provide the flame source. The assembly consisted of the usual gas cylinders, pressure regulators, and an assortment of welding torches with port openings of different sizes.

Records of the emission spectrum of acetylene-oxygen mixtures under various conditions of combustion and for selected regions in the figures that follow. In figure 1

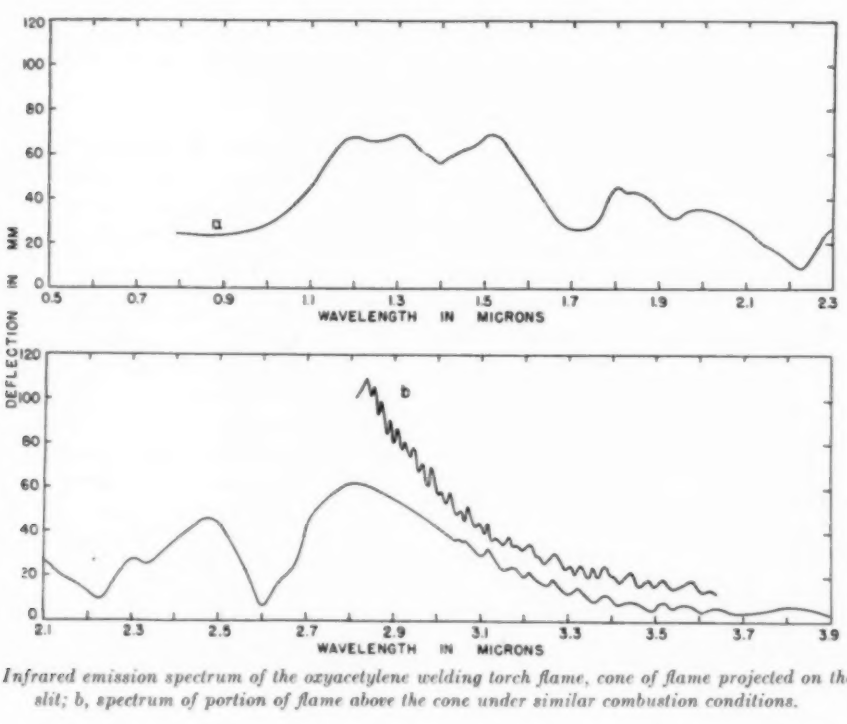

FIGURE 1. *a, Infrared emission spectrum of the oxyacetylene welding torch flame, cone of flame projected on the spectrometer slit; b, spectrum of portion of flame above the cone under similar combustion conditions.*

(curve *a*) is shown the emission spectrum of the cone of the flame. The amount of oxygen in the mixture was relatively small, so that a cone about 2 cm high was maintained above the tip of the torch. The emitted energy includes the spectrum originating in the cone, together with that from the portion of the surrounding flame at the same elevation. The figure shows emission bands at 1.2, 1.3, 1.5, 1.8, 2.0, 2.3, 2.5, and 2.8 μ. All these bands, except those at 1.52 and 2.30 μ, are produced by carbon dioxide and water vapor. There is considerable overlapping of portions of the P, Q, and R branches of some of the bands occurring in this spectral region. When the cone is focused on the slit, the carbon dioxide and water vapor spectra are reduced in intensity in comparison with higher portions of the flame. These spectra are much more intense above the cone, and previous studies on methane [2] have shown these bands in good detail. The purpose of the study of the emission from the cone was to ascertain if the spectrum originating in the heated acetylene molecules could be detected.

The band recorded at 1.52 μ was not present in the methane spectrum [1] and is attributed to the acetylene molecule. It checks well in position with the $\nu_1+\nu_3$ vibration of acetylene. The intensity is low, but the band appears in a region that is free of bands of water vapor and carbon dioxide and can be easily observed.

The band at 2.3 μ is interpreted as being part of the harmonic band of CO, observed in absorption with high resolution by Lagemann, Nielsen, and Dickey [4]. It should consist of P and R branches, but the P branch of this CO band is overlapped by the R branch of the ν_3 vibrational band of H_2O at 2.5 μ, which makes it impossible to observe its real profile. Further evidence of CO emission in the torch flame will be considered in a discussion of structural features observed in the 4.7-μ region.

The fundamental band, ν_3, of acetylene is located at 3 μ. In this series of observations its presence could not be clearly established. The *P* branch of the ν_3 vibrational band of H_2O is in the same region, and because of its great intensity could have completely obscured the emission from C_2H_2. It may be noted that the curve reproduced shows a broad emission band extending from 2.6 to beyond 3.1 μ, with almost no structure, in marked contrast to the traces obtained with methane. It is probable that the acetylene trace through this region represents a superposition of the spectra of H_2O, C_2H_2, and other molecules formed by combustion.

When the region of the flame above the cone was focused upon the slit, an energy trace illustrated by curve *b*, figure 1, was obtained. The conditions of combustion were maintained the same as for curve *a*. It is to be noted that much more fine structure is observed for the region from 2.8 to 3.6 μ, and the intensity of emission is greater than for the corresponding observations on the cone of the flame.

Figure 2, curve *a*, illustrates the emission pattern from 1.6 to 3.7 μ, when a moderate amount of oxygen, more than that used in the observations illustrated by figure 1, is introduced into the burning mixture. The region of the flame above the cone was selected for observation.

The zero branch of the 1.85-μ band originating in the H_2O molecule appears rather sharp, but the *P* branch at 2 μ is quite broad. This modification of its profile is caused by three CO_2 emission bands in this region. The 2.3-μ band, attributed to CO, is greatly reduced in intensity, whereas there is a marked increase in emitted energy throughout the 2.7- to 3.0-μ region. It was difficult to resolve the fine structure in the latter region. The rotational structure is clearly marked from 3 to 3.7 μ. These rotational lines have been studied previously in connection with the investigation of the methane flame. Although similar in appearance, some differences in clearness of the observed fine structures, attributed to different proportions of oxygen, are apparent.

In figure 2, curve *b*, is shown the region from 3.1 to 3.7 μ when still larger amounts of oxygen are supplied to the burning mixture. The flame is very hot, and the observed rotational lines, having a different spacing from that appearing when low oxygen is introduced, are very prominent. Altogether 10 emission maxima of nearly uniform spacing are clearly discernible in this wavelength interval. Of these, the five lines from 3.35 to 3.7 μ agree in position, within the limits of experimental error of these observations, with the rotational lines of OH as calculated by Dieke [5] for the $2\rightarrow1$ rotational-vibrational band, corresponding to the transitions, P(11) to P(15). The five emission maxima from 3.1 to 3.35 μ do not correspond in wave number to the $1\rightarrow0$ or $2\rightarrow1$ band. It is possible that these lines are blends

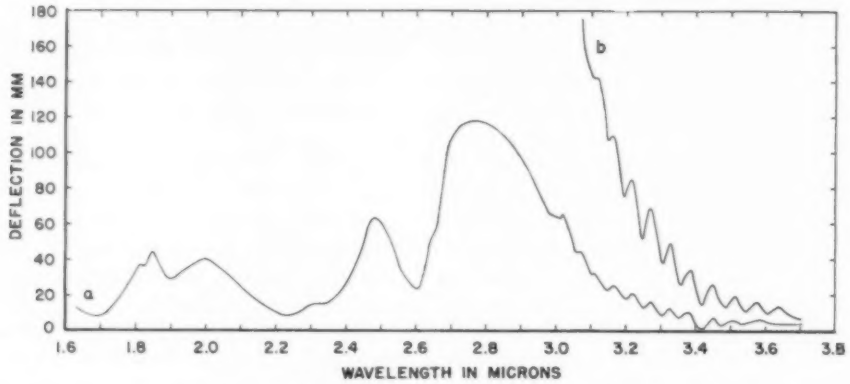

FIGURE 2. *a, Emission spectrum of the oxyacetylene flame, region above the cone, oxygen content greater than under conditions illustrated by figure 1; b, spectrum of oxyacetylene flame between 3.1 and 3.7μ, maximum oxygen content.*

of parts of each of these bands that are overlapped, and that the resolution of the instrument is not sufficient to separate the components of each band. Furthermore, some of the rotational components in the P-branch of the ν_3 band of H_2O may well extend into this region, particularly those associated with high-level transitions, which may be excited, at these elevated temperatures, and which would be located at longer wavelengths than transitions terminating in the normal state. In this connection it is particularly emphasized that the distribution and relative intensities of the fine structure components are extremely sensitive to proportions of the fuel mixtures, permitting considerable shifting of observed maxima where the resolution is insufficient to reveal all the details. The calculated and observed wave numbers as well as the line numbers, which are the K-values for the initial levels in absorption, are given in table 1. The calculated values for each band series are taken from Dieke's table. It is to be noted that the calculated wave numbers used for comparison with observed values are in each instance the average of four numbers, required by the existence of two electronic band systems, characterized by analogous vibrational levels, each of which is split by a spin doubling. The four possible transitions being of equal statistical probability, an arithmetical mean is taken. The experimentally observed rotational structure of the high-temperature acetylene flame corresponds almost identically with the spectrum observed in this region with the high temperature hydrogen-oxygen flame, which was recently measured with the same instrument.

TABLE 1. *Calculated and observed wave numbers for rotational lines in the P-branch of the 2→1 band of* OH

K	P (calculated [5])	P (observed)	P (observed)
	cm^{-1}	cm^{-1}	μ
11	2945.8	2952	3.388
12	2897.8	2899	3.449
13	2848.9	2848	3.511
14	2799.3	2801	3.570
15	2748.8	2749.5	3.637

The CO_2 emission band at 4.4 μ, originating in the hot acetylene flame, is of high intensity. The corresponding absorption band, located at 4.25 μ, is also very intense, being nearly opaque at 4.23 and 4.27 μ, where the respective minima of the two branches of the band are located. Part of this absorption may be produced by reversal in the flame. The concentration of CO_2 in the air in the room is also increased, with the result that there is increased absorption by CO_2 in the air path between source and spectrometer. The energy distribution pattern in this region is reproduced in figure 3. Comparison with the corresponding trace for a Bunsen burner flame [1] shows both absorption and emission to be more pronounced in the instance of acetylene, in line with a relatively much more rapid and abundant evolution of CO_2 in the burning of C_2H_2.

In the region between 4.8 and 4.9 μ, as shown in figure 3, a structural pattern was observed, which,

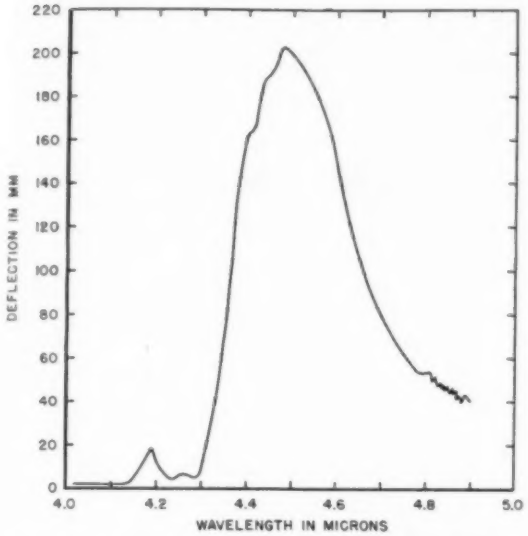

FIGURE 3. *Emission spectrum of the oxyacetylene flame in the region between 4.1 and 4.9μ, showing absorption and emission of* CO_2, *also fine structure attributed to* CO.

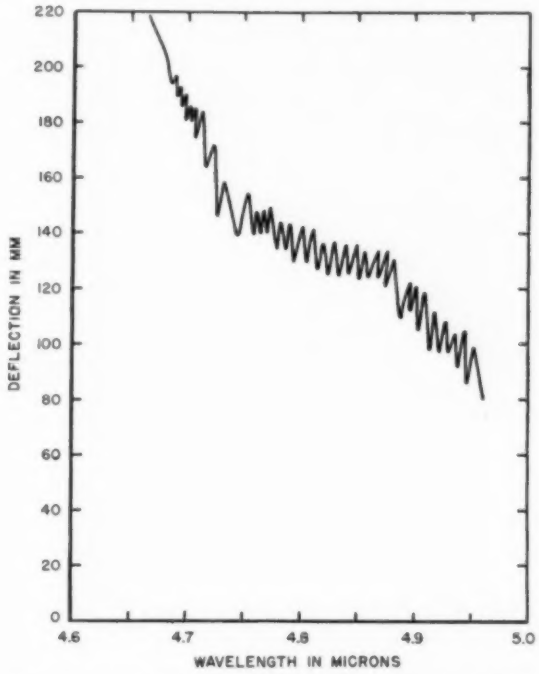

FIGURE 4. *Small-scale reproduction of fine structure pattern, attributed to* CO, *under optimum conditions for observation.*

although not of high contrast with respect to the background energy, exceeded the noise level of the amplifier. On the basis of preliminary observations, it was apparent that this structure might have been produced by variations in the flame intensity, or by the rotational structure originating in another molecule superposed on the portion of the CO_2 band extending into this region. By reducing the oxygen in the mixture, it was found possible to operate the flame in such a manner as to increase the contrast and cause the lines to stand out strongly above the background of the CO_2 emission band. This seemed to eliminate flickering as a cause of the effect. A trace of one of the records is reproduced in figure 4. This record was made under the most satisfactory conditions attained in these experiments. A possible interpretation of this structure, on the basis of the magnitude of the separation of the components and the probable presence of intermediate combustion products, is that it originates in CO, specifically the long wavelength portion of the negative branch of the $1 \rightarrow 0$ band. By comparing the wavelengths of the emission peaks with the absorption data of Lagemann, Nielsen and Dickey [4], it is found that seven, or roughly half of the measured maxima in the interval where reported data permit comparison, agree within experimental error with the absorption lines reported by those authors. This comparison is shown in table 2, which lists the positions of all maxima observed in this work. Possible reasons for disagreement of the other emission maxima are the presence of additional lines from the $2 \rightarrow 1$ band of CO, also the partially superposed $1 \rightarrow 0$ isotope band of $C^{13}O^{16}$, and that there may be considerable structure from high-level transitions of CO_2. All of these causes may be expected to produce shifts in the observed maxima where the resolution is incomplete. A reexamination of the recordings made with the methane flame showed the same structure to be present in the spectrum of burning mixtures. The overlapping of the CO_2 and CO spectra, and the fact that CO burns readily after formation, makes it difficult to observe this structural pattern unless the critical conditions are maintained. The use of a LiF prism, which reaches its highest dispersion in this region, has of course been highly advantageous in the current investigations of flame spectra.

834349—49——3

TABLE 2. *Comparison of data from the spectrum of CO with observed structural features in the flame spectrum of* C_2H_2

Observed rotational structure in the absorption spectrum of CO [4]		Observed emission maxima in the C_2H_2 flame
$C^{12}O^{16}$	$C^{13}O^{16}$	
Wave number cm^{-1}	*Wave number* cm^{-1}	*Wave number* cm^{-1}
P(10) 2103.12	.....	2103.0
P(11) 2099.01	.....	2100.3
.....	.....	2098.1
P(12) 2094.69	$P^{13}(1)$ 2092.35	2094.6
P(13) 2090.56	$P^{13}(2)$ 2088.57	2091.1
P(14) 2086.27	$P^{13}(3)$ 2084.85	2087.2
P(15) 2081.95	$P^{13}(4)$ 2081.12	2082.4
P(16) 2077.57	$P^{13}(5)$ 2077.33	2078.1
P(17) 2073.19	$P^{13}(6)$ 2073.49	2075.1
P(18) 2068.69	$P^{13}(7)$ 2069.52	2070.4
P(19) 2064.31	$P^{13}(8)$ 2065.73	2066.5
P(20) 2059.79	$P^{13}(9)$ 2061.81	2061.8
P(21) 2055.31	$P^{13}(10)$ 2057.81	2058.9
.....	$P^{13}(11)$ 2053.79	2054.6
P(22) 2050.72	$P^{13}(12)$ 2049.75	2051.3
P(23) 2046.14	$P^{13}(13)$ 2045.61	2048.3

III. Conclusions

The discussion of the results of this study of the acetylene flame is concerned with the evaluation of the evidence of emission spectra originating in C_2H_2 itself, and in CO, and OH. The presence of C_2H_2 is indicated by a relatively faint band at 1.52 μ, attributed to the $\nu_1+\nu_3$ vibration, which was not observed in the other flame spectra studied, also by a somewhat more pronounced background of emission in the 3-μ region where the fundamental band is expected to appear. No fine structure was observed in either of these features.

It is concluded that flames of all fuels mixed with high proportions of oxygen, hydrogen, methane, and acetylene emit the spectrum of the free radical OH, because of the appearance of an apparently identical set of five successive emission maxima that agree within experimental error with the positions of a succession of minima in the 2→1 absorption band as computed by Dieke. Support for this conclusion is weakened somewhat by the failure of the adjoining succession of five maxima on the short wavelength side to agree with computed positions in this or other OH series. A possible explanation of this lack of agreement on the basis of superposition of other structural features, mainly those originating in H_2O, will require further observation with improved resolution for confirmation. The excitation of the emission spectrum of CO in the acetylene flame is supported by the presence of a weak band at 2.3 μ, interpreted as a branch of the harmonic band, and by a set of emission maxima on the long wavelength side of the emission band, ν_3 of CO_2, which agree in part with the absorption minima for the CO fundamental. Here again the resolution is insufficient to separate any superposed structures that may cause an apparent displacement of the bands and prevent complete agreement with calculated values. It is to be emphasized that, although the evidence leading to the interpretations given is considered fairly strong, it is not altogether conclusive, so that the interpretations are to be regarded as tentative until the observations can be repeated with higher resolution. Such observations are expected to be undertaken in the near future with a grating spectrometer now rapidly approaching completion.

IV. References

[1] Earle K. Plyler, J. Research NBS **40,** 113 (1948) RP1860.

[2] Earle K. Plyler and Curtis J. Humphreys, J. Research NBS **40,** 449 (1948) RP1890.

[3] Earle K. Plyler, Ralph Stair, and Curtis J. Humphreys, J. Research NBS **38,** 211 (1947) RP1769.

[4] Robert T. Lagemann, Alvin H. Nielsen, and Fred P. Dickey, Phys. Rev. **72,** 284 (1947).

[5] G. H. Dieke, Table of OH bands, private communication.

WASHINGTON, February 8, 1949.

U. S. Department of Commerce
National Bureau of Standards

Research Paper RP1994
Volume 42, June 1949

Part of the Journal of Research of the National Bureau of Standards

Viscosity of Deuterium Oxide and Water in the Range 5° to 125° C

By Robert C. Hardy and Robert L. Cottington

Measurements of the absolute viscosity of deuterium oxide of 99.5 percent purity and of water were made over the range 5° to 125° C. It is estimated that these determinations are accurate within 0.1 percent in relation to the value 1.0050 centipoise for the viscosity of water at 20° C. The work also included determinations of the density of deuterium oxide over the range 90° to 125° C. Values for the viscosity and density of 100-percent deuterium oxide were obtained by linear extrapolations. The ratio of the viscosity of deuterium oxide to that of water at the same temperature was found to be 1.3052 at 5° C. This ratio decreased at a diminishing rate with increase in temperature to a value of 1.1456 at 125° C.

I. Introduction

The work reported here was undertaken to provide accurate data over a wide temperature range. The work was undertaken as two separate projects. The first project covered viscosity measurements with a Bingham viscometer [1] [1] over the range 5° to 95° C. The second project extended the temperature range above the boiling points of water and deuterium oxide, and it was necessary to operate the viscometer under pressure in order to prevent boiling of the test liquids. An Ostwald viscometer was selected for this project as being more readily adaptable to this type of operation.

II. Materials

The distilled water was obtained from a laboratory still of commercial type.

The deuterium oxide was obtained from the Atomic Energy Commission and was said to be of 99.56 mole percent purity. A portion of this material was used as received for the first project. Subsequently, it was learned through tests on other portions that the specific conductance was somewhat higher than for pure water, indicating that the impurities present probably included traces of inorganic salts. Mass-spectrograph analysis indicated the presence of approximately 0.9 mole percent of O^{18} in the oxygen of the material. A sample of distilled water was found to contain approximately 0.2 mole percent of O^{18}. The concentration of O^{17} in the D_2O was slightly higher than in the distilled water.

The material used in the second part of the work was subjected to a simple distillation under reduced pressure, and without boiling, to reduce or eliminate any inorganic impurities. The center fraction, representing 80 to 85 percent of the original volume, was selected for the viscosity measurements. The density of this fraction was found to be 1.10465 $\pm$0.00003 g/ml at 25° C. Calculations based on Longsworth's equation [2] using the numerical coefficients of Voskuyl [3] for the relation between density and mole fraction of D_2O, and corrected for abnormal O^{18} and O^{17} content, indicated that the mole fraction of D in the hydrogen was 99.53 mole percent. Similarly, calculations using the density of the sample as received, i. e., 1.10469 $\pm$0.00003 g/ml at 25° C, indicated that the concentration of D in the hydrogen of the original material was 99.57 mole percent.

III. Work with Bingham Viscometer in the Range 5° to 95° C

The Bingham viscometer [1] used was designed for low-viscosity liquids. The capillary was 12.3 cm long, and its diameter was approximately 0.022

[1] Figures in brackets indicate the literature references at the end of this paper.

cm. The volume of flow was 5.07 cm.[3] With this type of instrument, flow is caused by air pressure applied to one arm of the instrument. The pressure applied was measured with a mercury manometer. It is estimated that the corrected values for pressure causing flow were accurate within ± 0.05 percent.

In calibration tests and in viscosity measurements, times of flow were determined only for flow into the measuring bulb, the walls of which had been previously wetted and allowed to drain. Drainage times were approximately proportional to the viscosity of the liquid. In this way, error due to reduction in effective capacity of the bulb by the film of liquid on its walls was substantially eliminated. The working volume of liquid in this instrument is not highly critical, but it was adjusted at or near the test temperature when required.

Calibration of the Bingham viscometer was based on the usual equation

$$\eta = Cpt - C'\rho/t,$$

in which C and C' are instrumental constants, η is the absolute viscosity of the liquid, p the pressure causing flow, t the time of flow, and ρ is the density of the liquid. By observing the flow time for water at 20° C with several different values for p, data were obtained for evaluating C and C' by use of the usual pt versus $1/t$ plot. In this way, the calibration of the viscometer is made to rest entirely on the value assigned to the viscosity of water at 20° C. The viscosity of water at 20° C was assigned the value 1.0050[2] centipoises.

Test runs with water were made also at 5°, 40°, 60°, 80°, and 95° C to obtain comparative data on the viscosity of water and also to ascertain whether evaporation losses would cause serious error. Clear indications of slight losses by evaporation were observed, but the effects on the viscosity values were not significant.

A single filling of the viscometer with D_2O was used for observations of the flow time at 20°, 5°, 40°, 60°, 80°, and 95° C in the order named. As a check on possible contamination of the D_2O during these observations, the volume of charge as readjusted at room temperature and two runs made at 20° C for comparison with results of the initial runs at this temperature. This comparison indicated that the effect of any contamination was considerably less than the estimated accuracy of the determinations.

With the Bingham viscometer, the density of the liquid is of only minor importance. Values for the density of water were obtained from published data [4]. Data on the density of D_2O at temperatures below 50° C were in substantial agreement with those of Chang and Chien [5]. Values for density at 60°, 80°, and 95° C were obtained by extrapolation.

IV. Work With Ostwald Viscometer in the Range 90° to 125° C

The Ostwald viscometer was specially designed to provide for use of a capillary with "square-cut" ends and to minimize the effect of surface tension. The capillary was about 40 cm long, and its diameter was approximately 0.04 cm. The mean corrected time of flow for 10.31 cm³ of water at 20° C was 1620.13 sec, the hydrostatic head at mean time being 40.2 cm. The instrument was used with equal pressure applied to both arms to prevent boiling of the test liquid. Accurate values for the pressure were not required, and a Bourdon type pressure gage was used.

In this instrument, flow is caused by the hydrostatic pressure of the test liquid and is dependent on the density of the liquid, the volume of charge, and the dimensions of the instrument. The volume of charge was measured at room temperature with a special pipette. Corrections were applied to the observed time of flow to compensate for variations in the volume of charge caused by variations in room temperature and temperature of test.

The density of the D_2O at the test temperature was determined by use of a simple dilatometer that had been calibrated with water. The dilatometer was calibrated and used with an internal air pressure of 35 psi gage to prevent boiling.

For Ostwald type instruments the equation expressing the relation between η, ρ, and t is written

$$\frac{\eta}{\rho} = At - \frac{B}{t},$$

in which A and B are the instrumental constants,

[3] The value 1.005 centipoises has been used for many years at this Bureau as the basis for calibration of viscometers. The more recent value, 1.002 centipoises of Coe and Godfrey [11] has not been used because of its tentative nature, although results thus far obtained by J. F. Swindells in a continuation of their work indicate that the true value is in the neighborhood of 1.002 centipoises. Pending completion of Swindells' work, continued use of the value 1.005 seems desirable.

and the other symbols have the same significance as in eq 1. Determination of the values of the constants was made in the usual way by determining t for water at several temperatures for which η and ρ were known and constructing a Higgins diagram. In both the calibration and use of this instrument, flow times were corrected for the effect of the air column in the receiving arm and to a standard temperature, 20° C, with respect to volume of charge.

Distilled water was used at 20°, 40°, 60°, and 80° C in the calibration of this viscometer. The viscosity of water at 20° C was assigned the value 1.0050 centipoises, and the values for viscosity at the other temperatures were those determined with the Bingham viscometer and reported in table 1.

TABLE 1. *Absolute viscosity*

Temperature	Ordinary water	Deuterium oxide		
		99.53 mole percent	99.57 mole percent	100 mole percent [a]
°C	*Centipoises*	*Centipoises*	*Centipoises*	*Centipoises*
5	1.5230	.....	1.9858	1.9878
20	[b] 1.0050	.....	1.2503	1.2514
40	0.6551	.....	0.7866	0.7872
60	.4679	.....	.5509	.5513
80	.3558	.....	.4138	.4141
90	.3158	0.3656	.....	.3658
95	.2985	.....	.3452	.3454
100	.2830	.3263	.....	.3265
110	.2557	.2939	.....	.2941
120	.2328	.2668	.....	.2669
125	.2227	.2550	.....	.2551
20 [c]	.....	.....	[c] 1.2501	.....

[a] Extrapolated values not corrected for abnormal O^{18} content.
[b] Assigned value used as basis for calibration of instruments.
[c] Check for comparison with initial determination at 20° C to indicate possible extent of contamination.

Test runs were made with water at the higher temperatures and pressures to test the method and apparatus and to obtain comparative data on water at these temperatures. Usually observations at several temperatures were made on each filling, and for several fillings the temperature was returned to its initial value for final observations, which by comparison with the initial observations served as an indication of the possible maximum error (0.05%) due to loss of charge through evaporation.

Most runs were made by using an applied pressure of 35 psi gage. Although it was not anticipated that pressure of this magnitude would have significant effect on the viscosity of water due to air solubility or distortion of the viscometer, this was verified by data obtained in runs at 20° and 80° C at both atmospheric pressure and with an applied pressure of 35 psi. Since the agreement between data obtained under the two pressure conditions was within the experimental accuracy, no effect of pressure was observed.

A single filling of the instrument with D_2O was used for observations at 90°, 100°, 110°, 120°, and 125° C.

In both parts of the work, the temperature of the viscometer was controlled with an oil bath whose temperature was regulated to within approximately ± 0.01 deg for the Bingham viscometer and to within approximately ± 0.02 deg for the Ostwald viscometer.

Temperatures were measured with mercury-in-glass thermometers that had been calibrated in place with a platinum resistance thermometer.

Times of flow were measured with a manually controlled electric timer operating on a specially controlled constant-frequency circuit. It is estimated that time measurements were accurate within ± 0.02 percent.

After the completion of the work with water, the viscometers were cleaned with chromic-acid cleaning solution, washed with distilled water, and dried with a current of dry air.

In all the work with D_2O, a drying tube charged with Drierite was used in the pressure line to protect the D_2O from contamination with water vapor in the compressed air.

V. Results

Values obtained for the absolute viscosity of ordinary water and of deuterium oxide are given in table 1. As no data on the viscosity of D_2O^{18} are available, no correction for abnormal O^{18} content was attempted in the simple linear extrapolation used to obtain the values for D_2O of 100-percent purity with respect to D content.

Ratios of the viscosity of water and of deuterium oxide at various temperatures to the viscosity of water at 20° C are given in table 2. Values for the relative viscosity of water derived from values for absolute viscosity published in International Critical Tables [6] are included in table 2 for comparison. This table also includes values for the

ratio of the viscosity of deuterium oxide at various temperatures to the viscosity of water at the same temperatures. Table 3 contains values for the density of deuterium oxide that were determined at various temperatures in the range 90° to 125° C. Values for the density of 100-percent deuterium oxide, with normal and abnormal O^{18} content were obtained by linear extrapolations based on the assumption that the O^{18} and O^{17} compounds have the same molar volumes as the O^{16} compounds.

TABLE 2. *Relative viscosity*

Temperature	Relative to water at 20° C			Relative to water at t°
	Water		Deuterium oxide, 100 percent [b]	Deuterium oxide, 100 percent [b]
	Authors	ICT [a]		
° C				
5	1.5154	1.5057	1.9779	1.3052
20	1.0000	1.0000	1.2452	1.2452
40	0.6518	0.6480	0.7833	1.2017
60	.4656	.4638	.5485	1.1782
80	.3541	.3539	.4120	1.1637
90	.3142	.3139	.3640	1.1583
95	.2970	.2968	.3437	1.1570
100	.2816	.2815	.3250	1.1538
110	.2544	.254	.2927	1.1504
120	.2316	.230	.2656	1.1467
125	.2216	.....	.2538	1.1456

[a] Derived from values for absolute viscosity published in International Critical Tables [6].

[b] Extrapolated values not corrected for abnormal O^{18} content.

TABLE 3. *Density of deuterium oxide*

Temperature	Deuterium oxide		
	99.53 mole percent	100 percent [a]	100 percent [b]
° C	g/cm³	g/cm³	g/cm³
90	1.0711	1.0716	1.0708
100	1.0533	1.0538	1.0530
110	1.0549	1.0554	1.0547
120	1.0461	1.0466	1.0459
125	1.0416	1.0421	1.0414

[a] With 0.7 mole percent excess O^{18}.

[b] With normal O^{18} content.

VI. Discussion

The values for the absolute viscosity of deuterium oxide given in table 1 are based on the average of three or four determinations of the flow time at each temperature. The spread between the observed flow times at any one temperature was less than 0.1 percent and less than 0.05 percent for observations at 40° C and higher temperatures. One observation at 125° C was discarded because it departed from the mean of four other determinations by 0.12 percent. However, inclusion of this discarded observation would have changed the viscosity value at 125° C by only 0.0001 centipoise.

The limit of possible error of the determined values given in table 1 is believed to be about 0.25 percent in relation to the value 1.0050 centipoise for the viscosity of water at 20° C. The root mean square of the estimated maximum values for the various individual errors involved is 0.1 percent. The extrapolations to obtain values for the viscosity of D_2O of 100-percent purity neglected the effect on viscosity of the abnormal O^{18} and O^{17} content, since no data were available on the effect on viscosity of abnormal amounts of these oxygen isotopes.

Data obtained with both instruments over the entire temperature range are shown graphically in figure 1. It will be noted that the data for D_2O obtained with both instruments fall on one smooth curve. The same is true for the data on water.

However, some irregularities, notably at 95° C, will be noted on figure 2, which shows the variation of relative viscosity, η_t', with temperature. Points representing the results obtained by other investigators are included for comparison.

Only Lewis and MacDonald [7] have reported viscosity values over a range of temperatures. They observed that the relation between temperature and η_t' was approximately linear over the range 5° to 35° C; however, our results indicate an appreciable curvature in the relation in this temperature range. The agreement between their values and the curve representing our results is within the estimated accuracy of their data (0.5%), except at 35° C where their value is 1.0 percent lower than the curve and even a little lower than the present value determined at 40° C.

Taylor and Selwood [8] reported the same value as Lewis and MacDonald for the viscosity of D_2O at 20° C. This value is 0.3 percent higher than that obtained here.

Baker and La Mer [9] and Jones and Fornwalt [10] reported values for the relative viscosity of D_2O at 25° C only. Baker and La Mer's value

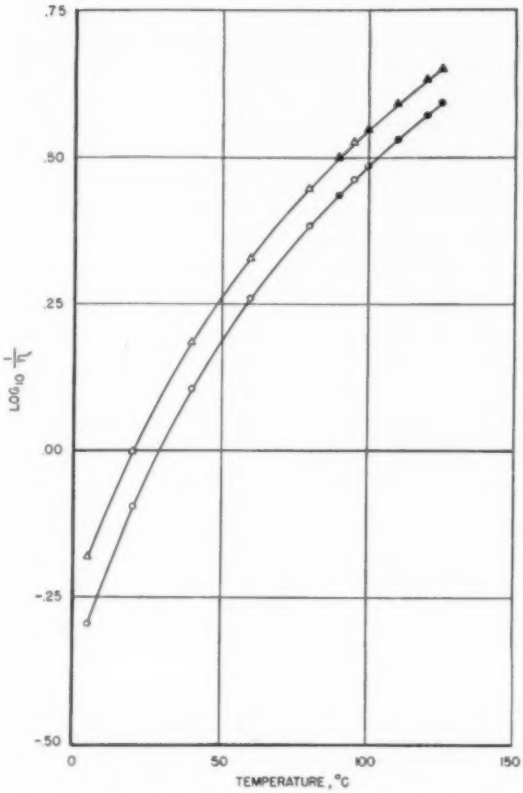

FIGURE 1. *Relation between temperature and logarithm of reciprocal viscosity for deuterium oxide and water, showing consistency of results obtained with the two types of instruments.*

Bingham viscometer: △, water; ○, deuterium oxide. Ostwald viscometer: ▲, water; ●, deuterium oxide.

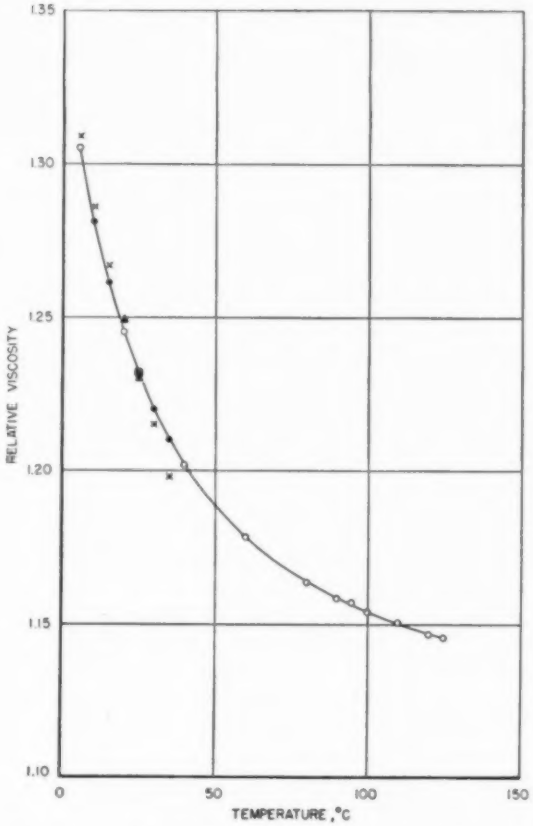

FIGURE 2. *Ratio of viscosity of deuterium oxide to the viscosity of water at the same temperature.*

○, Hardy and Cottington; ●, calculated interpolation; ×, Lewis and MacDonald; △, Taylor and Selwood; □, Baker and Lamer; ▲, Jones and Fornwalt.

agreed with that of Lewis and MacDonald and was only 0.05 percent higher than our curve. However, the value reported by Jones and Fornwalt appears to be the most accurate and is 0.12 percent lower than our curve. Part of this difference between our value and that of Jones and Fornwalt may be due to the abnormal O^{18} content of our sample.

This comparison with published data is shown more accurately in table 4, which contains interpolated values for η_t' at 10°, 15°, 25°, 30°, and 35° C that were calculated from our observed values at 5°, 20°, and 40° C. The interpolated values were obtained by use of the following relations to compute values for the absolute viscosity of D_2O and water at the desired temperatures:

For D_2O

$$\log_{10}\eta = \frac{1301}{930.349+7.8061(t-20)+0.000833(t-20)^2} - 3.30103.$$

For water

$$\log_{10}\eta = \frac{1301}{998.333+8.1855(t-20)+0.00585(t-20)^2} - 3.30103.$$

TABLE 4. *Relative viscosity, η_i'*

Ratio of the viscosity of D_2O to that of water at the same temperature. Comparison with published data.

Temperature	Hardy and Cottington [a]	Lewis and MacDonald, 1933	Taylor and Selwood, 1934	Baker and La Mer, 1935	Jones and Fornwalt, 1936
°C					
5	1.3052	1.309	.....	.....	.....
10	(1.2813)	1.286	.....	.....	.....
15	(1.2615	1.267	.....	.....	.....
20	1.2452	1.249	[b] 1.249	.....	.....
25	[c] (1.2314)	1.232	.....	1.232	1.22886
30	(1.2198)	1.215	.....	.....	.....
35	(1.2100)	1.198	.....	.....	.....
40	1.2017	.....	.....	.....	.....

[a] Values in parenthesis are interpolated.

[b] Derived from their reported value of 12.6 millipoises for absolute viscosity, using the ICT value for viscosity of H_2O, i. e., 1.0087 centipoise.

[c] This value is 0.12% higher than reported by Jones and Fornwalt. This may be due to the abnormally high O^{18} content of our sample.

The values for relative viscosity of water at 5° and 40° C derived from the ICT values are believed to be too low by amounts several times greater than 0.1 percent, the estimated accuracy of the ICT values between 5° and 40° C. The value reported here for 5° C is the mean of the values obtained with the two types of viscometers, i. e., 1.5155 with the Bingham and 1.5153 with the Ostwald. Our value at 40° C confirms the value 0.6518 reported by Coe and Godfrey [11] for the same temperature. The agreement with ICT values at other temperatures is within the estimated accuracy (0.5 to 1.0%) given for the ICT values above 40° C.

Unusual accuracy in determining the density of D_2O was not attempted. The values reported in table 3 are believed to be accurate to 0.0002 g/cm³, or a little better.

VII. Summary

Data are presented on the viscosity of deuterium oxide and water over the temperature range 5° to 125° C, and on the density of deuterium oxide in the range 90° to 125° C. Observations were made on deuterium oxide having more than 99.5 mole percent of D in the hydrogen, and values for the viscosity of deuterium oxide of 100-percent purity with respect to deuterium were obtained by linear extrapolation. The deuterium oxide contained 0.7 mole percent more O^{18} in the oxygen than the laboratory distilled water. The O^{17} concentration also was slightly higher than normal. No correction of the viscosity data was made to compensate for the abnormal content of the heavy oxygen isotopes.

The authors acknowledge the advice and assistance of J. F. Swindells of the Bureau staff in designing the special Ostwald viscometer and in performing part of the work of calibrating both viscometers. The cooperation and assistance of other members of the Bureau staff in supplying information on the composition of the deuterium oxide is acknowledged also. Credit is due the Atomic Energy Commission for financial support of the work.

VIII. References

[1] E. C. Bingham, Fluidity and plasticity, p. 76, fig. 29 (McGraw-Hill Book Co., New York, N. Y., 1922).

[2] L. G. Longsworth, J. Am. Chem. Soc. **59,** 1483 (1937).

[3] I. Kirschenbaum, Atomic Energy Commission Report AECD–1991 (1943).

[4] Smithsonian Physical Tables—Eighth Revised Ed., First Reprint, Table 121 (1934).

[5] Tsing-Lien Chang and Jen-Yan Chien, J. Am. Chem. Soc. **63,** 1709 (1941).

[6] International Critical Tables **5,** 10 (McGraw-Hill Book Co., New York, N. Y., 1929).

[7] Gilbert N. Lewis and Ronald T. MacDonald, J. Am. Chem. Soc. **55,** 4730 (1933).

[8] Hugh S. Taylor and P. W. Selwood, J. Am. Chem. Soc. **56,** 998 (1934).

[9] Weldon N. Baker and Victor K. La Mer, J. Chem. Phys. **3,** 406 (1935).

[10] Grinnell Jones and Holmes J. Fornwalt, J. Chem. Phys. **4,** 30 (1936).

[11] J. R. Coe and T. B. Godfrey, J. App. Phys. **15,** 625 (1944).

WASHINGTON, February 9, 1949.

U. S. Department of Commerce
National Bureau of Standards

Research Paper RP1995
Volume 42, June 1949

Part of the Journal of Research of the National Bureau of Standards

Determination of Efficiency of Microwave Bolometer Mounts from Impedance Data

By David M. Kerns

An impedance method of determining the input-to-bolometer-element power-transfer efficiency of bolometer mounts of the type used in microwave power measurements is formulated, and the theoretical basis of the method is outlined. The method stems from the consideration of the bolometer mount as a transducer. Under certain conditions, which are discussed, this transducer is representable as a two-terminal-pair network, and its parameters can be determined, essentially as in the case of ordinary networks, from observation of input impedance (in waveguide or coaxial line) as a function of load impedance (bolometer resistance). Convenient formulas are given for the calculation of power-transfer efficiency from such impedance data.

I. Introduction

Bolometric methods, employing fine platinum wires or bead thermistors as bolometers, have received wide use in power measurement at microwave and lower frequencies. The bolometer is mounted in a waveguide [1] structure (fig. 1) whose function is to enable the bolometer to absorb radio-frequency power from a source whose output is to be measured. The bolometer is also connected into a direct-current (or low-frequency alternating-current) network whose functions are to detect or measure changes of bolometer resistance, and to supply bias power to the bolometer. Thus radio-frequency power may be measured in terms of the change in bolometer resistance produced by the application of the power to be measured, or it may be measured by the change in bias power required to keep the resistance constant. Both methods are used; [2] the details, however, are not needed for the purpose of this paper, which is concerned only with what may be called the efficiency of bolometer mounts.

Bolometer mounts are ordinarily arranged to present very nearly a reflectionless load to the waveguide to which they are connected. If there is reflection, however, the net radio-frequency input power consists of that corresponding to an incident wave less that corresponding to a reflected wave. Let P_1 denote the net power input to the bolometer mount at a conveniently located terminal surface in the input waveguide. Let P_2 denote the radio-frequency power absorbed by the bolometer element itself. Then the efficiency of the bolometer mount is defined as

$$\eta = P_2/P_1 \tag{1}$$

Since P_2 may be considered to be the useful output, the efficiency is simply the ratio of output power to input power. P_2 is of course less than P_1, the difference being ordinarily accounted for largely by skin-effect losses on the metal surfaces constituting the interior surface of the bolometer mount.

A knowledge of bolometer-mount efficiency is not particularly important if a bolometric instrument is to be used only for relative measurements, or if it is to be used merely as a transfer instrument to be calibrated by some other means. If one is interested in attempting to establish absolute values of power (or of voltage or current in cases

[1] Throughout this paper the term *waveguide* is used in a somewhat general sense, in that two-conductor systems, such as coaxial line, are included within the meaning of the term. It is immaterial to the discussion whether the input waveguide is of a type that does or does not support a principal mode.

[2] See, for example, Technique of microwave measurements **11**, chap. 3 (Radiation Laboratory Series, McGraw-Hill Book Co., New York, N. Y., 1947).

834349—49——4

where these quantities are useful) by means of bolometric measurements, a knowledge of the efficiency of the mount used is important. Nevertheless, it appears that not much work has been done on the determination of the efficiency of bolometer mounts. It has in fact rather generally been assumed that the mount losses could be neglected in routine applications, even when absolute power is at least of nominal interest. But the negligibility of mount losses obviously depends not only on the actual value of the losses, but also upon the accuracy of measurement toward which one is working.

Unfortunately, it is rather difficult to determine the efficiency of a bolometer mount—at least when the determination is based upon power measurements. Comparison of two mounts can at best yield only the ratio of their efficiencies. Direct calorimetric measurements are handicapped by the fact that the powers involved are small, of the order of a few milliwatts, and by the fact that the heating effect of the losses gets distributed throughout a relatively large mass. Calorimetric measurements are somewhat easier to accomplish at higher power levels, but then one has the problem of attenuating the measured level by an accurately known amount down to the level at which bolometers are ordinarily used. The situation is, in short, that accurate measurement of microwave or UHF power at the milliwatt level is a difficult task. Bolometer-mount efficiency, however, is a power ratio—an attenuation, in fact—and does not fundamentally require power measurements for its determination.

The method of determining mount efficiency to be described stems from the consideration of the bolometer mount as a transducer. Under certain conditions, which will be discussed, this transducer becomes a four-pole (representable as a two-terminal-pair network) and its parameters can be determined, essentially as in the case of ordinary networks, from observation of input impedance as a function of load impedance. (In this case the load impedance is varied by varying the bias power supplied to the bolometer.) Once the parameters of the four-pole are found, the power-transfer efficiency can of course be calculated for any desired value of load impedance.

The formulation is based upon field concepts. As is to be expected, the formulas eventually obtained are formally the same as those for the same type of problem in conventional network theory. Thus the more basic portion of the development may be considered as an example of the reduction of what is in detail a problem described by field equations to a problem described by equations of the form of network equations, and the essential concepts and conditions on the basis of which the reduction is accomplished are those that in general underlie the treatment of waveguide and circuit problems by means of network equations. This paper is intended to be reasonably complete and self-contained; however, a much more elaborate discussion of the fundamentals is contained in a previous paper by the author.[3]

II. Formulation of the Method

Consider a bolometer mount, a structure of the general form indicated in figure 1, as a transducer.

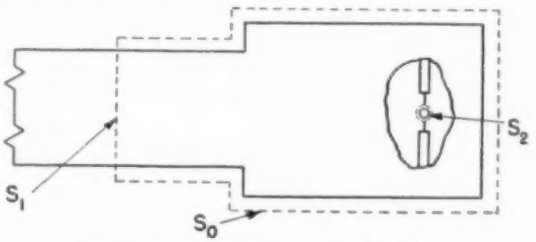

FIGURE 1. *Bolometer mount schematized.*

The terminal surfaces, through which radio-frequency power enters or leaves the system considered, are the surfaces S_1 and S_2. S_1 is a transverse surface in the input waveguide. This waveguide may be of any type or cross section (including, in particular, coaxial line); it is necessary merely that there exist a section that may be considered uniform and lossless. The terminal surface S_2 encloses the region occupied by the bolometer element. This surface is drawn as shown in figure 2, a, or 2, b, for a bolometer consisting of a fine wire or of a bead thermistor, respectively. S_2 is thus pierced by conductors that carry not only radio-frequency current but also bias current. (The bias current comes into consideration only insofar as it serves to establish the operating resistance of the bolometer.) If, as is ordinarily the case, the electromagnetic field

[3] David M. Kerns, Basis of the application of network equations to waveguide problems, J. Research NBS, **42**, 515 (1949) RP1980. (This reference is of a general nature and contains no discussion specifically directed to the bolometer problem).

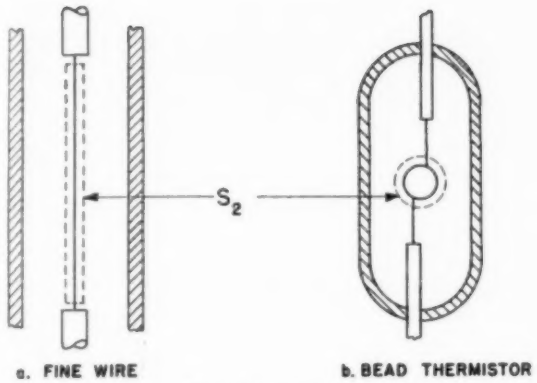

FIGURE 2. *Illustrating terminal surface S_2.*
Cross-hatching indicates protective dielectric enclosure.

of the transducer is effectively limited to a finite region by sufficiently thick metal walls, the interior of the transducer is (by definition) the region R bounded by the surface $S_0+S_1+S_2$, as illustrated in figure 1. S_0 is drawn outside the metallic walls of the structure, and the field may be assumed to be zero on this surface. It is, however, by no means necessary to assume that the transducer field is confined to a finite region. If the bolometer mount does not form a closed metallic structure, so that the electromagnetic field can extend to infinity, the surface S_0 and the region R would be chosen somewhat differently. But the subsequent argument would not be altered, so that it is not necessary to consider this case explicitly.

The whole structure within R, which may include auxiliary tuning devices, joints, bends, etc., may be counted simply as a (decidedly) nonhomogeneous medium. This medium is to be linear, i. e., such that Maxwell's equations become linear equations, and is to contain no sources. The electromagnetic field within R is then uniquely determined by the values of the tangential components of either the electric or the magnetic field on the boundary of R. (It is sufficient to consider only the case in which all field quantities vary harmonically with time at a given frequency, ω. The time dependence will be represented implicitly by a factor $\exp(j\omega t)$.) On the surface S_0, the boundary condition is simply that the field shall vanish; the fields on S_1 and S_2 will be specified in the manner outlined in the following two paragraphs.

In practice, only one waveguide mode need be considered in specifying the field on the waveguide terminal-surface S_1. The transverse components $\boldsymbol{E}_1$, $\boldsymbol{H}_1$ of the field on this surface may then be written

$$\left.\begin{aligned}\boldsymbol{E}_1&=V_1\boldsymbol{E}_{01},\\ \boldsymbol{H}_1&=I_1\boldsymbol{H}_{01},\end{aligned}\right\} \tag{2}$$

where $\boldsymbol{E}_{01}$, $\boldsymbol{H}_{01}$ are suitable two-component vector functions of coordinates in the transverse plane. V_1, I_1, are numbers, in general complex, which are respectively linear measures of $\boldsymbol{E}_1$, $\boldsymbol{H}_1$. It is convenient to choose $\boldsymbol{E}_{01}$, $\boldsymbol{H}_{01}$ as that field that corresponds to a waveguide field consisting solely of an incident wave, of unit power. The integral of the complex Poynting's vector $\frac{1}{2}(\boldsymbol{E}_{01}\times\boldsymbol{H}_{01}^*)$ taken over the surface S_1 becomes [4]

$$\tfrac{1}{2}\int_{S_1}\boldsymbol{E}_{01}\times\boldsymbol{H}_{01}^*\cdot\boldsymbol{n}dS=1\,\text{watt}, \tag{3}$$

where $\boldsymbol{n}$ is the unit normal vector on S_1 directed into the transducer. The complex power input to the transducer at terminal surface S_1 is then, for arbitrary values of V_1, I_1,

$$W_1=\tfrac{1}{2}\int_{S_1}\boldsymbol{E}_1\times\boldsymbol{H}_1^*\cdot\boldsymbol{n}dS=V_1I_1^*. \tag{4}$$

The looking-in impedance of the field on S_1 is defined as the ratio

$$z=V_1/I_1. \tag{5}$$

This impedance, which will be called the input impedance, can be determined by means of standing-wave measurements in the input waveguide.

It is assumed that the tangential components of the field on the surface S_2, which encloses the bolometer element, can be represented in the form 2

$$\left.\begin{aligned}\boldsymbol{E}_2&=V_2\boldsymbol{E}_{02},\\ \boldsymbol{H}_2&=I_2\boldsymbol{H}_{02},\end{aligned}\right\} \tag{6}$$

where $\boldsymbol{E}_{02}$, $\boldsymbol{H}_{02}$ denote suitable vector functions of coordinates designating points on S_2. The assumption 6 is justifiable if, in particular, the condition $kd \ll 1$ is satisfied, where d is a representative linear dimension of the region enclosed by S_2, and k is the wave-number $\omega\sqrt{\mu\epsilon}$ in the

[4] The rationalized meter-kilogram-second system of units is used.

medium (of permeability μ, dielectric constant ϵ) immediately surrounding the bolometer element.[5] For sufficiently small values of kd, equations of the form 6 will hold, with V_2 and I_2 equal (or proportional) to conventional voltage and current, respectively, at the bolometer terminals. Existence of voltage and current, however, is a sufficient but not a necessary condition. Validity of eq 6 insures formal validity of the method being set up; existence of voltage and current on S_2 is not essential in this respect (any more than existence of voltage and current on S_1 is essential). But for application to practical cases, the most favorable condition for knowing that eq 6 will hold to a good approximation occurs when voltage and current do in fact exist to a good approximation.

It is convenient to assume that $\boldsymbol{E}_{02}$, $\boldsymbol{H}_{02}$ satisfy the normalizing condition

$$\tfrac{1}{2}\int_{S_2} \boldsymbol{E}_{02}\times\boldsymbol{H}_{02}^{*}\cdot\boldsymbol{n}dS=1 \text{ watt},$$

where $\boldsymbol{n}$ is here the unit normal on S_2 directed into the transducer. The complex power input to the transducer at terminal surface S_2 is then

$$W_2=\tfrac{1}{2}\int_{S_2} \boldsymbol{E}_2\times\boldsymbol{H}_2^{*}\cdot\boldsymbol{n}dS=V_2I_2^{*}. \qquad (7)$$

The looking-in impedance on S_2 is defined as the ratio V_2/I_2; the load impedance, w, is defined as the negative of the same ratio:

$$w=-V_2/I_2. \qquad (8)$$

It is essential for the practical application of the method being formulated that the load impedance be known and variable through known (but not necessarily prescribed) values. The load impedance certainly can be varied by varying the bias power and hence the direct-current resistance of the bolometer; since the load impedance cannot be directly measured (except perhaps at sufficiently low frequencies), the essential problem is to relate it to the direct-current resistance in an adequate fashion. If, in addition to the previous condition $kd\ll 1$, the skin-depth $\sqrt{2/\mu\omega\sigma}$ (permeability μ, conductivity σ) is not less than the diameter of wire for a fine-wire bolometer or not less than bead-diameter for a bead thermistor[5] it is reasonable to expect the radio-frequency load impedance to be approximately equal to the direct-current resistance of the bolometer. The assumption of this equality is equivalent to the assumption that the current distribution in the bolometer is substantially independent of frequency from zero up to the radio frequency considered.[7] When the above-mentioned conditions are fulfilled, the use of the value of the direct-current resistance as an approximation to the value of the load impedance naturally suggests itself. This approximation is favored by the following facts (to be demonstrated later): (a) When the angle of the load impedance is considered to be a small quantity of the first order, the error in the determination of power-transfer efficiency caused by neglecting the angle and using real values for the load impedance tends to be small of the second order; (b) no error in the determination of efficiency is caused by the use of an arbitrary constant real multiple of the load impedance in place of the load impedance itself—the magnitude of the load impedance may indeed remain undefined to the extent of a constant real factor. This discussion outlines what appear to be the principal factors involved in judging the usefulness of the type of approximation considered.

The bolometer mount, as a transducer, is characterized by the relations that it imposes upon its four terminal variables V_1, I_1, V_2, I_2. Precisely two such relations must exist, since, by the uniqueness theorem mentioned above, the transducer field is determined by the boundary conditions, which in turn are fixed by fixing two of the four terminal variables. Since Maxwell's equations are, by hypothesis, linear and homogeneous in the interior of the transducer, it follows that the relations among V_1, I_1, V_2, I_2 must also be linear and homogeneous. The transducer is thus a linear, source-free four-pole, and its equations may be written

$$\left.\begin{aligned} V_1&=Z_{11}I_1+Z_{12}I_2,\\ V_2&=Z_{21}I_1+Z_{22}I_2.\end{aligned}\right\} \qquad (9)$$

[5] Typical dimensions for a platinum-wire bolometer are roughly 0.00015 cm. in diameter by 0.25 cm. in length; a typical bead thermistor has a bead diameter of roughly 0.05 cm. At a frequency of 10,000 Mc/s, the value of k for air is approximately 2.0/cm.

[6] For bolometers of the materials and dimensions mentioned in footnote 5, the skin depth becomes comparable to the respective dimensions in the two cases for frequencies in the neighborhood of 10,000 Mc/s.

[7] A condition of this kind is also important in assuring that radio-frequency power and direct-current power have equivalent heating effects in a bolometer. This question is of course basic in the measurement of absolute values of power by the bolometric method.

The Z's are constants in that they do not depend upon V's and I's, but they of course do depend upon frequency. Equation 9 can be interpreted and could be derived on the basis of the following remarks. If, for example, the boundary conditions

$$\boldsymbol{H}_1=0,\ \boldsymbol{H}_2=I_2\boldsymbol{H}_{02},$$

are prescribed, the corresponding field is determined and is proportional to I_2. Thus, in particular, the corresponding $\boldsymbol{E}_1$ and $\boldsymbol{E}_2$ are proportional to I_2, so that V_1 and V_2 are proportional to I_2, the factors of proportionality being Z_{12} and Z_{22}, respectively. The interpretation with $I_1\neq 0$ and $I_2=0$ is similar; eq 9 expresses the general case, with I_1 and I_2 both different from zero.

For the present purpose it is expedient to write equation 9 in a different form, viz,

$$\left.\begin{aligned} V_1&=aV_2+b\bar{I}_2,\\ I_1&=cV_2+d\bar{I}_2,\end{aligned}\right\} \tag{10}$$

where $\bar{I}_2=-I_2$ is used for convenience. The new parameters a, b, c, d are of course related in a simple manner to the Z's appearing in eq 9. These relations will not be written down, since they will not be needed explicity.

Under the assumptions that have been made, the reciprocity condition will apply.[8] Reciprocity must be assumed on theoretical grounds in the present problem, since it is not possible to make radio-frequency measurements at both ends of the transducer. The expression of the reciprocity condition is that $Z_{12}=Z_{21}$, or, equivalently, that the determinant of the coefficients in eq 10 is equal to unity:

$$ad-bc=1. \tag{11}$$

This equation, together with three further equations that are determined by measurement, provides the necessary number of equations to determine the four parameters a, b, c, d.

In accordance with eq 10, input impedance z is given as a function of load impedance w by a so-called linear fractional transformation,

$$z=\frac{aw+b}{cw+d}. \tag{12}$$

[8] A reciprocity theorem in a form adapted to the present application is derived in the reference in footnote 3.

It is noted that this equation may be written in the form

$$wa+b-wzc-zd=0. \tag{12a}$$

Suppose that, for any three distinct values of load impedance w_1, w_2, w_3, the corresponding values of input impedance z_1, z_2, z_3 are measured. Then, apart from a common constant multiplier, the values of a, b, c, d are determined by three simultaneous equations of the type 12, which may be written

$$\left.\begin{aligned} w_1a+b-w_1z_1c-z_1d&=0,\\ w_2a+b-w_2z_2c-z_2d&=0,\\ w_3a+b-w_3z_3c-z_3d&=0.\end{aligned}\right\} \tag{13}$$

If now these equations are solved by Cramer's rule for three of the parameters, say a, b, c, in terms of the remaining one, and if the resulting expressions are used to eliminate a, b, c, d from eq 12a, it may be seen that the final result is expressed by

$$\begin{vmatrix} w & 1 & wz & z\\ w_1 & 1 & w_1z_1 & z_1\\ w_2 & 1 & w_2z_2 & z_2\\ w_3 & 1 & w_3z_3 & z_3\end{vmatrix}=0. \tag{14}$$

(This equation may indeed be written down directly, by recognizing that it is the necessary condition that the system of *four* equations, consisting of eq 13 and 12a, shall form a compatible system for values of a, b, c, d not all zero). Equation 14 gives the relation between general values of z and w, as determined by three pairs of measured values of z and w. The equation may be reduced to

$$\frac{(z-z_3)(z_2-z_1)}{(z-z_1)(z_3-z_2)}=\frac{(w-w_3)(w_2-w_1)}{(w-w_1)(w_3-w_2)}. \tag{15}$$

It should be observed that there exists a transformation of the form 12, determined by eq 14 or 15, which will transform any three given distinct w-values into *any* three given z-values. Thus, in order to obtain a check on the consistency of experimental data, as well as on the validity of the method itself, it is necessary to observe more than three pairs of corresponding values of z and w, and to note whether all the data are represented by a transformation determined by just three pairs

of corresponding values. A check of this kind does not directly check the validity of the reciprocity condition, since the transformation of w depends only on the ratios of the values of a, b, c, d. But the reciprocity theorem applies rigorously, provided merely that the form of the description of the terminal fields (eq 2 and 6) is valid. Equation 12 is a rather direct consequence of eq 2 and 6; insofar as a verification of the existence of an equation of the form of eq 12 verifies the basic eq 2 and 6, it at the same time verifies the applicability of the reciprocity theorem.

Explicit formulas for the values of a, b, c, d will now be obtained. As an abbreviation let

$$\gamma=\frac{(w_2-w_1)(z_2-z_2)}{(z_2-z_1)(w_3-w_2)}$$

and solve eq 15 for z:

$$z=\frac{(z_3-\gamma z_1)w+(\gamma z_1 w_3-z_3 w_1)}{(1-\gamma)w+(\gamma w_3-w_1)}.$$

By comparison with eq 12

$$\left.\begin{aligned} a&=\alpha(z_3-\gamma z_1),\ b=\alpha(\gamma z_1 w_3-z_3 w_1),\\ c&=\alpha(1-\gamma),\quad d=\alpha(\gamma w_3-w_1),\end{aligned}\right\} \tag{16}$$

where α is a constant that must be determined with the aid of the reciprocity condition 11. This condition yields

$$\left.\begin{aligned} ad-bc&=\alpha^2\gamma(w_3-w_1)(z_3-z_1)=1,\\ \alpha&=[\gamma(w_3-w_1)(z_3-z_1)]^{-\frac{1}{2}}.\end{aligned}\right\} \tag{17}$$

Equations 16 and 17 together determine the values of a, b, c, d corresponding to the measured pairs of values of z and w.

Once a, b, c, d are known for a given bolometer mount, the power-transfer efficiency for a given load impedance can easily be calculated. By using the four-pole equations in the form 10, with load impedance w_0, one finds

$$V_1=(a+b/w_0)V_2,$$

$$I_1=(cw_0+d)\overline{I}_2.$$

Hence the complex power input W_1 and the complex power output $\overline{W}_2(=-W_2)$ are related by

$$W_1=(a+b/w_0)(cw_0+d)^*\overline{W}_2.$$

Let $(a+b/w_0)(cw_0+d)^*=N\exp(j\theta)$, with N and θ real; and let $\overline{W}_2=|W_2|\exp(j\phi)$ (ϕ is the angle of the load impedance w_0). Then the efficiency η_0 is

$$\eta_0=\frac{Re(\overline{W}_2)}{Re(W_1)}=\frac{\cos\phi}{N\cos(\theta+\phi)}. \tag{18}$$

On the basis of the foregoing formulas, the two supplementary facts invoked in the discussion of load impedance may be demonstrated. The formulas 16, 17, 18 enable one to calculate the parameters a, b, c, d and the efficiency η_0 with load w_0 for a four-pole that transforms w_i into z_i ($i=1, 2, 3$). Suppose that the load impedance is erroneously assumed to be $w'=m^2w$, where m^2 is a constant, and that the parameters a', b', c', d' and the efficiency η_0' with load impedance $w_0'=m^2w_0$ are calculated for a fictitious four-pole that transforms $w_i'=m^2w_i$ into z_i ($i=1, 2, 3$). By using eq 16 and 17, one obtains

$$a'=a/m,\qquad b'=mb,$$

$$c'=c/m,\qquad d'=md.$$

Defining δ by writing the constant m^2 in the form $m^2=|m|^2\exp(j\delta)$, and using eq 18, one obtains

$$\eta_0'\cos\phi=\eta_0\cos\phi', \tag{19}$$

where $\phi'=\phi/+\delta$ is the angle of w_0'. Since $|m|$ does not enter into eq 19, any constant real multiple of the load impedance may be used in place of the load impedance itself without affecting the calculated efficiency η_0'. If w_0' is real and ϕ is small,

$$\eta_0'=\eta_0/\cos\phi$$

$$\cong\eta_0(1+\phi^2/2).$$

Hence, under the stated conditions, the difference $\eta_0'-\eta_0$ is of the second order (and is positive). Thus the previous statements (b) and (a) are proved.

A bolometer mount (which may in particular include auxiliary tuning equipment in addition to the mount proper) is preferably and frequently arranged so that, with the bolometer at its desired operating resistance, there is substantially no reflected wave at the waveguide input. The corresponding value of input impedance is unity, according to the choice of an arbitrary real factor tacitly made in setting up the definitions of V_1, I_1

(eq 2, and 3). Further, when the load impedance is considered real, the arbitrary factor contained in this quantity may be chosen so that the normal operating load impedance is also represented by the value unity. These two conditions lead to useful, simplified formulas for the calculation of efficiency. Since input impedance $z=1$ corresponds to load impedance $w=1$, the parameters a, b, c, d must satisfy the relation

$$a+b=c+d.$$

Thus the efficiency for load impedance $w=1$, obtained by the appropriate specialization of 18, is given by

$$1/\eta=N=|a+b|^2=|c+d|^2. \tag{20}$$

The efficiency can of course be expressed directly in terms of w_i, z_i $(i=1, 2, 3)$, so that efficiency may be calculated without first calculating the four-pole parameters. It is convenient to incorporate the condition that $w=1$ is transformed into $z=1$ by taking w_3, z_3, say, as 1, 1. Then, by using eq 16 and 17 and the associated definition of γ to evaluate $|c+d|^2$, it is readily found that

$$\eta=\left|\frac{(1-z_1)(1-z_2)(w_2-w_1)}{(1-w_1)(1-w_2)(z_2-z_1)}\right|. \tag{21}$$

Although eq 20 and 21 are useful for the purpose intended, it should be remembered that they are based upon special conditions.

A number of measurements have been made, on the basis of the method described, at frequencies in the range 300 to 3,000 Mc/s on bolometer mounts having coaxial-line inputs and at approximately 9,000 Mc/s on mounts having rectangular-waveguide inputs. Values of efficiency calculated from the data range from 0.7 to 0.95 for different mounts, which included auxiliary tuning equipment in all cases and additional components in some cases. In all measurements made so far, it has been found that for suitably located input terminal surfaces, the four-pole could be represented in terms of real parameters. In the 9,000-Mc measurements, bolometers of the types and dimensions mentioned in footnote 5 were used, so that a moderate test of the approximations that have been discussed was provided. It was found that an equation of the form 12 represents these experimental data rather well.

The author is indebted to Harold Lyons, Chief of the Microwave Standards Section, National Bureau of Standards, for the opportunity to do this work and for encouragement in the preparation of this paper.

Washington, February 18, 1949.

U. S. Department of Commerce
National Bureau of Standards

Research Paper RP1996
Volume 42, June 1949

Part of the Journal of Research of the National Bureau of Standards

Ultraviolet Absorption Spectra of Seven Substituted Benzenes

By Ralph Stair

The ultraviolet absorption spectra of seven substituted benzenes have been measured in the region of 220 to 300 millimicrons. The substances were *n*-, *iso*-, *sec*-, and *tert*-butylbenzene and 1,2-, 1,3-, and 1,4-diethylbenzene. The wavelengths (also frequencies in centimeters^{-1}) are shown for the absorption bands for each substance. Spectral absorbancy curves are given for the same concentration in each case. The hydrocarbons were NBS Standard Samples prepared in connection with American Petroleum Research Project 6 and were highly purified in the Chemistry Division of this Bureau. These spectral data should be of value in chemical analysis in the field of ultraviolet absorption spectroscopy.

The measurements were made with a Beckman quartz spectrophotometer on 1-centimeter cells of the hydrocarbons in a solution of isooctane (2,2,4-trimethylpentane).

I. Introduction

This work is an extension of the contribution [1] [1] of the radiometry laboratory of this Bureau in the cooperative research program with the American Petroleum Institute Research Project 44 in the study of the absorption spectra of the constituents of petroleum that have been extensively purified. This report deals with the liquid phase of two series of compounds, butylbenzenes and diethylbenzenes, that are closely related and that have significant selective absorption in the ultraviolet region between 220 and 280 mμ.

No attempt has been made, in this report, to give a detailed theoretical interpretation of the structural features of the observed spectra. Primary emphasis has been placed on the precise mapping of these features in order to make available reference data [5] for analytical purposes. Particular attention is called to the similarities between these spectra of closely related compounds and to the small displacements of analogous features associated with the substitution of different chemical groups in the benzene structure.

There is within the published literature a vast amount of empirical data on the spectra of complex molecules—especially in the liquid phase—and it has been fairly well established that the general appearance and intensity of an ultraviolet absorption spectrum depend upon the nature of the electronic states between which the electronic transition takes place. Each transition is presumed to be associated with a characteristic vibrational structure of the molecule, which is fundamentally different for "allowed" and "forbidden" transitions [6, 7]. Nevertheless, the interpretation of the spectra is often quite difficult because of lack of complete knowledge of the vibrations of the molecule in the ground state, and because in many cases bands can be interpreted in different ways, resulting in an ambiguity that makes such an interpretation meaningless [8] and confusing to other workers in the field.

Probably more is known about the structure of benzene and some of the simple benzene derivatives than any other polyatomic molecules. In any case, benzene appears to be unique in a number of characteristics and has undergone many investigations in the liquid, vapor, and solid phases by investigators in the ultraviolet and infrared, as well as for Raman and fluorescence spectra for both the regular and the deutero-substituted material.

[1] Figures in brackets indicate the literature references at the end of this paper.

II. Instrument and Method of Measurement

A Beckman quartz-spectrophotometer [2, 3] was employed, without modification, except that it had been specially supplied with a "blue sensitive" phototube in an envelope of Corning 9740 glass. By using a hydrogen lamp in an envelope of similar glass, measurements were possible down to 200 mμ.

In this spectrophotometer the photometric ("density," equivalent to absorbancy) scale is based on electrical principles, in that the photoelectric current through a load resistor produces a voltage drop that is balanced by a potentiometer, thus giving a null reading for each condition of balance. To make this null setting possible, any voltage unbalance is electronically amplified and impressed across the terminals of a sensitive direct-current milliammeter. The precision of the instrument thus becomes largely a function of the linearity of the potentiometer circuits and the irradiation-current characteristic of the vacuum caesium-antimony silver phototube employed. Since the operation of the instrument is based on these principles and conditions, a high degree of precision and accuracy may be expected when care is taken in its use.

In this work the hydrocarbons were examined in the liquid phase. Five concentrations of each material were employed, and the absorbancy observed at intervals of 0,5 to 1.0 mμ throughout the range from 220 to about 280 mμ for all values of absorbancy less than about 1.0.

The concentration of the hydrocarbon was determined by carefully weighing about 0.5 g of the pure material and then diluting it in isooctane (2,2,4-trimethylpentane). For example, to obtain the 10 g/liter solution the procedure was as follows: First a 50 ml-flask containing a few cubic centimeters of isooctane was placed in the balance and carefully weighed. Then a 0.5-g weight was placed on the opposite pan and the hydrocarbon carefully added (in small drops) until the amount slightly exceeded the required 0.5 g. Next, a careful balance was obtained to determine the exact amount of hydrocarbons added—for example, 0.503 g. Finally, the flask was filled with isooctane to the 50 ml mark, after which an additional 0.3 ml was added to give the total of 50.3 ml to produce a 10 g/liter solution. The other concentrations were simply obtained by diluting samples of the 10 g/liter solution. All operations were performed at room temperature, with the flasks kept "stopped" to prevent errors due to selective evaporation. The prepared samples were kept in a refrigerator until immediately preceding the filling of the absorption cells.

The reflection loss from the absorption-cell windows and the possible absorption by the isooctane solution were annulled by using a comparison cell filled only with isooctane taken from the same container as that employed in preparing the hydrocarbon solutions. Thus the data recorded here are the specific absorbancies of the concentrations of the hydrocarbons employed.

All of the substances that were measured were obtained from F. D. Rossini of the Chemistry Division of this Bureau. They were purified under his direction in connection with the American Petroleum Institute Research Project No. 6. The substances studied and the amount of impurity in each one is given in table 1 [4]. The absorption-spectra data on the butylbenzenes and diethylbenzenes have been made a part of the catalog of ultraviolet spectrograms of the American Petroleum Institute Research Project No. 44 [16].

TABLE 1. *Purity of compounds*

Substance	Standard Sample number	Amount of impurity
		Mole percent
Benzene	210	0.03±0.02
1,2-Diethylbenzene	523	.05±0.03
1,3-Diethylbenzene	524	.07±0.04
1,4-Diethylbenzene	525	.07±0.02
n-Butylbenzene	501	.12±0.08
Isobutylbenzene	502	.13±0.09
sec-Butylbenzene	503	.12±0.06
tert-Butylbenzene	504	.06±0.03
Toluene	211	.04±0.02

III. Results and Discussion

The ultraviolet spectral absorbancies of each of the seven substituted benzenes were measured at room temperature in solutions having concentrations of 10.0, 1.0, 0.5, 0.2, and 0.1 g/liter (all for a 1-cm cell length). In all cases the results for the different concentrations were in close agreement with Beer's law, indicating that for these hydrocarbons no change in chemical or physical constitution occurs as the result of association or

interaction upon placing them in an isooctane solution. It was therefore felt unnecessary to display in the illustrations and tables data for more than one concentration (that for 0.5 g/liter), since any other values can be calculated from the recorded data in accordance with Beer's law. The spectral absorbancy data for a concentration of 0.5 g/liter were chosen for purposes of illustration because, in general, they were within the absorption range (specific absorbancy 0.2 to 0.8) most suitable for analysis considerations (see figs. 1 and 2 and tables 2 and 3).

The analysis of the ultraviolet absorption spectrum of benzene [10] has shown the vibrational structure to be in agreement with the selection rules for the forbidden electronic transition $A_{1g} \rightarrow B_{2u}$. It is held that this transition is rendered possible through the distortion of the benzene molecule by E_g^+ vibrations. Each of the eight absorption bands (see fig. 1) results from a series of more or less superimposed lines or bands. Sponer, et. al [10] list eight numerical equations principally in terms of the 0,0 band frequency (38,089 cm^{-1}), and the totally symmetrical carbon vibrations of 992 cm^{-1} and 923 cm^{-1} belonging to the ground and upper states, respectively, of the benzene molecule, which define the positions of the integral parts of these absorption bands (in the vapor state). The uniform spacing of 923 cm^{-1} of the principal component (the A series) of these bands is indicative of the important part played by the totally symmetrical vibrations of the benzene molecule in the excited state.

When a substitution has been made for one or more of the H atoms of the benzene ring, the symmetry is changed from the type D_{6h} to another, depending upon the particular substituent. Often the substituent, as is the case in the present work, contains groups such as CH, CH_2, CH_3, which have mobile electrons that can resonate or migrate into the benzene ring and thus produce a continuum or other special characteristic in the absorption spectrum.

All of the substituted benzenes herein reported

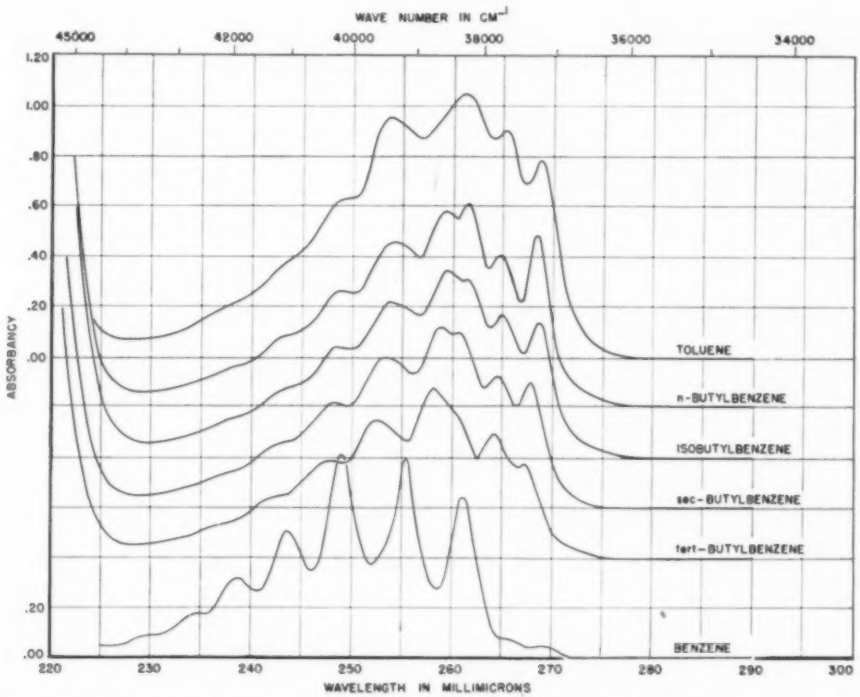

FIGURE 1. *Spectral absorbancies of benzene, toluene, and the four butylbenzenes, all for a concentration of 0.5 g/liter, cell thickness 1.000 cm.*

Although the ordinates are displaced for the different curves, all are reduced to the same scale.

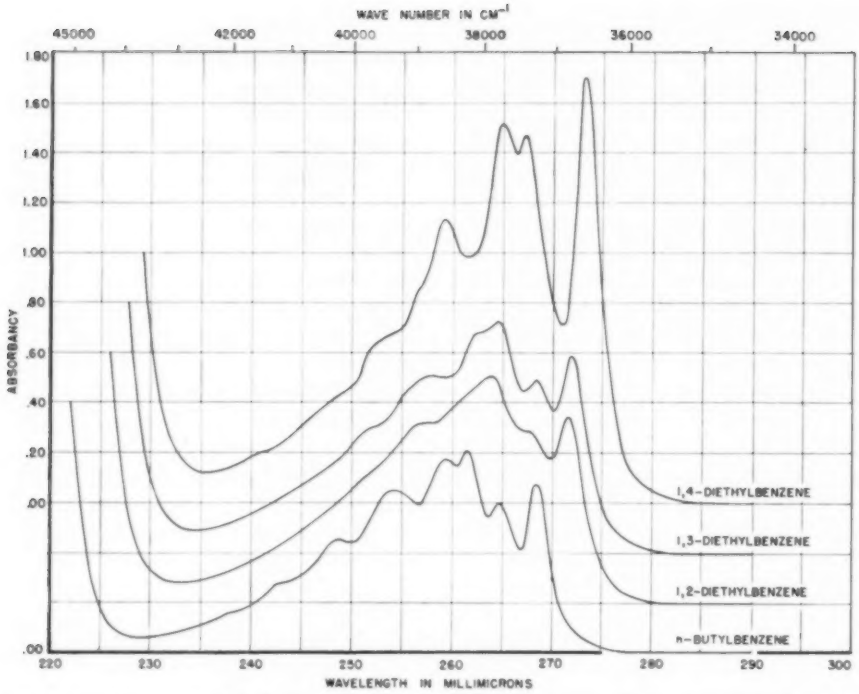

FIGURE 2. *Spectral absorbancies of n-butylbenzene and the three diethylbenzenes, all for a concentration of 0.5 g/liter, cell thickness 1.000 cm.*

Although the ordinates are displaced for the different curves, all are reduced to the same scale.

have similar absorption characteristics in the ultraviolet. In all cases the spectra are shifted nearer to the visible than that for benzene. Also it appears that all the materials have a double set of spectra [12, 13]. One of these corresponds to the *A* series in benzene. The other (denoted as *M* series below) is probably the result of electron migration or other change in the symmetry of the molecule, since it does not occur within a frequency range to be associated with any of the eight series for benzene. Since a major portion of the spectra of all of these substituted benzenes is carried over from benzene, it appears that the mechanism that brought the benzene spectrum into existence remains relatively important. Furthermore, since the carbon atoms enter into the important vibrations responsible for the benzene spectrum the benzene ring must undergo only slight perturbations for the butyl- and diethyl-substitutions. The general shift of the spectra toward longer wavelengths (lower frequencies) is indicative of slight spatial increases between the carbon atoms in the ring structure and to the increase in mass of the substituted molecule.

The spectrum of liquid *n*-butylbenzene at room temperature (about 24° C) is shown in both figures 1 and 2. It is apparently composed of two series of bands, designated *A* and *M* in this report. The *A* series, presumably corresponding to the *A* series in benzene, has its first band located at approximately 37,780 cm^{-1} (see table 3) with a second member spaced at an interval of about 770 cm^{-1} to higher frequencies. The *M* series has a 0,0 band at a frequency of about 37,240 cm^{-1} with a second member spaced at an interval of about 990 cm^{-1} toward the higher frequencies. Only the first two pairs of bands are resolved, since they approach each other toward shorter wavelengths and are no doubt further complicated through overlapping of spectra from weaker series, band splitting, rotational effects, etc. The ratio of the intensities of the *M* to the *A* bands appears to decrease with frequency.

For comparative purposes the absorption spec-

tra of the four butylbenzenes are placed together with those for liquid benzene and toluene in figure 1. The marked similarity between the four butylbenzenes and toluene is impressive. Whereas the spectra are similar, their differences are real and easily measured. In general there is a progressive decrease in absorbancy in the order; *n-*, *iso-*, *sec-*, *tert*-butylbenzene. It is interesting to note the gradual shift in the position of the important absorption bands to higher frequencies in progressing toward the more complicated molecules in this series of *mono*-substituted benzenes from the simple toluene to *tert*-butylbenzene. In some respects the absorption spectrum of *tert*-butylbenzene appears to be more like that of benzene than that of the others of this group.

The spectra of the 1,2-, 1,3-, and 1,4-diethyl-

TABLE 2. *Values of spectral ultraviolet absorbancy for a 0.5-g/liter solution of the seven substituted benzenes, cell thickness 1.000 cm*

Wavelength	*n*-Butylbenzene	Isobutylbenzene	*sec*-Butylbenzene	*tert*-Butylbenzene	1,2-Diethylbenzene	1,3-Diethylbenzene	1,4-Diethylbenzene
mμ							
222	0.990	.....	0.717	0.582	.....	.....	.....
224	.317	0.418	.242	.198	.....	.....	.....
226	.111	.138	.087	.079	0.960	.....	.....
228	.063	.066	.052	.053	.308	0.866	.....
230	.062	.058	.056	.061	.123	.296	0.642
232	.079	.072	.070	.074	.081	.126	.236
234	.096	.089	.091	.095	.087	.094	.137
236	.128	.119	.123	.128	.106	.100	.127
238	.161	.153	.149	.151	.134	.124	.146
240	.192	.182	.190	.198	.169	.157	.185
241	.220	.210	.225	.228	.189	.174	.202
242	.259	.246	.253	.245	.210	.195	.218
243	.284	.272	.286	.251	.237	.218	.242
244	.291	.282	.274	.272	.266	.244	.275
245	.305	.297	.302	.313	.293	.274	.312
246	.340	.327	.347	.354	.321	.296	.342
247	.396	.376	.399	.396	.350	.323	.383
248	.452	.428	.424	.389	.379	.350	.412
249	.459	.438	.417	.381	.416	.382	.438
250	.452	.434	.424	.413	.460	.427	.472
251	.473	.457	.483	.500	.499	.470	.550
252	.554	.527	.565	.551	.532	.498	.629
253	.628	.600	.601	.545	.564	.514	.658
254	.648	.619	.598	.518	.602	.558	.678
255	.647	.602	.570	.480	.652	.620	.702
256	.620	.580	.540	.497	.703	.668	.700
257	.600	.572	.600	.616	.722	.694	.884
258	.695	.650	.700	.681	.720	.708	.969
259	.768	.740	.722	.641	.742	.704	1.09
260	.768	.740	.700	.598	.790	.708	1.07
261	.774	.706	.689	.533	.826	.782	1.00
262	.780	.693	.576	.428	.856	.808	.99
263	.610	.574	.488	.431	.900	.887	1.05
264	.559	.523	.518	.495	.905	.910	1.32
265	.566	.564	.508	.451	.859	.899	1.50
266	.492	.496	.427	.380	.734	.746	1.40
267	.420	.416	.452	.378	.662	.644	1.45
268	.611	.484	.495	.330	.686	.681	1.33
269	.600	.509	.352	.206	.617	.650	1.04
270	.352	.334	.187	.113	.578	.598	.816
272	.095	.098	.063	.048	.706	.785	.958
274	.043	.046	.029	.021	.276	.332	1.420
276	.014	.017	.010	.008	.087	.102	.444
278	.004	.007	.002	.003	.033	.038	.129

TABLE 3. *Frequencies in centimeters^{-1} (also wavelengths in millimicrons) of the first 2 bands of each absorption spectra syste*

Absorbancies of a 0.5-g/liter solution, thickness 1.000 cm

Substance	First M band			Second M band			First A band			Second A band		
	$m\mu$	cm^{-1}	Absorbancy	$m\mu$	cm^{-1}	Absorbancy	$m\mu$	cm^{-1}	Absorbancy	$m\mu$	cm^{-1}	Absorbancy
n-Butylbenzene	268.5	37240	0.677	261.6	38230	0.812	264.7	37780	0.600	259.4	38550	0.780
Isobutylbenzene	268.7	37220	.538	261.5	38240	.710	265.0	37740	.570	259.4	38550	.750
sec-Butylbenzene	267.8	37340	.508	260.3	38420	.703	264.3	37840	.533	258.6	38670	.725
tert-Butylbenzene	267.2	37420	.381	*260.3	38420	.580	264.2	37850	.500	258.0	38760	.683
1,2-Diethylbenzene	271.6	36820	.749	263.7	37910	.931	267.7	37355	.691	*262.0	38170	.825
1,3-Diethylbenzene	271.8	36790	.700	264.5	37810	.927	268.3	37270	.693	262.3	38120	.875
1,4-Diethylbenzene	273.3	36590	1.700	267.2	37420	1.470	*270.0	37035	.800	264.8	37765	1.505

benzenes (see fig. 2) are distinctly different from those for the butylbenzenes, and they are more intense. The spectrum for 1,4-diethylbenzene differs noticeably from the other two diethylbenzenes. In general the two-spectra characteristic is less distinct, probably because of greater electronic migration, dissociation, and band splitting. The *A* series is relatively weak, and in the 1,4-diethylbenzene the first band of the *A* series is barely perceptible.

For comparative purposes the absorption spectrum of *n*-butylbenzene is displayed also with the diethylbenzenes. Here, again, it is interesting to note the gradual shift in the position of the important absorption bands in progressing from *n*-butylbenzene to 1,4-diethylbenzene. In this case the shift is toward the lower frequencies (longer wavelengths), resulting in the greatest shift for 1,4-diethylbenzene, although its spectrum is in some respects most like that for benzene of any of the substituents. A comparison of the two illustrations is interesting in displaying the gradual wavelength shift of the absorption bands in progressing through the seven substituted benzenes from 1,4-diethylbenzene to *tert*-butylbenzene.

The ratio of the specific absorbancies of the diethylbenzenes is in general agreement with the predictions of Sklar [11]. The value of absorbancy of the 1,4- spectrum is near twice that for the 1,2- and 1,3- substituents, as predicted. The spectra for both the butylbenzenes and the diethylbenzenes are in general agreement with other measurements upon similar materials both qualitatively and quantitatively where such data exist [13, 14, 15].

In view of the similarity of the absorption spectra of these compounds, both in general appearance and in intensity, chemical analysis by ultraviolet absorption data alone would be impractical. The data should, however, serve a useful purpose in supplement to other measurements.

Acknowledgment is gratefully given to Nicolo Acquista for valuable assistance in the careful measurement of the concentrations of the various materials.

IV. References

[1] Earle K. Plyler, Ralph Stair, and Curtis J. Humphreys, J. Research NBS **38,** 211 (1947) RP1769.
[2] H. H. Cary and Arnold O. Beckman, J. Opt. Soc. Am. **31,** 682 (1941).
[3] Kasson S. Gibson and Margaret M. Balcom, J. Research NBS **38,** 601 (1947) RP1798.
[4] Supplement to NBS Circular C398, p. 7 (1949).
[5] Robert S. Mulliken, Chem. Rev. **41,** 201 (1947).
[6] H. Sponer and E. Teller, Rev. Mod. Phys. **13,** 76 (1941).
[7] G. Herzberg and E. Teller, Z. Physik Chem. **B21,** 410 (1933).
[8] H. Sponer, Chem. Rev. **41,** 281 (1947).
[9] American Petroleum Institute Research Project 44. National Bureau of Standards. Catalog of ultraviolet spectrograms. Serial No. 1, Benzene, contributed by the Beacon Laboratory of the Texas Co.
[10] H. Sponer, G. Nordheim, A. L. Sklar, and E. Teller, J. Chem. Phys. **7,** 207 (1939).
[11] A. L. Sklar, J. Chem. Phys. **7,** 984 (1939); **10,** 135 (1942).
[12] H. Sponer, and S. H. Wollman, J. Chem. Phys. **9,** 816 (1941).
[13] F. A. Matsen, W. W. Robertson, and R. L. Chuoke, Chem. Rev. **41,** 273 (1947).

[14] American Petroleum Institute Research Project 44. National Bureau of Standards. Catalog of ultraviolet spectrograms. Serial No. 3, *n*-Butylbenzene; Serial No. 4, Isobutylbenzene; Serial No. 5, sec-Butylbenzene; Serial No. 6, tert-Butylbenzene, all contributed by the Ethyl Corp., Research Laboratories, Detroit, Mich. Serial No. 32, tert-Butylbenzene, Union Oil Co. of California. Serial No. 60, *n*-Butylbenzene; Serial No. 61, sec-Butylbenzene; Serial No. 69, Isobutylbenzene; Serial No. 70, tert-Butylbenzene, all contributed by the Beacon Laboratory of The Texas Co. Serial No. 165, Isobutylbenzene; Serial No. 166, both contributed by the Shell Development Co.

[15] American Petroleum Institute Research Project 44. National Bureau of Standards. Catalog of ultraviolet spectrograms. Serial No. 77, Ortho-diethylbenzene; Serial No. 78, Meta-diethylbenzene; Serial No. 79, Para-diethylbenzene, all contributed by the Anglo-Iranian Oil Co., Ltd., Research Laboratories, Sunbury-on-Thames, Eng.

[16] American Petroleum Institute Research Project 44. National Bureau of Standards. Catalog of ultraviolet spectrograms. Serial No. 176, *n*-Butylbenzene; Serial No. 177, Isobutylbenzene; Serial No. 178, sec-Butylbenzene; Serial No. 179, tert-Butylbenzene; Serial No. 186, 1,2-Diethylbenzene; Serial No. 187, 1,3-Diethylbenzene; Serial No. 1,4-Diethylbenzene, all contributed by the Radiometry Laboratory, National Bureau of Standards, Washington, D. C.

WASHINGTON, August 6, 1948.

U. S. Department of Commerce
National Bureau of Standards

Research Paper RP1997
Volume 42, June 1949

Part of the Journal of Research of the National Bureau of Standards

Acid-Base Equilibrium Constants for the Reaction of Tribenzylamine with Picric Acid and with Trinitro-*m*-Cresol in Benzene, from Spectrophotometric Data

By Marion Maclean Davis and E. Anne McDonald

The relative acidic strengths of picric acid and trinitro-*m*-cresol in benzene have been measured spectrophotometrically in terms of their reactivity with the base, tribenzylamine. The respective constants found for the combination of tribenzylamine with picric acid and with trinitro-*m*-cresol in benzene at 25° C are 1.58×10^{3} and 4.48×10^{2}. The same relative order of strengths would be predicted on theoretical grounds. The constant for picric acid is in close agreement with previous measurements of the dielectric constant of benzene solutions of tribenzylammonium picrate. The method used for assessment of the relative strengths of the two acids is superior to measurements of their ionic dissociation in water.

I. Introduction

During the first quarter of this century, the definitions of an acid and a base most commonly taught and applied were founded on the behavior of aqueous solutions. As is well known, acidic and basic properties were referred, respectively, to hydrogen and hydroxyl ions, numerous investigators undertook the measurement of the ionic dissociation constants of acids and bases in water, and the pH scale came into widespread use as a means of expressing relative acidities and basicities. The currently popular Brønsted-Lowry proton-transfer theory of acidity and basicity has clarified the role of the solvent.[1] It is now recognized that water can function both as a base and as an acid, and this, of course, is the reason a continuous pH scale for aqueous solutions can exist. Moreover, the effect of other solvents on dissolved acids and bases is now to some degree predictable, because the electronic structure of a molecule reveals whether it can serve as a proton donor, as a proton acceptor, or as both donor and acceptor. But whenever the solvent displays acidic or basic character, the nature of the reaction between a dissolved acid and base is partially masked. The ideal condition for studying the reaction between an acid and a base would be to use no solvent at all. The nearest practicable approach to such a condition, when organic acids and bases are concerned, is to use an inert or "aprotic" solvent; that is, a solvent that can neither add nor release protons. Benzene and carbon tetrachloride are examples of aprotic solvents that are suitable for such studies. At one time many proponents of the ionization theory assumed, from an overemphasis of the role of ions in chemical reactions and inadequate experimental evidence, that acid-base reactions do not occur in any medium of such low dielectric constant. Subsequently, Hantzsch, Brønsted, LaMer, and others demonstrated that instantaneous acid-base reactions occur as readily in an aprotic medium as in an ionizing medium. However, widespread awareness of their work does not yet exist, acid-base reactions in aprotic media remain a neglected field of study, and a general tendency persists to employ, in analytical procedures and as media for reactions, only solvents that promote ionization.

In two previous publications from this Bureau

[1] The authors do not reject the much broader Lewis concept of acidity, but it offers no advantage over the Brønsted-Lowry concept when hydrogen acids only are considered, as in this paper. Furthermore, acid-base reactions that involve the formation of a hydrogen bridge do not entirely parallel reactions in which a coordinate covalent bond is formed between the acid and the base.

[1, 2],[2] some of the earlier studies of acid-base reactions in aprotic media were reviewed, and new experimental data, both qualitative and quantitative, were presented. The method employed by us was to study, by means of the spectrophotometer, the reaction between different acidic indicator dyes and various organic bases in benzene and other organic solvents. Of particular interest was the discovery that organic bases of various types—for example, primary, secondary, and tertiary aliphatic amines—exhibit specific differences in their behavior with acids in an aprotic solvent, such as benzene. These differences are masked in an amphiprotic solvent, like water. Other studies still in progress provide additional evidence of the specificity of the behavior of bases and of acids in inert solvents. Such experiments point to the need for further investigations of acid-base reactions in inert solvents, as a prerequisite both to the development of methods for the measurement of acidity and basicity in such media and to a better understanding of acid-base relationships in water and other "active" solvents.

This paper deals with the reaction of tribenzylamine with picric acid and with trinitro-*m*-cresol in benzene. The acid-base equilibrium constants of the reactions were determined spectrophotometrically. As will be shown, the results are in agreement with conclusions arrived at from other experimental procedures.

II. Equipment and Procedure

The spectrophotometric equipment used was the same as that described in the preceding paper of this series [2], except for changes designed for protection of the solutions from the heating effect of the light source. The cell compartment was replaced by a new box with double walls at the bottom, sides, and top. In the space between the two walls, water from a constant-temperature bath circulates continuously. The temperature of the bath is maintained at 25.0° ±0.1° C, and the contents of the cell can be kept at a temperature not more than 0.2° C above that of the bath. The light source was also moved about 1 in. farther away from the cell compartment.

The procedure followed in the preparation and dilution of solutions and in the recording of data has already been described [1, 2]. In some of the measurements, one cell contained the pure solvent and the other the solution under investigation. However, when working with a considerable excess of tribenzylamine in the solution, an equivalent amount of tribenzylamine was placed in the reference cell. Such cases will be noted in section IV.

The symbols and terminology used are as follows: T_s (transmittancy of the solute)$=T_{soln}/T_{solv}$; a_s (absorbancy or optical density of the solute)$=-\log_{10}T_s$; a_M (molar absorbancy of the solute)$=a_s/(b\times M)$; b=length in centimeters of the absorption cell; M=molar concentration of the solution [3].

III. Materials

Benzene.—The high grade of commercial benzene used in previous work became unavailable while these investigations were in progress. However, benzene from another source was found to be equally satisfactory when dried over Drierite and then redistilled [4].

Picric acid.—A practical grade of picric acid, containing 10 percent of water, was recrystallized twice from boiling water, dried in a vacuum oven at 100° C, then precipitated from benzene solution by cyclohexane, and finally dried in a vacuum oven at 80° C. The melting point was 122.1° to 122.3° C.[3]

Tribenzylamine.—A high grade of commercial tribenzylamine was recrystallized from 95-percent ethyl alcohol and then dried in a vacuum oven at 80° C. The melting point was 92.0° to 92.1° C.

Trinitro-m-cresol.—A high grade of commercial trinitro-*m*-cresol was recrystallized once from 95-percent ethyl alcohol and twice from benzene. After drying in a vacuum oven at 80° C, the melting point was 107.0° to 107.2° C.

IV. Data and Calculations

Reaction of tribenzylamine with picric acid.—In the pure, dry state, tribenzylamine and picric acid are colorless solids and give colorless solutions in benzene. When solutions of the acid and the base are mixed, an instantaneous reaction occurs, as

[2] Figures in brackets indicate the literature references at the end of this paper.

[3] Melting points were determined in an electrically heated bath containing silicone oil, with an ASTM thermometer for 3-in. immersion.

shown by the appearance of a yellow color.[4] The reaction was studied quantitatively by measurement of the spectral transmittancy of solutions that contained a constant amount of picric acid mixed with varying amounts of the amine. A series of transmittancy curves obtained for such solutions are presented in figure 1. Curve 0 is for

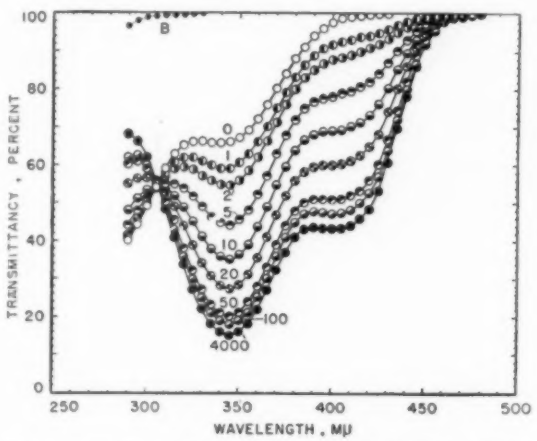

FIGURE 1. *Transmittancy curves for picric acid, for tribenzylamine, and for their mixtures in benzene (1-cm cell).*

0, Picric acid, 5×10^{-5}-*M*; (1) to (4,000), 5×10^{-5}-*M* picric acid with from 1 to 4,000 molar equivalents of tribenzylamine; B, tribenzylamine, 5×10^{-3}-*M*.

5×10^{-5}-*M* picric acid in benzene, and the curves designated 1 through 4,000 are for solutions that contained the same concentration of picric acid mixed with from 1 to 4,000 molar equivalents of tribenzylamine. In the case of the curve marked 4,000, the reference cell contained 4,000 molar equivalents of tribenzylamine; in all other cases, it contained benzene only. The change produced by 4,000 molar equivalents of tribenzylamine was no greater than that produced by 2,000 molar equivalents of the base, and the curve marked 4,000 is therefore the limiting curve for the reaction.[5] Measurements cannot be made for wavelengths shorter than 280 mμ, because of the high absorbancy of the solvent.

A benzene solution of tribenzylamine more dilute than 10^{-3}-*M* shows almost complete transmittancy at wavelengths greater than 300 mμ. More concentrated solutions exhibit measurable absorbancy at wavelengths shorter than about 350 mμ, as indicated by the transmittancy curve for 5×10^{-3}-*M* tribenzylamine (curve B, fig. 1). Determination of the applicability of Beer's law is not easy, because of the steepness of the transmittancy curves for the higher concentrations of the base. However, in the range 5×10^{-4}-*M* to 5×10^{-2}-*M*, the values for molar absorbancies agreed within experimental error, and there is no reason for expecting the molar absorbancy to show any effect of concentration. It is not possible to determine with certainty the change in transmittancy that occurs when tribenzylamine is converted to the tribenzylammonium group, but it is reasonable to assume that the change is inappreciable for a 5×10^{-5}-*M* solution, even at the shortest wavelengths.

The curve for picric acid shows a shallow transmission band near 325 mμ and a shallow absorption band near 340 mμ. At the concentration employed, there was no measurable absorbancy at wavelengths greater than about 430 mμ. Molar absorbancies for $5\times10^{-5}-M$ and $5\times10^{-4}-M$ solutions were the same within experimental error. Picric acid has been shown by cryoscopic measurements to exist in the monomeric state in benzene [5], and infrared studies indicate a hydrogen bridge between the phenolic oxygen and the nitro group in ortho-substituted phenols [6]. Conformity of its benzene solution to Beer's law is therefore to be anticipated.

The transmittancy curve for tribenzylammonium picrate in benzene shows a fairly deep absorption band near 342 mμ and a very shallow band near 410 mμ. Curves 0 through 10 in figure 1 show a well-marked isosbestic point at approximately 304.5 mμ. With concentrations of tribenzylamine greater than 10 molar equivalents, the isosbestic point was shifted to about 305.5 mμ.

Solutions of tribenzylammonium salts are all colorless if the acidic component is colorless, whereas all picrates give yellow solutions. The absorption bands that give rise to the yellow color of tribenzylammonium picrate are therefore attributable to a loosening of electrons in the

[4] The presence of traces of water adsorbed from the air by any of the materials or glassware also produces a yellow color. It is therefore necessary to take every possible precaution to exclude moisture and to prepare fresh stock solutions of the materials at frequent intervals. Little difficulty is experienced if measurements are performed in cool, dry weather.

[5] In the preparation of solutions that contained 2,000 or 4,000 molar equivalents of tribenzylamine, the slight evaporation of solvent upon exposure of the 0.25-*M* stock solution to the air caused some of the base to be deposited on the surface of the flasks and pipettes. The actual concentration of tribenzylamine was therefore not quite 2,000 or 4,000 molar equivalents. However, it was evident that a further increase in concentration would not produce a measurable change in transmittancy.

$-OC_6H_2(NO_2)_3$ group. This loosening is not so great as in quaternary ammonium picrates, because the transmittancy curves for the latter compounds in benzene are displaced appreciably toward longer wavelengths [7]. For a dilute solution of a quaternary ammonium picrate in benzene, for example, tetraethylammonium picrate, the studies of Kraus and his collaborators indicate the structure $Et_4\overset{+}{N}\overset{-}{Pi}$. This formula signifies an ion pair, held together by Coulombic attraction. The formula for tribenzylammonium picrate, $(C_6H_5CH_2)_3\overset{+}{N}H \ldots \overset{-}{O}C_6H_2(NO_2)_3$, accounts for the difference in the spectral absorption of the two salts. It is also in harmony with the views of Kraus, who wrote: "When a partially substituted ammonium salt is dissolved in a solvent medium the molecules of which have no affinity for the proton, interaction takes place between the negative ion and the proton of the positive ion. In other words, there is formed what is commonly known as a hydrogen bond, the energy of rupture of which may be much higher than the energy necessary to overcome the Coulombic forces acting between the ions [8]." The conclusion cited was derived from measurements of conductance.

The reaction under discussion may be formulated quite simply as the union of one molecule of tribenzylamine with one molecule of picric acid to give a molecule of tribenzylammonium picrate. The hydrogen bond (or bridge) is generally much weaker than a covalent bond. A rupture of the hydrogen bridge in tribenzylammonium picrate can occur in two places. If the break comes between nitrogen and hydrogen, the products are tribenzylamine and picric acid. A break between hydrogen and oxygen gives tribenzylammonium and picrate ions. Experimental data indicate that appreciable dissociation of the salt into tribenzylamine and picric acid occurs in benzene solution. Spectrophotometric measurements furnish no evidence of ionic dissociation. The possibility of extremely minute concentrations of ions, is not excluded, however. Kraus and Fuoss, from measurements of conductance, calculated for tetraisoamylammonium picrate and for triisoamylammonium picrate in benzene the respective ionic dissociation constants, 8.9×10^{-18} and 2.5×10^{-21} at 25° C [9, 10]. These values correspond to an ionic dissociation of approximately a millionth of a percent in the case of tetraisoamylammonium picrate, and approximately a billionth of a percent in the case of triisoamylammonium picrate. The ionic dissociation of tribenzylammonium picrate in benzene has not been measured, but it probably does not differ greatly from that of triisoamylammonium picrate.

If, now, the equation for this reaction is written in the form,

$$\underset{\text{(acid)}}{A} + \underset{\text{(base)}}{B} \rightleftharpoons \underset{\text{(salt)}}{S}, \tag{1}$$

the association constant is expressed according to the familiar law of mass action as

$$K_{assoc.}=[S]/\{[A][B]\}. \tag{2}$$

The value obtained for $K_{assoc.}$ will be a measure of the acidic strength of picric acid and of the basic strength of tribenzylamine. In order to compute the values of $[S]$, $[A]$, and $[B]$ for various mixtures, it is necessary to know the initial concentrations C_a and C_b of the acid and base, respectively, and the values of a_s for the acid, for the salt, and for mixtures of the two, at one or more wavelengths. The quotient, $[a_s\text{ (mixture)}-a_s\text{ (acid)}]/[a_s\text{ (salt)}-a_s\text{ (acid)}]$, gives the fraction of the acid converted to the salt. This fraction multiplied by the initial concentration of the acid (5×10^{-5}-M) gives $[S]$, the molar concentration of salt in the mixture. The concentrations of acid and base in the equilibrium mixture are, respectively, $C_a-[S]$ and $C_b-[S]$. Experimental values of a_s for the acid, salt, and 19 mixtures of the two at the wavelength 410 mμ are given in table 1, together with the calculated values for $[S]$, $[A]$, $[B]$, and $K_{assoc.}$. Values of $K_{assoc.}$ computed for data at 342 mμ are also included. The precision of the data is obviously less for mixtures that contain very small quantities of the acid or the salt. The average of 16 intermediate values for K is 1.58×10^3 for measurements at 410 mμ and 1.52×10^3 for measurements at 342 mμ. Because of uncertainty as to a possible contribution from basic components to the absorbancy at 342 mμ, the value obtained for 410 mμ is probably the more reliable one.

The manner in which the fraction of picric acid converted to tribenzylammonium picrate varies with C_b is shown in figure 2, curve 1. The open circles represent values for 410 mμ and the solid circles values for 342 mμ. The change produced

TABLE 1. *Experimental data and association constant for the reaction of tribenzylamine and picric acid in benzene*

Initial concentration of base [a]	From measurements at—					
	410 mμ					342 mμ
	a_o	$[S]\times10^3$ [b]	$[A]\times10^3$ [b]	$[B]\times10^3$ [b]	$K\times10^{-3}$	$K\times10^{-3}$
0	0.0039					
1	.0311	0.3857	4.614	4.614	*1.81	*1.69
2	.0501	.6551	4.345	9.345	1.61	1.53
4	*.0857	1.160	3.840	18.84	1.60	1.47
5	.1002	1.366	3.634	23.63	1.59	1.57
6	*.1135	1.554	3.446	28.45	1.58	1.53
8	*.1355	1.866	3.134	38.13	1.56	1.45
10	.1537	2.124	2.876	47.88	1.54	1.52
12	*.1733	2.402	2.598	57.60	1.61	1.52
15	.1938	2.693	2.307	72.31	1.61	1.58
16	*.1993	2.771	2.229	77.23	1.61	1.51
20	.2140	2.979	2.021	97.02	1.52	1.52
25	.2358	3.288	1.712	121.7	1.58	1.54
30	.2510	3.504	1.496	146.5	1.60	1.48
35	.2604	3.637	1.363	171.4	1.56	1.48
40	.2700	3.773	1.227	196.2	1.57	1.51
50	.2840	3.972	1.028	246.0	1.57	1.58
100	.3179	4.453	0.547	495.5	1.64	1.49
500	.3382	4.741	.259	2,495.	*0.73	*0.63
1,000	.3487	4.889	.111	4,995.	*.88	*.74
Limiting value	[d].3565	5.000				
				Average	*1.58	*1.52

[a] Expressed as molar equivalents of 5×10^{-4}-*M* picric acid.
[b] In moles per liter of solution.
[c] Average of 5 values.
[d] Observed value; calculated value is the same.
[e] Values marked with an asterisk are excluded from the average.

in the absorbancy is relatively great for small values of C_b. When the value of C_b is greater than about 50 molar equivalents, much larger increments are necessary to cause measurable changes in the absorbancy and to determine the limiting value. For example, when C_b=200 or 500 molar equivalents, identical values of a_z were obtained. Calculations of K using this provisional limiting value showed a slight trend. Calculations were then made with various assumed limiting values for a_z. The value that gave the most consistent results was 0.3565. The validity of this number was confirmed experimentally for solutions that contained C_b=2,000 and 4,000 molar equivalents, in which the minute residual quantities of picric acid are not detectable spectrophotometrically.

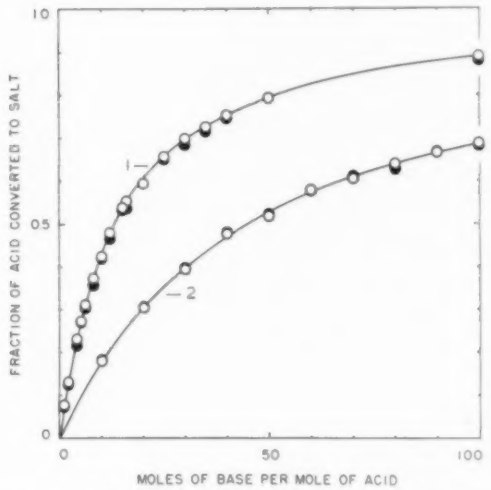

FIGURE 2. *Effect of the concentration of tribenzylamine, expressed in molar equivalents, on the fraction of the acid converted to salt in benzene.*

1, 5×10^{-4}-*M* picric acid. Open circles, values for 410 mμ; solid circles, values for 342 mμ. 2, 5×10^{-4}-*M* trinitro-*m*-cresol. Open circles, values for 400 mμ; solid circles, values for 345 mμ.

Equation 2 may also be expressed in logarithmic terms as follows:

$$\text{Log } [S]/[A]=\log [B]+\log K_{assoc.} \qquad (3)$$

Equation 3 has the form of the familiar equation for the straight line, $y=mx+b$, in which m signifies the slope of the line and b is its intercept on the x-axis. For the reaction postulated (eq. 1), m should equal 1. In figure 3, for convenience, the values for log $[S]/[A]$ and $-\log [B]$ are plotted along the vertical and horizontal axes, respectively. The slope then becomes negative in sign. The line shown in figure 3 was drawn with the theoretical slope, minus 1. Log $K_{assoc.}$ is the intercept on the horizontal axis for log $[S]/[A]=0$. It is evident from inspection of figure 3 as well as of table 1 that the experimental values showed no trend when the concentration of the base was varied but conformed closely to the equation assumed for the reaction. The validity of eq 1 is therefore supported by the experimental results as well as by the fact that any reaction other than the one postulated would be inconsistent with the properties of tribenzylamine and picric acid.

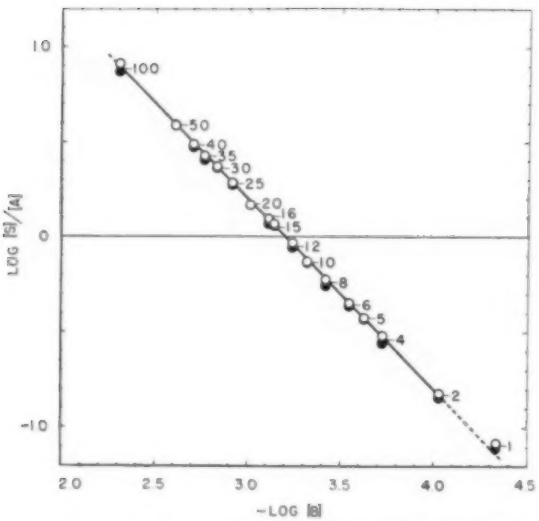

FIGURE 3. *Graphical evaluation of association constant for the reaction of 5×10^{-5}-M picric acid with tribenzylamine in benzene.*

Experimental points marked 1 through 100 indicate the number of molar equivalents of tribenzylamine per mole of picric acid. Open circles, values for 410 mμ; solid circles, values for 342 mμ.

From the association constant, 1.58×10^{3}, it may be calculated that in a 5×10^{-5}-M solution of tribenzylammonium picrate in benzene approximately 93 percent of the salt would be dissociated into tribenzylamine and picric acid at 25° C.

Reaction of tribenzylamine with trinitro-m-cresol.—Trinitro-*m*-cresol (3-methylpicric acid) is a colorless solid and gives a colorless solution in benzene. The transmittancy curve for 5×10^{-5}-M trinitro-*m*-cresol in benzene (fig. 4, curve 0) resembles that of equimolar picric acid in benzene but is shifted slightly toward shorter wavelengths. Instead of a shallow absorption band near 340 mμ, there is a plateau in the region 325 to 335 mμ. No measurable absorbancy was observed for a 5×10^{-5}-M solution at wavelengths greater than about 440 mμ. Deviations from Beer's law were not detected for solutions of four different concentrations in the range 5×10^{-5}-M to 5×10^{-4}-M, and there is no reason to expect either association or dissociation of the acid in a benzene solution of the concentration used in the investigation.

Comparison of curves 1 and 2 in figure 2 reveals that a greater excess of tribenzylamine is required for the conversion of trinitrocresol to its tribenzylammonium salt in benzene than is required for

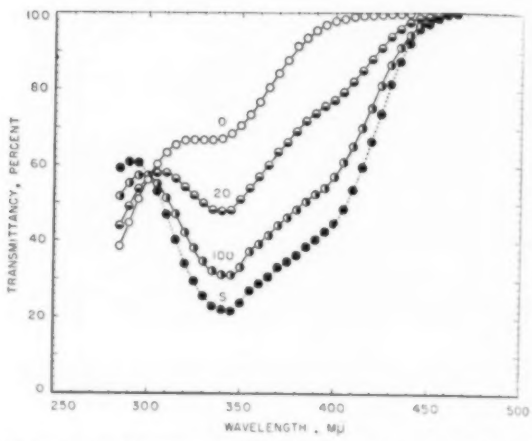

FIGURE 4. *Transmittancy curves for trinitro-m-cresol and for its mixtures with tribenzylamine in benzene (1-cm cell).*

0, Trinitro-*m*-cresol, 5×10^{-5}-M; (20) and (100), 5×10^{-5}-M trinitro-*m*-cresol, with 20 and 100 molar equivalents of tribenzylamine, respectively; S, calculated limiting curve for the reaction of 5×10^{-5}-M trinitro-*m*-cresol with tribenzylamine.

the conversion of picric acid to tribenzylammonium picrate. When about 2,000 molar equivalents of tribenzylamine were added to 5×10^{-5}-M trinitrocresol, precipitation occurred. The limiting value was therefore not measurable, but it was calculated in the manner described for tri-

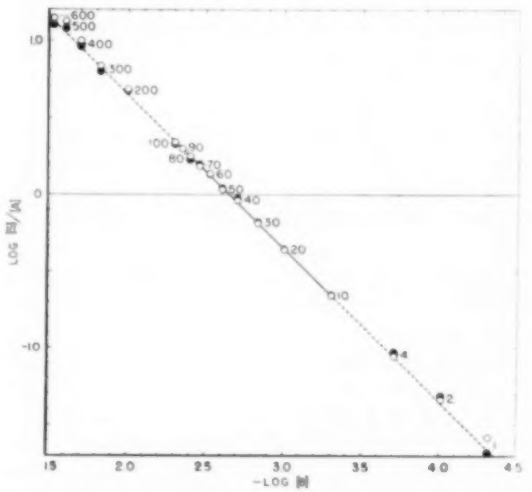

FIGURE 5. *Graphical evaluation of association constant for the reaction of 5×10^{-5}-M trinitro-m-cresol with tribenzylamine in benzene.*

Experimental points marked 1 through 600 indicate the number of molar equivalents of tribenzylamine per mole of trinitro-*m*-cresol. Open circles, values for 400 mμ; solid circles, values for 345 mμ.

benzylammonium picrate. The data presented in table 2 are for trinitro-*m*-cresol and 18 mixtures with tribenzylamine and correspond to those already discussed for mixtures of picric acid with tribenzylamine. Measurements at 400 mμ and 345 mμ gave the same average value, 448, for $K_{assoc.}$. From inspection of figure 5 it may be seen that all of the experimental values for log $[S]/[A]$ versus $-\log [B]$ fall on or very close to the theoretical curve. In view of the unlikelihood of a reaction other than the one postulated and the consistency of the results, the value 448 for $K_{assoc.}$ may be accepted with confidence. From this result it may be computed that in 5×10^{-5}-M benzene solution, the tribenzylammonium salt of trinitro-*m*-cresol would be 98 percent dissociated into tribenzylamine and trinitro-*m*-cresol at 25° C.

Although it was not possible to measure the transmittancy curve for the tribenzylammonium salt of trinitro-*m*-cresol, the curve was calculated from the transmittancy curves for 5×10^{-5}-M trinitrocresol and for its mixtures with 20 and 100 molar equivalents of tribenzylamine and the calculated limiting value of a_s at 400 mμ (used in the computation of $K_{assoc.}$). The quotient, $[a_s\text{ (salt)}-a_s\text{ (acid)}]/[a_s\text{(mixture)}-a_s\text{ (acid)}]$ should be the same for all wavelengths. Two sets of values for the absorbancy versus wavelength were calculated for the salt, one set based on the absorbancy values for the solution that contained 20 molar equivalents of tribenzylamine and the other set based on the values for the solution with 100 molar equivalents of tribenzylamine. The final curve was computed from the average of the two sets of values. The computed curve (dotted line marked *S* in fig. 4) intersects the three experimentally determined curves at their isosbestic point, which is near 300 mμ, and is probably correct within ±1 percent.

TABLE 2. *Experimental data and association constant for the reaction of tribenzylamine and trinitro-m-cresol in benzene*

Initial concentration of base [a]	From measurements at—					
	400 mμ					345 mμ
	a_s [b]	$[S]\times10^5$ [c]	$[A]\times10^5$ [c]	$[B]\times10^5$ [c]	$K\times10^{-2}$	$K\times10^{-2}$
0	0.0090	.....	.....	.....	.....	.....
1	.0177	0.1273	4.873	4.873	*5.36	*4.24
2	.0241	.2209	4.779	9.779	*4.73	*4.98
4	.0367	.4052	4.595	19.60	*4.49	*4.79
10	.0706	.9012	4.099	49.10	4.48	4.54
20	.1129	1.520	3.480	98.48	4.44	4.47
30	.1439	1.974	3.026	148.0	4.41	4.46
40	.1726	2.393	2.607	197.6	4.65	4.70
50	.1864	2.595	2.405	247.4	4.36	4.46
60	.2069	2.895	2.105	297.1	4.63	4.59
70	.2161	3.030	1.970	347.0	4.43	4.55
80	.2277	3.200	1.800	396.8	4.48	4.24
90	.2386	3.330	1.670	446.7	4.46	4.49
100	.2441	3.440	1.560	496.6	4.44	4.30
200	.2924	4.146	0.854	995.8	*4.88	*4.77
300	.3072	4.363	.637	1,496.	*4.58	*4.20
400	.3197	4.546	.454	1,995.	*5.02	*4.58
500	.3270	4.652	.348	2,496.	*5.36	*4.80
600	.3279	4.666	.334	2,996.	*4.66	*4.23
Limiting value	[d] (.3507)	5.000	.....	.....	.....	.....
				Average	*4.48	*4.48

[a] Expressed as molar equivalents of 5×10^{-5}-M trinitro-*m*-cresol.
[b] Average of 10 values.
[c] In moles per liter of solution.
[d] Calculated as explained in the text.
[e] Values marked with an asterisk are excluded from the average.

V. Discussion

So far as we are aware, the association constants given in section IV are the first values for solutions of acids and bases in benzene to be measured with precision by the spectrophotometric method. In an earlier publication [1], provisional values were given for the association of the indicator acid, bromophthalein magenta, with five different bases in benzene. These values were determined under less favorable experimental conditions but are probably close to the correct values. Nearly 20 years ago, Weissberger and Fasold [11] attempted to measure spectrophotometrically the extent of salt formation in benzene and chloroform solutions of *p*-dimethylaminoazobenzene (methyl yellow) and trichloroacetic acid. The values for K were not constant and showed a trend. Hantzsch had previously emphasized the tendency toward salt formation in an inert solvent as the most logical measure of the strength of acids, and had estimated the relative strengths of several acids by semiquantitative measurements of the extent to which they formed colored salts with basic indicator dyes [12, 13]. Carboxylic acids are known to be dimerized in inert solvents and, according to Hantzsch, sulfonic acids are associated in chloroform [14]. In titrating acids conductimetrically with aliphatic amines in benzene, Maryott observed unusual inflections in the curves for the titration of trichloroacetic and camphorsulfonic acids that were not present in the curves for the titration of picric

acid. The peculiarities were interpreted in terms of a reaction between salt and acid, leading to the formation of a complex anion [15]. In all probability, the reaction studied by Weissberger and Fasold was complicated by similar effects.

Maryott has measured the dipole moment at 30° C of tribenzylammonium picrate in benzene. The value, 12.0×10^{-18} esu, is substantially the same as that found previously for the picrates of more strongly basic amines [16, 17].[6] From the variation of dielectric constant with concentration, the constant for the dissociation of tribenzylammonium picrate into tribenzylamine and picric acid in benzene was determined at 30° and 40° C [17]. On the assumption that the change in enthalpy (ΔH) is constant over the limited range of temperature involved, the value calculated for K_N at 25° C is 5.58×10^{-5}. The corresponding value for the dissociation constant expressed in terms of moles per liter rather than mole fraction is 6.25×10^{-4}. The reciprocal of this value, $K_{assoc.}$, is 1.60×10^{3}, or almost exactly the value obtained by the spectrophotometric method.

The extent of ionic dissociation of picric acid and trinitro-*m*-cresol in water and in absolute methyl and ethyl alcohols has been measured by Goldschmidt and his collaborators. The two acids were found to be highly ionized and of practically equivalent strength in water, in agreement with earlier work of Kendall [21, 22]. Differences were found, however, in the strengths of the two acids in alcoholic solutions. For picric acid, the thermodynamic ionization constants found were 1.547×10^{-4} in methyl alcohol [23] and 8.32×10^{-5} in ethyl alcohol [24].[7] For trinitro-*m*-cresol, the respective values were 3.47×10^{-5} [21] and 1.59×10^{-5} [24]. The results for methyl and ethyl alcohol solutions indicate a lower acidic strength for trinitro-*m*-cresol, in agreement with our results for benzene solutions.

On theoretical grounds, this difference in the strength of the two acids could have been predicted. The introduction of a nitro group into the phenol molecule is most effective in increasing the acidic strength when the substituent is in the ortho or para position. This indicates that resonance with quinoid structures is involved, as well as electrostatic interactions between the ionizable proton and the dipole moment of the nitro group [26 to 28]. In picric acid, with two nitro groups ortho and one para to the —OH group, both the electrostatic and the resonance effects operate in the same direction, thus accounting for its high strength. If resonance with quinoid structures is prevented from occurring, only the electrostatic effect of nitro groups remains. Wheland and coworkers have shown that in *p*-nitrophenol the introduction of methyl groups ortho to the nitro group causes a diminution in acidity. It is assumed that such groups cause the nitro group to be twisted out of the plane of the benzene ring, thereby preventing quinoid resonance. This effect, which is termed "steric inhibition of resonance," has been observed by other investigators, for bases as well as for acids. The lower acidic strength of trinitro-*m*-cresol as compared with picric acid can be explained by similar arguments, for the two acids differ in structure by the presence in trinitro-*m*-cresol of a methyl group adjacent to the para and one of the ortho nitro groups. In this connection, it is interesting to recall that the absorption curve for trinitro-*m*-cresol in benzene was found to be shifted a little—toward shorter wavelengths—from the position of the curves for picric acid. (See p. 600.) This difference is in harmony with current theories of absorption spectra, according to which the energy of excitation is lower for a molecule in which there is resonance among various structures, and hence spectral absorption occurs at longer wavelengths than if there were no resonance. Partial inhibition of resonance should lead to an opposite effect. Remington [29] and several others have observed such effects.

The discovery that acids that appear equally strong in water show differences in acidity in other solvents is not new. Some of the earliest work in this field was by Hantzsch, who showed, for example, that perchloric acid, the halogen acids, nitric acid, and sulfonic acids—all of which appear equally strong in water—exhibit marked differences in intrinsic acidity when comparisons are made in solvents such as chloroform and ether [14]. Numerous workers have pointed out the advantage of working with aprotic solvents, but the use of such media to date has largely been limited to studies of the catalytic effects of different acids and bases.

The intrinsic strength of an acid or base can be

[6] The values found for tetraalkylammonium picrates in benzene are of the order 18×10^{-18} esu at 25° C [18 to 20].

[7] The value 6.23×10^{-5} has been reported for picric acid in butyl alcohol [25].

determined only by the study of a reaction that is reversible to a measurable degree. In water, the ionization of an acid—which is customarily formulated as $HX+H_2O \rightleftharpoons H_3O^+ + X^-$—goes practically to completion when the acid, HX, relinquishes its proton readily. The great excess of the base, H_2O, is partly responsible for the completeness of the reaction. The strength of the acid can be measured only when the relative strengths of the acid and the base and their relative proportions in various mixtures are such that the reaction is only partly complete.

The results reported in this paper show that the combination of tribenzylamine with picric acid or trinitro-*m*-cresol would be unsuitable for titrimetric analyses. It is an advantage, however, for the determination of relative strengths that the reactions do not proceed to completion. Tables of relative acidic and basic strengths similar to the electromotive series of metals can eventually be constructed when more data are available, but much work remains to be done.

VI. References

[1] M. M. Davis and P. J. Schuhmann, J. Research NBS **39,** 221 (1947) RP1825.

[2] M. M. Davis, P. J. Schuhmann, and M. E. Lovelace, J. Research NBS **41,** 27 (1948) RP1900.

[3] Terminology and symbols for use in ultraviolet, visible, and infrared absorptometry, NBS Letter Circular LC857 (May 19, 1947).

[4] M. E. Maclean, P. J. Jencks, and S. F. Acree, J. Research NBS **34,** 271 (1945) RP1643.

[5] J. N. Brønsted and R. P. Bell, J. Am. Chem. Soc. **53,** 2478 (1931).

[6] G. E. Hilbert, O. R. Wulf, S. B. Hendricks, and U. Liddel, J. Am. Chem. Soc. **58,** 548 (1936).

[7] M. M. Davis, E. A. McDonald, and P. J. Schuhmann, unpublished data.

[8] C. A. Kraus, J. Phys. Chem. **43,** 231 (1939).

[9] C. A. Kraus and R. M. Fuoss, J. Am. Chem. Soc. **55,** 21 (1933).

[10] R. M. Fuoss and C. A. Kraus, J. Am. Chem. Soc. **55,** 3614 (1933).

[11] A. Weissberger and K. Fasold, Z. physik. Chem. [A] **157,** 65 (1931).

[12] A. Hantzsch, Z. Elektrochem. **29,** 221 (1923); **30,** 194 (1924).

[13] A. Hantzsch and W. Voigt, Ber. deut. chem. Ges. **62,** 975 (1929).

[14] A. Hantzsch, Ber. deut. chem. Ges. **60,** 1933 (1927).

[15] A. A. Maryott, J. Research NBS **38,** 527 (1947) RP1794.

[16] A. A. Maryott, J. Research NBS **41,** 1 (1948) RP1896.

[17] A. A. Maryott, J. Research NBS **41,** 7 (1948) RP1897.

[18] G. S. Hooper and C. A. Kraus, J. Am. Chem. Soc. **56,** 2265 (1934).

[19] J. A. Geddes and C. A. Kraus, Trans. Faraday Soc. **32,** 585 (1936).

[20] P. Mortier, Wis. Natuurkund. Tijdschr. **10,** 114 (1941).

[21] H. Goldschmidt, E. Marum, and L. Thomas, Z. physik. Chem. **129,** 223 (1927).

[22] J. Kendall, Proc. Roy. Soc. (London) [A] **85,** 200 (1911).

[23] H. Goldschmidt and H. Aarflot, Z. physik. Chem. **117,** 312 (1925).

[24] H. Goldschmidt, E. Marum, and L. Thomas, Z. physik. Chem. **132,** 257 (1928).

[25] R. B. Mason and M. Kilpatrick, J. Am. Chem. Soc. **59,** 576 (1937).

[26] F. H. Westheimer, J. Am. Chem. Soc. **61,** 1977 (1939).

[27] G. W. Wheland, The theory of resonance and its application to organic chemistry, p. 172 (John Wiley & Sons, Inc., New York, N. Y., 1944).

[28] G. W. Wheland, R. M. Brownell, and E. C. Mayo, J. Am. Chem. Soc. **70,** 2492 (1948).

[29] W. R. Remington, J. Am. Chem. Soc. **67,** 1838 (1945).

WASHINGTON, January 29, 1948.

U. S. Department of Commerce
National Bureau of Standards

Research Paper RP1998
Volume 42, June 1949

Part of the Journal of Research of the National Bureau of Standards

Transmission of Reverberant Sound Through Single Walls

By Albert London

The transmission of reverberant sound through homogeneous single walls has been investigated theoretically and experimentally. Random incidence sound-transmission measurements were made on homogeneous walls of aluminum, plywood, and plasterboard. The results were found to be in satisfactory agreement with a modified version of a theoretical treatment first given by Cremer, which postulates that the wall impedance has a resistive component in addition to its mass reactance and a stiffness reactance resulting from the occurrence of flexural waves. Two of three parameters that are required to predict the transmission loss, namely, resistance, and critical flexure frequency, the third one being mass, are evaluated from the experimental data in such a way as to obtain the best fit between the theoretical and experimental results. Conditions under which the mass law of sound transmission may be assumed to be valid are investigated in detail by studying the behavior of Rayleigh's transmission law, which takes into account the compressional waves induced in the wall.

Experimentally, it was found that considerable improvement in transmission loss could be obtained by applying a fairly substantial sound-absorbent blanket to one of the faces of a homogeneous wall.

I. Introduction

Previous investigators [1 to 5][1] have given theoretical treatments for the attenuation of a plane sound wave upon transmission through multiple partitions consisting of two or more septa separated by airspaces. In all of these derivations only normally incident sound waves are considered. Consequently, it is difficult to compare the theoretical predictions with the experimental results obtained on walls for which transmission loss characteristics are determined [6] under the excitation of reverberant sound fields containing random waves with random angles of incidence.

Also in the previous derivations [1 to 5], it has usually been assumed that each panel of the double wall combination has a mass reactance only. This is equivalent to assuming that each individual septum obeys the familiar mass law. However, it is well known that many homogeneous walls deviate considerably from the mass law. Consequently, it was necessary to investigate the transmission of reverberant sound through single walls. By utilizing a modified version of a treatment first given by Cremer [7], it was possible to determine a suitable equation of motion for each septum, which could then be inserted into the equations governing the transmission through the double wall.

In this paper, the attenuation of an obliquely incident plane sound wave upon transmission through a single wall is computed. By using the customary reverberant sound field statistics, the attenuation is integrated over all angles of incidence to give the average transmission loss. The same technique is applied in studying the transmission loss through double walls, which will be given in a subsequent paper. In addition to the theoretical treatment, experimental results on single and double walls will be given.

[1] Figures in brackets indicate the literature references at the end of this paper.

834349—49——6

II. Transmission Through Single Walls

1. Attenuation of an Obliquely Incident Wave

In figure 1, an oblique plane wave is incident at an angle θ on the infinite wall. If p_i is the acoustic pressure in the incident wave, then there will be a reflected wave with pressure p_r, and a transmitted wave with pressure p_t. It is required to determine the ratio p_i/p_t. Consider any small area of the wall located at point (0,0). Then

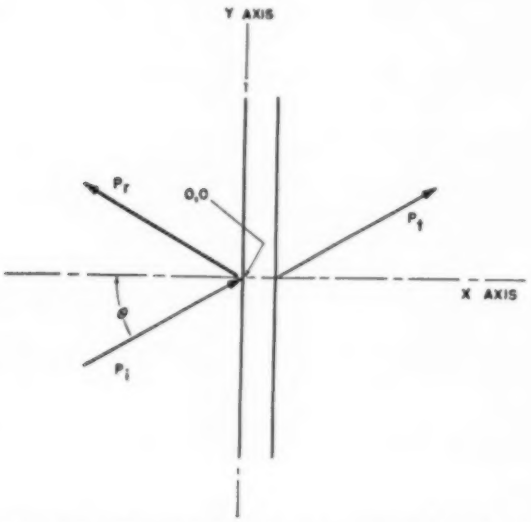

FIGURE 1. *Geometrical relation between incident, reflected and transmitted pressure waves.*

there are two conditions which obtain at the boundary between the sound field and the wall, which suffice to determine the desired ratio, that is, (1) continuity of X-component of particle velocity, and (2) the relation between the acoustic pressure difference acting across the interface and the motion of the wall.

Let the pressures be represented by expressions of the form:

$$\left.\begin{aligned} p_i &= P_i e^{i\omega t - ik(x\cos\theta + y\sin\theta)}, \\ p_r &= P_r e^{i\omega t - ik(-x\cos\theta + y\sin\theta)}, \\ p_t &= P_t e^{i\omega t - ik(x\cos\theta + y\sin\theta)}, \end{aligned}\right\} \tag{1.1}$$

where

$$k = \frac{2\pi}{\lambda} = \frac{\omega}{c},\ \lambda = \text{wavelength in air.} \tag{1.2}$$

The directions of propagation of the waves are in the x–y plane. As the particle velocity is related to the pressure by the expression

$$\dot{\xi}x = \frac{i}{\rho\omega}\frac{\partial p}{\partial x}, \tag{1.3}$$

the first boundary condition at point (0,0), results in the following:

$$P_i - P_r = P_t = \frac{\rho c \dot{\eta}_0}{\cos\theta}, \tag{1.4}$$

where $\dot{\eta}_0$ is the velocity amplitude of the wall in the x-direction, whereas the second boundary condition requires that

$$(P_i + P_r) - P_t = Z_w \dot{\eta}_0. \tag{1.5}$$

Here Z_w is the mechanical impedance per unit area of the wall. Whence, α, the ratio of the incident to transmitted amplitude becomes

$$\alpha = \frac{Pi}{P_t} = 1 + \frac{Z_w \cos\theta}{2\rho c}. \tag{1.6}$$

2. Basic Assumptions

In the derivation of eq. 1.6 it has been assumed that it is only necessary to consider a small area of the wall for which the projection of the wave front on it has practically constant phase. This treatment may be justified by the consideration that a reverberant sound field may be treated as the resultant of effects due to sections, having a small area, of wave packets with random angles of incidence and random phases. Also, use may be made of Schoch's [8] asymptotic law, which states that at sufficiently high frequencies above the fundamental frequency of a vibrating plate, the plate breaks up into small zones that vibrate independently of all other zones. Any small area of the plate vibrates in accordance with the sound pressure acting on this small area only.

Other assumptions that are implicit in this derivation can best be discussed with reference to a specific type of Z_w, that is, one in which the wall is assumed to have a mass reactance only, corresponding to which

$$Z_w = i\omega m, \tag{2.1}$$

where m = mass of wall per unit area. Now, Rayleigh [9], by considering the compressional waves induced in the wall by the action of the

sound waves, has shown that the attenuation is more generally given by

$$\alpha=\cos\,(a_1 l)+\frac{i}{2}\sin\,(a_1 l)\left[\frac{\rho_1 c_1}{\rho c}\frac{\cos\,\theta}{\cos\,\theta_1}+\frac{\rho c\,\cos\,\theta_1}{\rho_1 c_1\,\cos\,\theta}\right], \tag{2.2}$$

where

$$a_1=\frac{2\pi}{\lambda_1}\cos\,\theta_1.$$

l = thickness of wall.
θ_1 = angle of refraction of wave in wall.
ρ_1 = density of wall material.
c_1 = velocity of sound in wall material.
λ_1 = wavelength of sound in wall material.

In eq 2.2 a phase factor given by Rayleigh that does not effect the magnitude of $|\alpha|$ has been ignored since we shall concern ourselves only with absolute values. For $a_1 l \ll 1$, or $2\pi l/\lambda_1(\cos\,\theta_1)\ll 1$, eq 2.2 becomes

$$\alpha=1+\frac{i}{2}\frac{2\pi l}{\lambda_1}\cos\,\theta_1\left(\frac{\rho_1 c_1\,\cos\,\theta}{\rho c\,\cos\,\theta_1}+\frac{\rho c\,\cos\,\theta_1}{\rho_1 c_1\,\cos\,\theta}\right). \tag{2.3}$$

If we restrict ourselves to angles less than the critical angle as defined by Snell's law and as is explained below, then if $(\rho c\,\cos\,\theta_1)/(\rho_1 c_1\,\cos\,\theta)\ll 1$, which is equivalent to $(\rho c)/(\rho_1 c_1)\ll 1$ since $\cos\,\theta_1$ and $\cos\,\theta$ are of the same order of magnitude, eq 2.3 reduces to

$$\alpha=1+\frac{i\omega m\,\cos\,\theta}{2\rho c}, \tag{2.4}$$

which is identical with eq 1.6 when eq 2.1 is substituted in the latter equation. Thus, it will be seen that eq 2.4, which we shall call the mass law α is valid, provided the specific acoustic impedance of air, ρc, is much less than that for the wall material, and the thickness of the wall is much less than the wavelength of sound in the wall.

It is of interest to investigate the behavior of eq 2.2 in the vicinity of $\theta=90°$, since the mass law α, (eq 2.4) predicts that the incident wave will be totally transmitted at grazing incidence. First, it is to be noted that, in accordance with Snell's law

$$\frac{\sin\,\theta_1}{\sin\,\theta}=\frac{c_1}{c}, \tag{2.5}$$

and the critical angle of incidence θ_c is given by

$$\sin\,\theta_c=\frac{c}{c_1}, \tag{2.6}$$

or since for ordinary materials $c_1/c\gg 1$, we see that the critical angle of incidence is rather small. Thus, for a brick wall $c_1/c\approx 10$, and therefore $\theta_c\approx 6°$. For angles greater that θ_c $\cos\,\theta_1$, which may be written as

$$\cos\,\theta_1=\left\{1-\left(\frac{c_1}{c}\right)^2\sin^2\,\theta\right\}^{\frac{1}{2}}, \tag{2.7}$$

becomes imaginary, i. e., $\sin\,\theta>c/c_1$. Then let

$$\cos\,\theta_1=i\left\{\left(\frac{c_1}{c}\right)^2\sin^2\,\theta-1\right\}^{\frac{1}{2}}=i\,\cos\,\theta_1', \tag{2.8}$$

where $\cos\,\theta_1'$, from its definition, may be greater than unity, and also $a_1=ia_1'=i(2\pi/\lambda_1)\,\cos\,\theta_1'$. Equation 2.2 becomes

$$\alpha=\cosh\,(a_1' l)-\frac{i}{2}\sinh\,(a_1' l)\left[\frac{\rho c\,\cos\,\theta_1'}{\rho_1 c_1\,\cos\,\theta}-\frac{\rho_1 c_1\,\cos\,\theta}{\rho c\,\cos\,\theta_1'}\right]. \tag{2.9}$$

If $a_1' l\ll 1$, for $\theta>\theta_c$, then

$$\frac{l\omega}{c_1}\cos\,\theta_1'\approx\frac{l\omega}{c}\sin\,\theta\ll 1,$$

so that this condition corresponds to $l\ll\lambda<\lambda_1$, and is to be compared with the condition $l\ll\lambda_1$ when $\theta<\theta_c$, previously derived. Equation 2.9 by a first-order expansion of $\cosh\,(a_1' l)$ and $\sinh\,(a_1' l)$ becomes

$$\alpha=1+\frac{i}{2}\frac{m\omega}{\rho c}\cos\,\theta\left\{1-\left(\frac{\rho c}{\rho_1 c_1}\right)^2\frac{\left[\left(\frac{c_1}{c}\right)^2\sin^2\,\theta-1\right]}{\cos^2\,\theta}\right\}, \tag{2.10}$$

which for angles close to 90° reduces to

$$\alpha=1+\frac{i}{2}\frac{m\omega\,\cos\,\theta}{\rho c}\left\{1-\left(\frac{\rho}{\rho_1}\tan\,\theta\right)^2\right\}. \tag{2.11}$$

Thus total transmission occurs at an angle less than 90° when $\tan\,\theta=\rho_1/\rho$, and since $\rho_1/\rho\approx 10^3$, θ is very close to 90°. At 90°, however, the attenuation becomes infinitely great. Furthermore for angles not close to 90°, eq 2.11 reduces to the mass law α, (eq 2.4), even though $\theta>\theta_c$.

3. Average Attenuation for a Reverberant Sound Field

In a reverberant room, waves are incident at the transmitting wall from all possible directions. Since the phases are distributed at random, the

energy of the resultant wave is a summation of the energy of each individual wave component. Each packet of energy incident at angle θ, is greater than its corresponding transmitted packet by the factor $|\alpha|^2$. Let τ be the ratio of the total energy transmitted by the wall to the total energy incident on the wall, then in accordance with the usual reverberant sound field statistics [6]

$$\tau=\frac{\int_0^{\frac{\pi}{2}}\frac{\cos\theta\sin\theta\,d\theta}{|\alpha|^2}}{\int_0^{\frac{\pi}{2}}\cos\theta\sin\theta\,d\theta}=2\int_0^{\frac{\pi}{2}}\frac{\cos\theta\sin\theta\,d\theta}{|\alpha|^2}. \quad (3.1)$$

For a wall having a pure mass reactance, i. e. α defined by eq 2.4, the transmission loss (TL), which is defined as $10\log_{10}(1/\tau)$ is given by

$$TL=10\log\left(\frac{1}{\tau}\right)=10\log a^2-10\log[\ln(1+a^2)], \quad (3.2)$$

where

$$a=\frac{\omega m}{2\rho c}.$$

Equation 3.2 is the random incidence mass law, which is to be distinguished from the normal incidence mass law given by

$$TL=10\log(1+a^2), \quad (3.3)$$

which is readily obtained from eq. 1.6 and eq 2.1 by setting $\theta=0°$ and noting that in this case $1/\tau=|\alpha|^2$.

In table 1, a comparison between the normal and random incidence transmission loss values is made. Thus, it will be seen that the effect of random incidence is to materially reduce the transmission loss relative to what would be observed in the case of normal incidence.

TABLE 1. *Transmission loss*

Normal incidence	Random incidence	Difference
db	*db*	*db*
10	5.9	4.1
20	13.3	6.7
30	21.6	8.4
40	30.4	9.6
50	39.4	10.6
60	48.6	11.4

Neither the normal nor the random incidence mass law agrees with experimental results on lightweight walls to be described below. However, it is possible to obtain reasonable agreement with experiment if it is postulated that the wall impedance Z_w contains in addition to its mass reactance a resistive term. For this purpose it is assumed that

$$Z_w=\frac{2r}{\cos\theta}+i\omega m, \quad (3.4)$$

and in accordance with eq 1.6, there results

$$\alpha=1+R+i\frac{\omega m\cos\theta}{2\rho c}, \quad (3.5)$$

where $R=r/\rho c$, the resistance in ρc units. Furthermore, in this case the transmission loss becomes

$$TL=10\log a^2-10\log\left[ln\left\{1+\left(\frac{a}{1+R}\right)^2\right\}\right]. \quad (3.6)$$

From the method used in introducing the resistance coefficient r in eq. 3.4, it will be seen that it has been assumed that a normally incident wave experience much less resistance than a wave at oblique incidence. This seems to be a natural assumption to make, since it is to be expected that a wave at almost grazing incidence would have high attenuation in passing through the material because of its long path length, whereas a normally incident wave would have little attenuation because of its short path length. In addition, from eq 3.5 it will be seen that the effect of the resistive term is to reduce the high transmission obtained at grazing incidence for the random incidence mass law. Since at low frequencies the mass reactance is rather small, while R is independent of frequency, the effect of R will be to increase the low frequency transmission loss, whereas at high frequencies it will have negligible effect.

In figure 2, application of the random incidence mass law, eq 3.2, and the more general equation that includes the resistance term, eq 3.6, to experimental results obtained on a $\frac{1}{64}$-in. aluminum wall are shown. It will be seen that eq 3.6 may be made to fit the experimental data if R is taken to be 2.16. The optimum value of R was determined empirically so as to give the best fit with the data.

In the next section we shall consider modifications required in Z_w when flexural waves are excited in the wall. Before taking leave of the

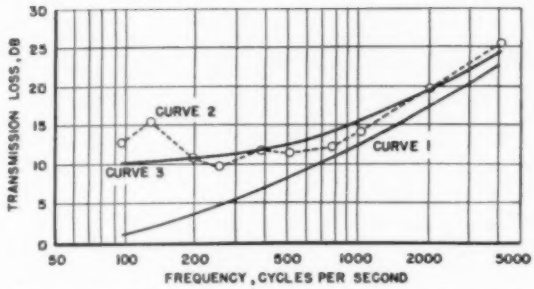

FIGURE 2. *Transmission loss of a 1/64-in. aluminum wall.*

$m=0.12$ g/cm^2. Curve 1: transmission loss $=10 \log a^2-10 \log [\ln(1+a^2)]$; curve 2: experimental; curve 3:

$$\text{transmission loss}=10 \log a^2-10 \log\left[\ln\left\{1+\left(\frac{a}{1+R}\right)^2\right\}\right], \text{ where } R=2.16.$$

present discussion we need to investigate further the relationship between Rayleigh's exact expressions (eq 2.2 and 2.9) and the random incidence mass law.

Since the mass law in the form of eq 2.11 holds only when $a_1'l \ll 1$, it is of interest to determine what limitations occur as a result of this restriction. From eq 2.9, for $\rho c \cos \theta_1' \ll \rho_1 c_1 \cos \theta$, which is valid for all values of θ except those very close to 90°, provided $\rho \ll \rho_1$, we may write

$$|\alpha|^2=\cosh^2 (a_1'l)+\frac{1}{4} \sinh^2 (a_1'l) \left(\frac{\rho_1 c_1 \cos \theta}{\rho c \cos \theta_1'}\right)^2. \quad (3.7)$$

For small $a_1'l$ we take $\cosh a_1'l=1$ and $\sinh a_1'l=a_1'l$. This substitution results in the mass law $|\alpha|^2$. Since both the cosh and sinh increase with increasing argument, we wish to find an upper bound to $a_1'l$ such that the deviation of eq 3.7 from the mass law will not be too great. Furthermore, the second term of the right-hand side of eq 3.7 is much greater than the first, so that practically all of the deviation will be due to $\sinh (a_1'l) > a_1'l$. If we use the value of $a_1'l$ such that $\sinh^2(a_1'l)/(a_1'l)^2=2$, there will be approximately 3 db more loss for this value of $a_1'l$ as compared to the mass law. When $a_1'l=1.5$, $[\sinh(a_1'l)]/(a_1'l)=1.4195$, which is a sufficiently close approximation to $\sqrt{2}$. This results in

$$\sin \theta=\frac{1.5c}{\omega l} \leqslant 1, \quad (3.8)$$

where ω is 2π times the frequency in c/s, l is the thickness in centimeters. The value of θ, provided $\theta \leqslant 90°$, defined by eq 3.8, say θ_m, may be taken as the maximum angle of incidence for which the mass law expression (eq 2.4) represents very closely the Rayleigh expression (eq 2.9).

The whole state of affairs is pictured in figures 3 and 4 for the case of a brick wall for which the physical constants were taken as $\rho_1=1.5$ g/cm^3, $c_1=4.3\times10^5$ cm/sec, $c_1/c=12.5$, $l=2$ in. for $f=4{,}096$ cps, or $l=4$ in. for $f=2{,}048$ cps, etc. It will be seen from figure 3 that θ_m in this case is about 24°, and the Rayleigh expression (eq 3.7) for angles greater than θ_m results in values for $|\alpha|^2$, which are much larger than the $|\alpha|^2$ obtained from the mass law. Figure 4 shows that the τ integral (eq 3.1), using the integrand ν_m corresponding to the mass law and integrating to 90° will result in a value of τ that is much larger than that which the Rayleigh expression would give. To obtain an accurate value of τ under such circumstances, it would be necessary to integrate the exact Rayleigh expression. However, a rough approximation to the integral could be obtained by integrating the mass law expression from $\theta=0°$ to $\theta=\theta_m$. The accuracy of this approximation would increase as θ_m increases. Thus, if we let $u=\cos^2\theta$, and θ_m be the maximum angle

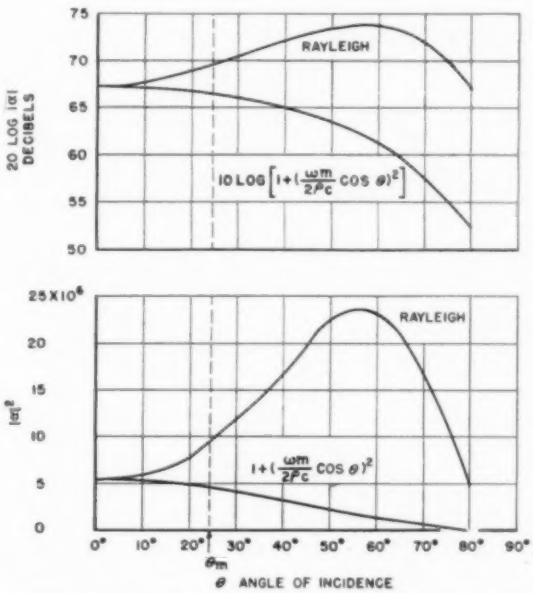

FIGURE 3. *Comparison between $|\alpha|^2$ obtained from Rayleigh's expression, eq 2.9 and mass law $|\alpha|^2$.*

Calculations for a brick wall: 2 in. thick at 4,096 c/s; 4 in. thick at 2,048 c/s; 8 in. thick at 1,024 c/s, etc.

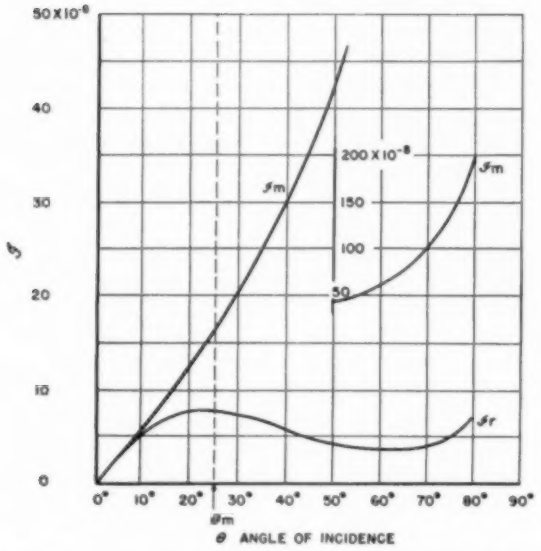

FIGURE 4. *Comparison between τ integrand obtained from Rayleigh's expression, eq 2.9, and from mass law* $|\alpha|^2$ *(plotted in fig. 3).*

$\mathcal{J}=\frac{2\sin\theta\cos\theta}{|\alpha|^2}$, i. e., $\tau=\int_0^{\frac{\pi}{2}}\mathcal{J}d\theta$; $\mathcal{J}_r$ corresponds to the Rayleigh expression $\mathcal{J}$; $\mathcal{J}_m$ corresponds to the mass law $\mathcal{J}$.

of incidence for which the integral (eq 3.1) will be evaluated, we have from eq 3.8

$$u_m=\cos^2\theta_m=1-\frac{2.25c^2}{\omega^2l^2}, \tag{3.9}$$

where $0\leq u_m\leq 1$
and eq 3.1 becomes (using $Z_w=i\omega m$)

$$\tau=\int_{u_m}^{1}\frac{du}{1+a^2u}=\frac{1}{a^2}\,ln\,\frac{1+a^2}{1+a^2u_m}. \tag{3.10}$$

Now

$$a^2u_m=\frac{\omega^2\rho_1{}^2l^2}{4\rho^2c^2}\left[1-\frac{2.25c^2}{\omega^2l^2}\right],$$

or

$$u_m=1-\frac{0.56\rho_1{}^2}{a^2\rho^2}. \tag{3.11}$$

Since $u_m=0$, when $\theta_m=90°$, we see that restrictions on the maximum angle of integration begin to occur only when $0.56\rho_1{}^2/a^2\rho^2\approx 1$, which, since $(\rho_1/\rho)^2\approx 10^6$, means that this phenomenon should be taken into account only when the wall is of such a nature that its normal incidence transmission loss is of the order of magnitude of 60 db or greater. In this case it would be much better to use the exact Rayleigh expression than to attempt to use eq 3.10.

4. Flexural Waves; Experimental Results

The case of flexural waves has been discussed in some detail by Cremer [7]. We shall state his results and point out wherein the present method differs somewhat from his presentation.

By using the wave equation for the motion of an infinite plate, Cremer shows that the wall impedance for a plane wave incident at any angle becomes

$$Z_w=i\omega m\left[1-\frac{P\omega^2}{mc_1{}^4}\right], \tag{4.1}$$

where

$$P=\frac{Qf^3}{12(1-s^2)}$$

Q = Young's modulus

s = Poisson's ratio

c_1 = Velocity of flexural wave.

In the above the velocity of the wall in the x-direction is represented by

$$\dot{\eta}=\dot{\eta}_0e^{i\omega t-ik_1x},$$

where $k_1=\omega/c_1=2\pi/\lambda_1$, λ_1 = wavelength of sound in the wall. The wall thickness is assumed to be small compared to λ and λ_1. Hence no x-dependent term occurs in $\dot{\eta}$.

The appearance of the negative reactance term in the wall impedance is evidently due to the plate stiffness. It will be seen that it is possible for Z_w to become zero at the frequencies for which the bracketed term goes to zero in eq 4.1. The coupling between the acoustic wave and the flexural wave is given by the condition

$$c=c_1\sin\theta, \tag{4.2}$$

where c is the velocity of sound in air. Furthermore, it is readily shown that if c_f is the velocity of a flexural wave in the absence of driving forces, then

$$c_f{}^4=\frac{P\omega^2}{m} \tag{4.3}$$

so that Z_w becomes

$$Z_w=i\omega m\left(1-\frac{c_f{}^4}{c^4}\sin^4\theta\right). \tag{4.4}$$

It is to be noted that Z_w becomes zero when $c_f=c_1$, that is, when the velocity of the free flexural wave is the same as that of the driven flexural wave. This phenomenon Cremer has called the coincidence effect. The lowest frequency, f_c, at which the coincidence effect takes place occurs when $\theta=\pi/2$ and is given by

$$\frac{P\omega_c^2}{mc^4}=1. \tag{4.5}$$

Now

$$\frac{c_f^4}{c^4}=\frac{P}{mc^4}\omega^2=\frac{f^2}{f_c^2},$$

or eq. 4.4 may be written as

$$Z_w=i\omega m\left(1-\frac{f^2}{f_c^2}\sin^4\theta\right). \tag{4.6}$$

By determining Young's Modulus from measurements on longitudinal waves in a long bar of the wall material, an expression for P in eq 4.5 can be derived that results in the following expression for f_c

$$f_c=\frac{\sqrt{3}c^2(1-s^2)^{\frac{1}{2}}}{\pi c_l l}, \tag{4.7}$$

where c_l is the velocity of a longitudinal wave in the bar, and l is the plate thickness.

So far we have not considered the effect of a resistance term in Z_w. Cremer introduces the dissipation effect by replacing Q by $Q\ (1+i\ \epsilon)$, where $\epsilon\ Q$ is the complex part of Young's Modulus which results in damping. However, when it was attempted to use this method in experiments described below, extremely large values of ϵ were required to give any reasonable answers. In addition, the dissipation term had the wrong functional dependence on angle of incidence. It will also be seen that for frequencies much below f_c, eq 4.6 regains its simple mass law form, the complex Young's Modulus would have no effect, and this theory would predict no dissipation for thin partitions. Thus, for the $\frac{1}{64}$-in. aluminum wall shown in figure 2, $f_c=30{,}000$ cps, so that no flexural effects would appear at audio frequencies, and consequently no dissipation would appear if we followed Cremer's treatment. Accordingly, we introduce the resistance term here in the same way as in section II, 3. The complete expression for α, including flexural effects is then

$$\alpha=1+R+\frac{i\omega m\cos\theta}{2\rho c}\left(1-\frac{f^2}{f_c^2}\sin^4\theta\right), \tag{4.8}$$

and τ is obtained from $|\alpha|^2$ by eq 3.1. Unfortunately, the integral (eq 3.1) appears to be unintegrable in general in terms of elementary functions. Hence in what follows, numerical integration was utilized.

From eq 4.8 it will be seen that the transmission loss will depend on three constants R, m, and f_c. Of these three constants, m is known, f_c can be computed from eq 4.7 if all the other constants in this equation are known or measured, while R is unknown. Experimental measurements of transmission loss were made on ½-in. plywood, and ½-, 1-, and 2-in. plasterboard walls. The R and f_c were determined empirically by choosing those values that gave the best fit with experimental results. R was determined by fitting an equation of the form eq 3.6 to the experimental data for frequencies from the lowest up to about one octave below the value of f_c.

In the case of figure 5, which is the transmission loss for a ½-in. plywood wall, two critical flexure frequencies were computed, i. e., $f_c=900$ c/s, or $f_c=1{,}885$ c/s. The first value corresponds to c_l for fir wood for a wave parallel to the wood fiber of 5.2×10^5 cm/s. The second value corresponds to c_l for a wave perpendicular to the fibers equal to 2.4×10^5 cm/sec. The best fit was obtained for $f_c=1{,}885$ c/s. In addition to $f_c=900$ c/s, an $f_c=2{,}048$ c/s, where the dip in the experimental curve occurs, was also tried.

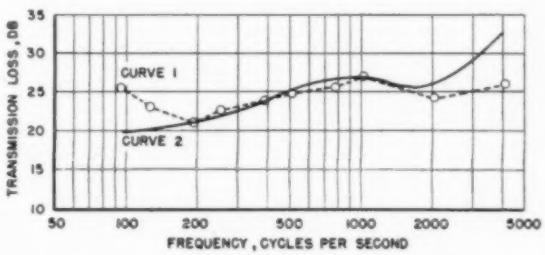

FIGURE 5. *Transmission loss of a ½-in. plywood wall.* $m=0.70$ g/cm². Curve 1: experimental; curve 2: $R=8.3$, $f_c=1885$.

Figures 6, 7, and 8 give the results obtained on different thicknesses of plasterboard. In the ½-in. plasterboard case, there is some doubt as to which is a better fit, $f_c=2{,}048$ c/s or $f_c=4{,}096$ c/s. From eq 4.7 it is to be expected that f_c for the various thicknesses of plasterboard should be inversely proportional to thickness. Consequently, if $f_c=512$ c/s be taken as correct for the 2-in. wall,

then f_c should be 1,024 c/s for the 1-in. and 2,048 c/s for the ½-in. wall. The experimental results roughly approximate this sequence of values for f_c.

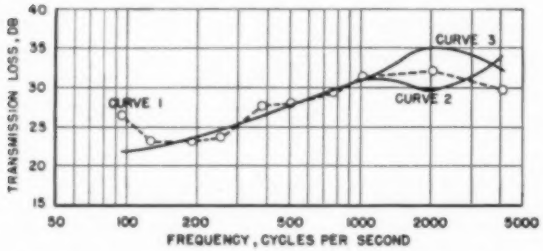

FIGURE 6. *Transmission loss of a ½-in. plasterboard wall.*
$m = 1.02$ g/cm². Curve 1: experimental; curve 2: $R = 10.5$, $f_c = 2{,}048$; curve 3, $R = 10.5$, $f_c = 4{,}096$.

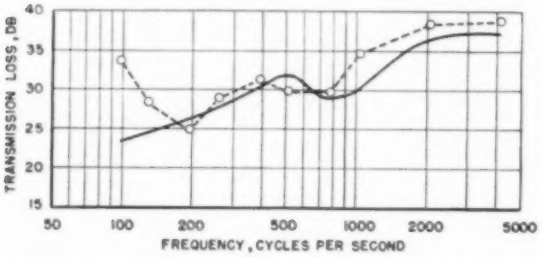

FIGURE 7. *Transmission loss of a 1-in. plasterboard wall.*
$m = 2.03$ g/cm². Dotted curve: experimental; solid curve 2: $R = 10.5$, $f_c = 768$.

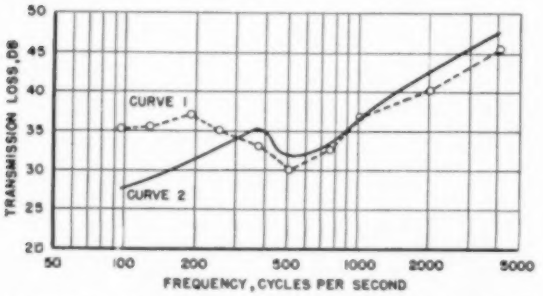

FIGURE 8. *Transmission loss of a 2-in. plasterboard wall.*
$m = 4.06$ g/cm². Curve 1: experimental; curve 2, $R = 15.3$, $f_c = 512$.

The variation of R with thickness is worth noting. No appreciable change was observed between the ½-in. and 1-in. wall, whereas an approximately 50-percent increase occurred between the 1-in. and 2-in. wall. Although the experimental points lie above the theoretical curves at the lowest frequencies, it is not possible to change R without changing the predicted transmission loss at the minimum point at which flexural effects are pronounced, and also the theoretical transmission loss curve in the low-frequency region will go up or down accordingly as R is increased or decreased. To some extent, the rather slow variation of R with thickness indicates that some of the dissipation may be due to the type of mounting or restraints at the boundaries of the wall. Since this was the same for all three walls, it would not be expected to change. The walls were slightly less than 6 by 7½ ft in size and were wedged in place in an opening of this size and then sealed in with a gypsum plaster seal. Experimental details are given in [6].

5. Transmission Through Inhomogeneous Walls

In this section we consider some additional experimental data bearing on the transmission of sound through single walls of an inhomogeneous character.

We consider the case of a wall having a thin veneer of a different material on its surface. The wall has a flexual frequency of f_c, occurring in the audio range, whereas the veneer has an f_c outside of the audio range. It might be expected that such a combination would have an f_c somewhere between the two extreme values, so that the composite panel would begin to deviate from its mass law characteristics at a frequency somewhat higher than that of the wall without the veneer, thus resulting in an over-all higher transmission loss. In figure 9 are shown the results on a composite panel of this type. In this experiment the base panel was the ½-in. plywood wall of figure 5, to which was applied a 1/64-in. aluminum sheet on both faces by glue and tacks. No significant in-

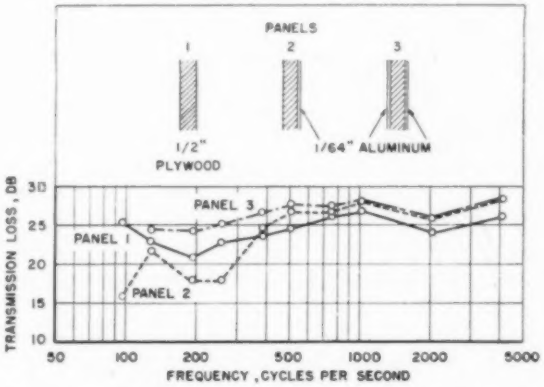

FIGURE 9. *Transmission loss of a ½-in. plywood wall with 1/64-in. aluminum faces.*

crease was observed over and above what would be expected on the basis of an increase in mass. Thus, it may be concluded that a thin veneer relative to a thicker core can have little effect on the over-all transmission loss. This bears on the question of the acoustic effectiveness of lining doors with metal.

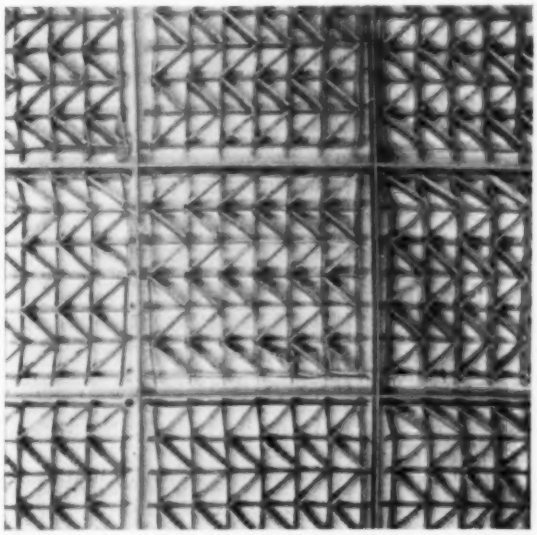

FIGURE 10. *Egg-crate separators used to prevent transverse modes at wall surface.*

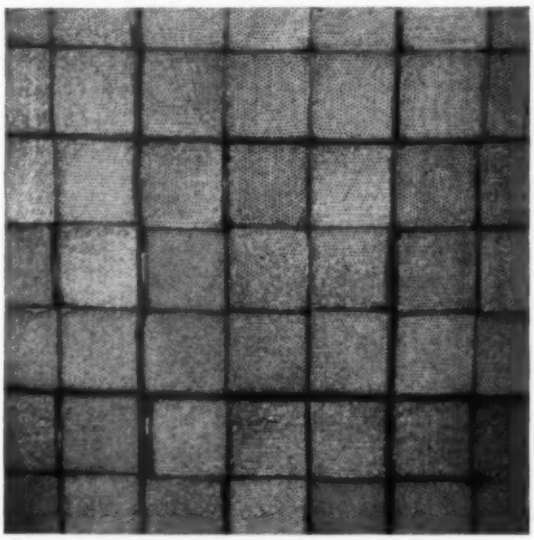

FIGURE 11. *Strawcomb used in attempt to filter out waves incident at oblique angles.*

Another type of experiment that was tried is illustrated in figures 10 and 11. Here it was attempted to filter out obliquely incident waves by inserting a honeycomb structure in front of the wall so that waves travelling at or near grazing incidence would be impeded. The first structure tried consisted of egg crate separators shown in figure 10. The next structure consisted of soda straws about 2¾ in. long placed in front of the wall (fig. 11). There were approximately 150,000 straws used in the "strawcomb" shown in the figure. The principle involved is that if obliquely incident waves can be filtered out, then the transmission phenomena would be due solely to normally incident waves, thus eliminating flexural vibrations and raising the transmission loss compared to the random incidence case. The results obtained in a series of tests in which the strawcomb was placed in front of various thicknesses of plasterboard are shown in figure 12. Although some increase in transmission loss was experienced, it was hardly as much as one might expect. Upon considering the action of the straws in greater detail it will be seen that for frequencies such that the wavelength is much greater than the

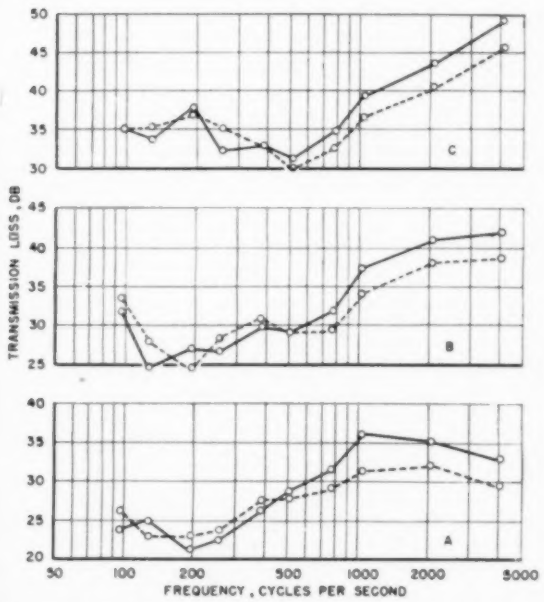

FIGURE 12. *Effect of placing strawcomb of figure 11 in front of plasterboard walls.*

A, ½-in. plasterboard; B, 1-in. plasterboard; C, 2-in. plasterboard. ——, tests made with 2⅞-in. strawcomb in front of wall; — —, strawcomb removed.

834349——7——49

2¼-in. straw length, the straws do not essentially change the boundary conditions (1) and (2) given in section II, 1. Thus the total pressure acting at the mouth of each straw is p_i+p_r, whereas the x-component of particle velocity is certainly continuous, inasmuch as this is the only component that would be transmitted down the straw. The particle velocity is increased somewhat inside the straw because the solidity, i. e., the ratio of wall volume to total volume, was of the order of 10 percent. We are thus led to the conclusion that a strawcomb of this type could not change the behavior of the wall to any great extent with the exception that transverse interference patterns or normal modes in the room located at the wall face would be broken up by the strawcomb. Meyer [2, 3] has indicated that in the case of double walls such modes tend to reduce the effectiveness of the double wall. We shall discuss this use of the strawcomb in double walls in a subsequent paper.

The improvement in transmission loss obtained at the higher frequencies by use of the strawcomb may have been due to an absorbent effect of such a structure. Some measurements of the improvement in transmission loss obtained by hanging an absorbent blanket immediately in front on the source side of the plasterboard walls of figure 12 (without strawcomb) are shown in figure 13,

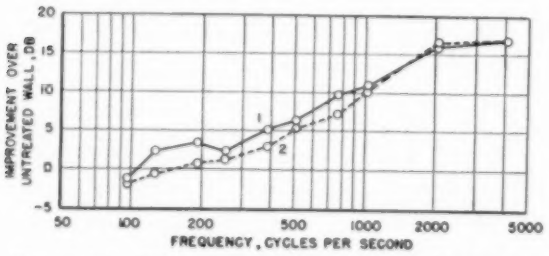

FIGURE 13. *Effect of applying an absorbing blanket to a homogeneous wall.*

---○---, 3-in. glasswool, 1.0 lb/ft³ on plasterboard walls; —○—, 1¾-in. hairfelt, 1.2 lb/ft³ on plywood walls.

curve 1. The absorbent in this case was 3 in. of glass wool having an average density of 1 lb/ft². The improvement resulting from the addition of the glass wool blanket was approximately the same for the ½-, 1-, and 2-in walls. Accordingly, the average increase in loss for these three walls is plotted in figure 13. Curve 2 of figure 13 gives the results obtained on the improvement resulting from gluing on to the far or receiving room side of a ½-in. plywood wall, 1¾-in. hair felt having an average density of 1.2 lb/ft². Some additional improvement, of the order of 3 db, is obtained by gluing rather than hanging the blanket loosely. A general discussion of this problem has been given by Cook [10]. It will be seen from figure 13 that this type of treatment produces a rather large effect. Consequently, it should be borne in mind in practical noise reduction problems. In addition to the improvement in transmission loss, use may be made of the absorption provided by the blanket to increase the over-all noise reduction.

One other observation is probably pertinent from a practical point of view. In the case of the plasterboard wall series, if the improvement in transmission loss that results from doubling the mass of the wall is averaged over all 10 test frequencies, it will be found that doubling the mass results in an average improvement of approximately 4 db. This result is in accord with previous data [11, 12].

III. Conclusion

The experimental results and theoretical treatment show that there are three important physical properties of a homogeneous wall, namely, its mass, internal damping or dissipation, and its ability to propagate flexural waves, which determine its sound transmission loss. Furthermore, the importance of the effect caused by random angles of incidence of the sound waves in a reverberant room has been demonstrated. The experimental results were utilized to determine the values of R and f_c for the different walls in question. This effectively determines the value of the wall impedance, Z_w. Knowing Z_w it will be possible to investigate the performance of double walls consisting of two single walls separated by an airspace. This will be considered in a subsequent paper.

The author acknowledges the assistance of Seymour Edelman and Henry J. Leinbach, Jr., who carried out the experimental observations.

IV. References

[1] J. E. R. Constable, Phil. Mag. **18,** 321 (1934).
[2] E. Meyer, Elek. Nachr. Tech. **12,** 393 (1935).
[3] E. Meyer, Z. Tech. Phys. **16,** 565 (1935).
[4] D. G. Hunt, Can. J. Research **12,** 398 (1935).
[5] A. L. Kimball, J. Acous. Soc. Am. **7,** 222 (1936).
[6] A. London, J. Research NBS **26,** 419 (1941) RP1388.
[7] L. Cremer, Akust. Z. **7,** 81 (1942).
[8] A. Schoch, Akust. Z. **2,** 113 (1937).
[9] Lord Rayleigh, Theory of sound **2,** sec. 271, p. 186 (Dover, N. Y., 1945).
[10] R. K. Cook, Radiation of sound by a vibrating absorber, J. Acous. Soc. Am. **19,** Abstract No. 35, p. 729 (1947).
[11] V. L. Chrisler and W. F. Snyder, Soundproofing of airplane cabins, BS J. Research **2,** 897 (1929) RP63.
[12] Albert London, Principles, practice, and progress of noise reduction in airplanes, Tech. Note No. 748, National Advisory Committee for Aeronautics (Jan. 1940).

WASHINGTON, February 16, 1949.

U. S. Department of Commerce
National Bureau of Standards

Research Paper RP1999
Volume 42, June 1949

Part of the Journal of Research of the National Bureau of Standards

Separation and Identification of the Major C_7 to C_{10} Components of Triptene Residue

By Philip Pomerantz, Thomas W. Mears, and Frank L. Howard

As a part of an investigation conducted under the auspices of the National Advisory Committee for Aeronautics, the Bureau of Aeronautics of the Department of the Navy, and the Department of the Air Force, embracing the synthesis and isolation of highly branched hydrocarbons, a series of systematic distillations was carried out on "triptene residue," a synthetic alkylate made at the Radford Laboratories of the General Motors Corporation.

This report describes the isolation thereby of two heptenes, four octenes, and three nonenes; the identification of four heptenes, two octenes, three nonenes, and six decenes not resolvable by fractional distillation; and the isolation of two heptanes, two octanes, one nonane, and five decanes formed by hydrogenation of mixtures of olefins. Physical constants for the isolated products and graphs showing the course of the several distillations are presented.

The analysis presented is based, where individual olefins were isolated, on the distillation curves; where the mixtures obtained by distillation were more complex, the analysis is based on ozonolysis data and/or distillation data of the hydrogenated product.

The mechanism of successive methylation by which the several olefins in the mixture were derived has been shown to be valid.

I. Introduction

The work described herein is part of an investigation conducted for the National Advisory Committee for Aeronautics, the Bureau of Aeronautics of the Department of the Navy, and the Department of the Air Force on the synthesis and purification of highly branched hydrocarbons for the determination of their physical properties and for a study of their antiknock characteristics. This report describes the isolation and physical properties of a number of hydrocarbons obtained from triptene residue by systematic fractionation and the identification of several others not isolated.

Triptene residue is a byproduct of the manufacture of 2,3,3-trimethyl-1-butene (triptene). The details of the process and the mechanism of the chemical reactions involved have been presented [22][1] by Verle A. Miller and W. G. Lovell.

As shown by Miller and Lovell, the process consists essentially of reacting methyl chloride with the dehydration products of tertiary amyl alcohol, in the presence of a specially prepared lime, to yield hydrocarbons of higher molecular weight.

The olefin reactants consist primarily of 2-methyl-2-butene and lesser amounts of 2-methyl-1-butene and 3-methyl-1-butene. Under the proper conditions, the olefins are methylated at the double bond to yield a more complex mixture of hexenes. The first step in the methylation is believed to proceed as illustrated below.[2]

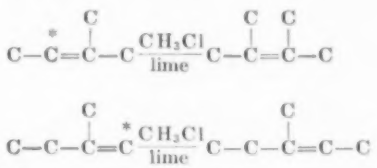

[1] Figures in brackets indicate the literature references at the end of this paper.

[2] Asterisks indicate point of methylation.

The hexenes can react further to yield heptenes, the most important of these being triptene. This methylation step is shown below.

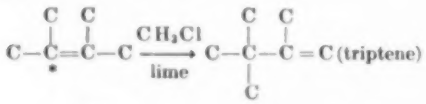

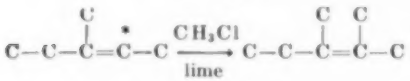

Successive, stepwise methylations of portions of the heptenes yield octenes, nonenes, decenes, and higher boiling materials.

Figure 1 [3] shows the postulated course of the methylations of the methylbutenes and the olefins isolated and/or identified in this work.

The compound 2,3,3-trimethyl-1-butene (triptene) is the component of the methylation products that is of the greatest interest, the methylation reaction being used primarily to produce this olefin. Besides having a high knock-rating, triptene is the precursor, by hydrogenation, of 2,2,3-trimethylbutane (triptane), a compound having exceptional engine behavior. Large amounts of

[3] This figure was adapted from the one published by Miller and Lovell [22]. This altered chart is reproduced by permission of the Editor of Industrial and Engineering Chemistry.

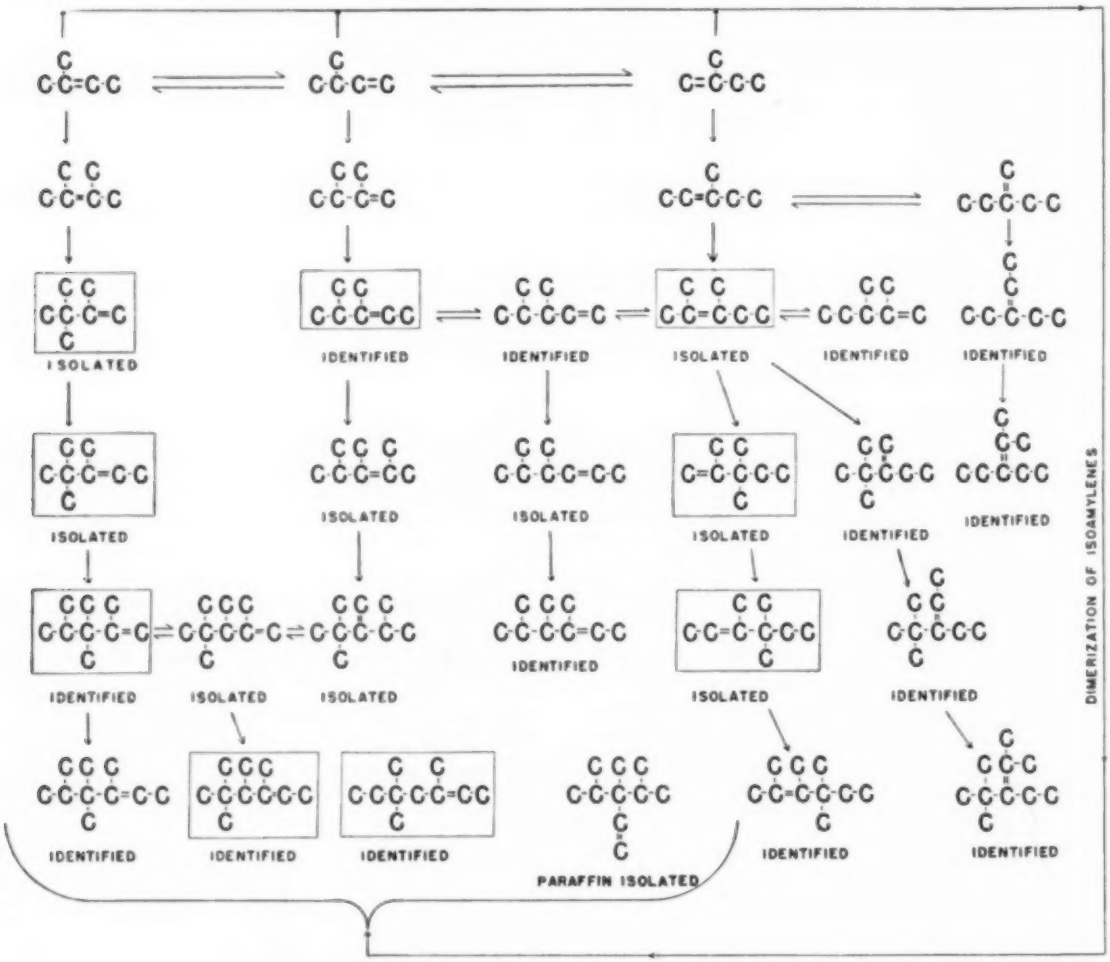

FIGURE 1. *Olefins isolated or identified in triptene residue.*

Principle products are enclosed by rectangles.

triptene were made by methylation at the Redford Laboratories of the General Motors Corporation, separated from the reaction mixture by distillation, and then hydrogenated to triptane. The "bottoms" from this distillation is designated as triptene residue.

The identity of the components of triptene residue aroused considerable interest at the Redford Laboratories, because the verification of the presence of certain structures as formulated in figure 1 would throw light on the mode of methylation. The work that had been done on this problem at the Redford Laboratories had been performed on the hydrogenated heptene and octene portions. More conclusive evidence, in the form of the identification of olefins, was needed, particularly in the nonene and decene range.

In addition, interest was directed in this laboratory to the composition of triptene residue because several highly branched members shown in figure 1 were needed in large quantities for engine tests and for synthetic work, and this alkylate appeared to be the most promising source of these compounds. Accordingly, by arrangement with General Motors Corporation, work was started on the fractionation of triptene residue in order to identify the major constituents of the alkylate through the decene range, and to isolate any hydrocarbons that could be obtained by fractional distillation.

II. Equipment and Methods

1. Distillation Equipment

There were seven stills available for this study; these are listed in table 1. A more complete description of these stills is given in a previous report [14]. Still 9, having an efficiency of about 40 theoretical plates at total reflex, was used for the fractionation of the oily layer arising from the ozonization of fractions of triptene residue.

TABLE 1. *Distillation columns*

Still number	Type	Size	Material of construction	Packing	Number of theoretical plates (approx.)	Operating reflux	Pot capacity
		In.				*Liters/hr.*	*Gal.*
9	Total reflux variable takeoff.	16 by ¼	Glass	3/64-in. stainless steel helices made from 0.006-in. wire.	40		0.1
11	do	240 by 2	Monel	3/32-in. stainless steel helices made from 0.010-in. wire.	65	4 to 6	15
12	do	600 by 4	Galvanized steel	3/8-in. unglazed porcelain raschig rings	100	45 to 50	55
13	do	600 by 4	do	do	100	45 to 50	55
14	do	600 by 2	Stainless steel	3/32 in. stainless steel helices made from 0.010-in. wire.	200	4 to 6	55
17	Podbelniak Hypercal	72 by 1	Glass	Heli-Grid	100	2 to 3	1
22	Total reflux variable takeoff.	72 by 1	do	3/16-in. glass helices	35	2 to 3	1

Stills 11 to 14, inclusive, are of the total condensation partial-takeoff type and were constructed for analysis of commercial crudes, purification of large amounts of materials, and for isolation of hydrocarbons from commercial mixtures. Stills 12, 13, and 14 were used to process the bulk of the triptene residue, whereas still 11 was used for redistillation of several cuts and for the isolation of paraffins from several of the hydrogenated cuts. Still 17 was used for analytical distillation of small amounts of material and of hydrogenated cuts and for redistillation of "heart cuts" of the several plateaus obtained from distillation of the triptene residue.

Still 22 is a glass column of the Whitmore-Lux type; it was used for exploratory distillations of material as received from the General Motors Corporation.

2. Fractionations

The material available for the present study was a 980-gallon shipment from the Redford Laboratories, which consisted of triptene residue, as defined previously, containing all of the material from the methylation product boiling above triptene.

An exploratory distillation of a 2,850-ml sample of triptene residue as received was conducted in still 22 at a reflux ratio of 25 to 1. This was done to serve as a guide in conducting the later distilla-

tions of large quantities of material. The results obtained from this distillation of triptene residue are shown in figure 2.

Since this preliminary test showed that the triptene residue could be separated readily into four portions containing, respectively, heptenes, octenes, nonenes, and decenes, a series of distillations were performed on the bulk of the material in stills 12 to 14 inclusive, and at a reflux ratio of 25 to 1, to separate the entire material and to obtain larger quantities for subsequent investigation. In this series of distillations, material boiling in the range 75° to 171° C from each run of triptene residue was collected in 1-quart samples. (Distillation was carried out to 171° C in order to assure inclusion of all the decenes). Corresponding fractions from the several distillations were then combined. This operation yielded four major fractions designated as H, O, N, and D, which were concentrates, respectively, of the heptene, octene, nonene, and decene portions of the triptene residue. These fractions are listed below:

Fraction	Boiling point range	Volume	Volume
	°C	gal	%
H	75 to 100	320	33
O	100 to 118	390	40
N	118 to 143	54	5
D	143 to 171	98	10
Residue and loss		118	12

Each of the four portions, H, O, N, and D was redistilled at a reflux ratio of about 100 to 1 in stills 12 and 13. In several cases, plateaus representing relatively pure substances were obtained. Figures 3 to 6 represent the results of this operation. In this series of distillations, the residue of the heptene cut was added to the octene cut; the residue from this was added to the nonene portion, and so on. Table 2 lists some of the physical properties of the plateaus obtained from this series of redistillations.

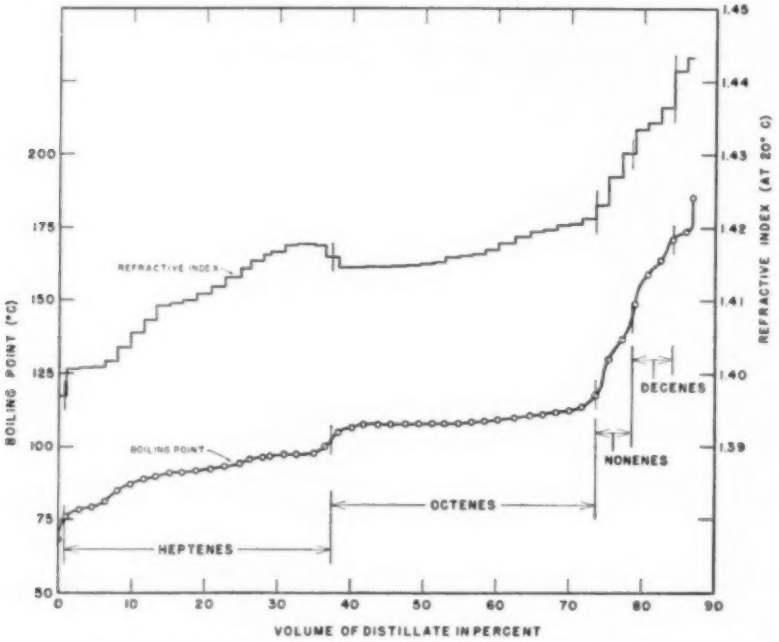

FIGURE 2. *Exploratory distillation of triptene residue as received.*

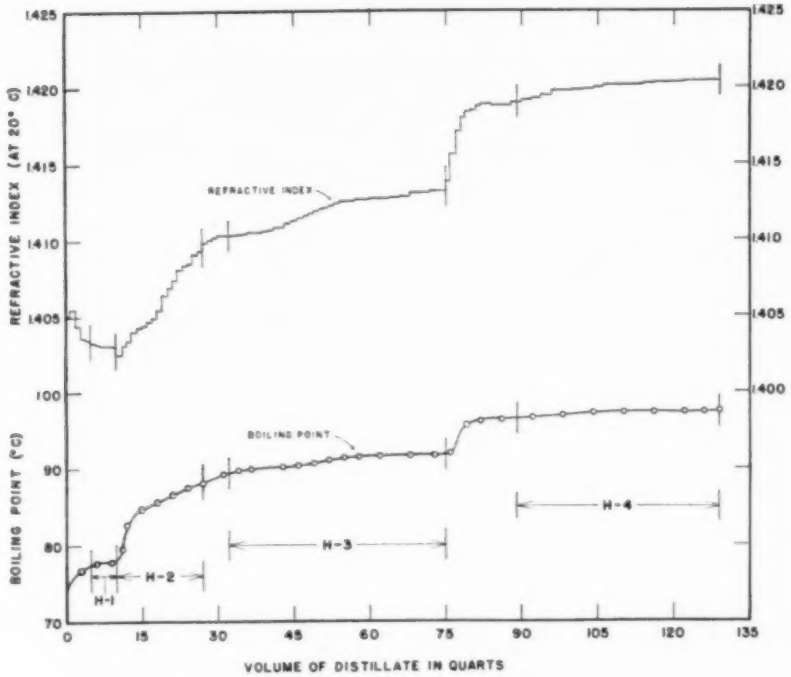

FIGURE 3. *Redistillation of the preliminary heptene cut.*

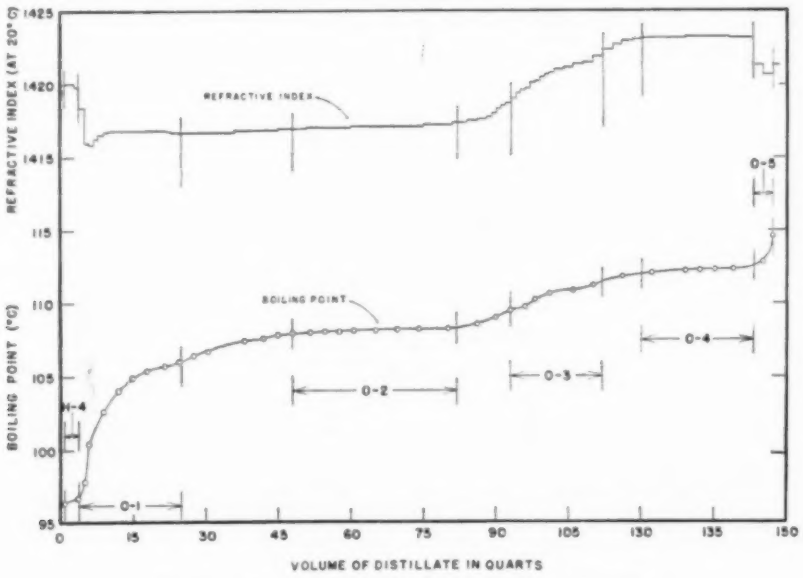

FIGURE 4. *Redistillation of the preliminary octene cut.*

Cut	Boiling range of cut	Refractive index of cut n_D^{20}	Compounds identified in cut	Method of identification [a]	Physical constants		
					Olefin		
					Boiling point at 760 mm Hg	Refractive index n_D^{20}	Density at 20° C
	°C				°C		g/ml
H-1	77.6 to 77.8	1.4034 to 1.4030	2,3,3-Trimethyl-1-butene	PCO	77.8 77.87[2]	1.4030 1.4029[2]	
H-2	79.5 to 88.0	1.4025 to 1.4093	2,3,3-Trimethyl-1-butene 3,4-Dimethyl-2-pentene 2,3-Dimethyl-1-pentene	O O O			
H-3	89.8 to 91.8	1.4016 to 1.4133	3,4-Dimethyl-2-pentene 3,4-Dimethyl-1-pentene	PCP, O PCP, O			
H-4	96.9 to 97.4	1.4192 to 1.4206	2,3-Dimethyl-2-pentene 3-Ethyl-2-pentene	PCO, PCP PCO, PCP	97.43 97.6 to 97.7[4] 96.9 95[29]	1.4206 1.4211[4]	0.7280 0.7282[4]
O-1	100.4 to 106.0	1.4158 to 1.4167	3,3-Dimethly-2-ethyl-1-butene	O			
O-2	108.3 to 108.4	1.4170 to 1.4172	2,3,3-Trimethyl-1-pentene	PCO, PCP	108.31 108.4[14]	1.4172 1.4174[14]	0.7322 0.7352[14]
O-3	109.5 to 111.2	1.4190 to 1.4219	4,5-Dimethly-2-hexene	PCO	109.8 110[7]	1.4131 1.413[7]	
O-4	112.2 to 112.3	1.4232 to 1.4233	3,4,4-Trimethyl-2-pentene	PCO, O	112.2 to 112.3 112.3[14]	1.4232 to 1.4233 1.4235[14]	
O-5	112.8 to 115.0	1.4206 to 1.4253	3,4,4-Trimethyl-2-pentene 2,3,4-Trimethyl-2-pentene	O O			
O-6	115.9 to 116.2	1.4262 to 1.4266	2,3,4-Trimethyl-2-pentene	PCO	116.2 116.26[14]	1.4266 1.42736[14]	
O-7	116.8 to 119.0	1.4286 to 1.4263	2-Methyl-3-ethyl-2-pentene	O, PCP			
N-1	121.5 to 123.0	1.4225 to 1.4186	3,3-Dimethyl-2-isopropyl-1-butene	PCO, PCP	122.0 122.21[14]	1.4175 1.41669[14]	
N-2	127.7 to 128.1	1.4222 to 1.4227	2,3,4,4-Tetramethyl-1-pentene	PCP, O	127.97 132–133[34]	1.4220 1.4275[34]	0.7544
N-3	133.9 to 135.5	1.4295 to 1.4302	4,4-Dimethyl-3-ethyl-2-pentene 3,4,5-Trimethyl-2-hexene 2,3,3,4-Tetramethyl-1-pentene	O O PCP, O			
N-4	137.4 to 137.6	1.4324 to 1.4328	3,4,4-Trimethyl-2-hexene	O	137.2 135.6[24] [b]	1.4324 1.4320[24]	0.7620 0.7612[24]
D-1	144 to 147	1.4300 to 1.4290	2,4,4-Trimethyl-3-ethyl-2-pentene	O	146.2 to 147.0	1.4280 to 1.4289	
D-2	151.5 to 155.2	1.4340 to 1.4356	3,4,5,5-Tetramethyl-2-hexene	O			
D-3	159.0 to 160.8	1.4372 to 1.4388	3,5,5-Trimethyl-2-heptene 2,3,4,4-Tetramethyl-2-hexene 3,4,4,5-Tetramethyl 2-hexene 3,4-Dimethyl-3-isopropyl-2-hexene	O PCP PCP PCP			

[a] The abbreviations and their significance are: PCO, material identified by the physical constants of the olefin; PCP, material identified by physical constants of the paraffin formed by hydrogenation of the olefin; O, material identified by ozonolysis.

[b] The letter *M* after the melting point of the derivative indicates that no depression of melting point occurred when the derivative was mixed with an authentic sample.

[c] Identifications of acetaldehyde, formaldehyde, and acetone, if any, are described in the text. Only the larger fragments from ozonolyses are included here.

[d] Semicarbazone of 3,4,4-trimethyl-2-pentanone, mp (found) 150° to 150.5° C, mp (lit) [34] 151° C, [8] 148° C.

[e] Semicarbazone of 2,2-dimethyl-3-pentanone, mp (found) 143.5° to 145° C, mp (lit) [18] 144° C. The mixed melting point was determined with 2,4-

Physical constants—Continued				Ozonolyses			
Paraffin				Oily fraction		2,4-Dinitrophenylhydrazone	
Compound	Boiling point at 760 mm Hg	Refractive index n_D^{20}	Density at 20° C	Compounds identified [a]	bp	mp	mp [Reference]
	° C		g/ml		° C	° C	° C
				3,3-Dimethyl-2-butanone	104 to 106	126 to 126.5M [b]	126 to 126.5[14].
				3-Methyl-2-butanone	92 to 93	117 to 118M	119 to 120 [21].
				3-Methyl-2-pentanone	117 to 118	67 to 69M	71.2[9].
2,3-Dimethylpentane	89.82	1.3920	0.6951	3-Methyl-2-butanone	92 to 95	117 to 118M	119 to 120[21].
	89.787[14]	1.3919[14]	0.69510[14]	2,3-Dimethylbutanal	111 to 112	119.5 to 121.0	123 to 123.5[3].
2,3-Dimethylpentane	89.8	1.3920	0.6951				
	89.787[14]	1.3919[14]	0.69510[14]				
3-Ethylpentane	93.42	1.39330	0.69788				
	93.473[2]	1.39337[2]	0.69818[2]				
				2,2-Dimethyl-3-pentanone	126.0	144 to 145M	143.5 to 144.5[35].
2,3,3-Trimethylpentane	114.5	1.4073					
	114.767[14]	1.40757[14]					
				3,3-Dimethyl-2-butanone	105 to 106	126 to 126.5M	126 to 126.5[14].
				3,3-Dimethyl-2-butanone	105 to 106	125 to 126M	126 to 126.5[14].
				3-Methyl-2-butanone	90 to 92	117 to 118M	119 to 120[21].
2-Methyl-3-ethylpentane	115.5	1.4042		3-Pentanone	101 to 101.5	154 to 156M	156[36].
	115.653[14]	1.40403[14]					
2,2,3,4-Tetramethylpentane	133	1.4146					
	133.0[14]	1.4146[14]					
2,2,3,4-Tetramethylpentane	133	1.4146		3,4,4-Trimethyl-2-pentanone [c]	147	112 to 113	112[8,34].
	133.01[14]	1.4146[14]		2,2-Dimethyl-3-pentanone [c]	125 to 126	143 to 144M	143.5 to 144.5[35].
				3,4-Dimethyl-2-pentanone [d]	136 to 140	100 to 102M	98[6].
2,3,3,4-Tetramethylpentane	141.4	1.4218		3,3,4-Trimethyl-2-pentanone [e]	152 to 153	146 to 147	148[11].
	141.54[14]	1.4222[14]					
3,3,4-Trimethylhexane	140.424	1.41736	0.74540	3,3-Dimethyl-2-pentanone		111.0 to 111.5M	111 to 112[14].
	140.2[26]	1.4178[26]	0.7460[26]				
2,2,4-Trimethyl-3-ethylpentane.	155.3	1.4223	0.7571	2,2-Dimethyl-3-pentanone	125 to 130	140 to 141M	143.5 to 144.5[35]
	154.3[12]	1.4230[12]	0.7537[12]	3,4,4-Trimethyl-2-pentanone	145 to 147	111 to 112M	112[8, 34].
3,3,5-Trimethylheptane	155.68	1.41701	0.74278	4,4-Dimethyl-2-hexanone [f]	153.5 to 154	75 to 75.5	75[20, 27]
	155.2[13]	1.4171[13]	0.7418[13]				
2,3,4,4-Tetramethylhexane	161.6	1.4267	0.7624				
	161.0[13]	1.4274[13]	0.7623[13]				
2,3,3,4-Tetramethylhexane	164.59	1.4298	0.7694				
	164.3[13]	1.4306[13]	0.7690[13]				
2,3,4-Trimethyl-3-ethylpentane.	169.44	1.4333	0.7773				
	167.8[13]	1.4335[13]	0.7761[13]				

dinitrophenylhydrazone of a synthetically prepared sample of ketone. Kharasch et al [19] report the 2,4-dinitrophenylhydrazone mp to be 175° C, which is believed to be in error.

[c] A somewhat impure sample of this 2,4-dinitrophenylhydrazone was kindly supplied by Dr. Cook [6]. A mixed melting point determination showed no depression.

[d] Semicarbazone of 3,3,4-trimethyl-2-pentanone, mp (found) 147° to 148° C, mp (lit) [11] 150.5° to 151° C, [5] 150° C.

[e] Semicarbazone of 4,4-dimethyl-2-hexanone, mp (found) 170° to 171° C, mp (lit) [8] 169.5° C, [27] 169° to 170° C. Drake et al [8] report the 2,4-dinitrophenylhydrazone to be 146.5° to 147° C, which is believed to be in error.

[f] Drake and Welsh [10] obtained a boiling point of 159.1° C and a refractive index (corrected to 20° C) of 1.4230. These values are at variance with those from other investigators [12], [17] and are believed to be in error.

[g] Measured at a pressure of 738 mm Hg.

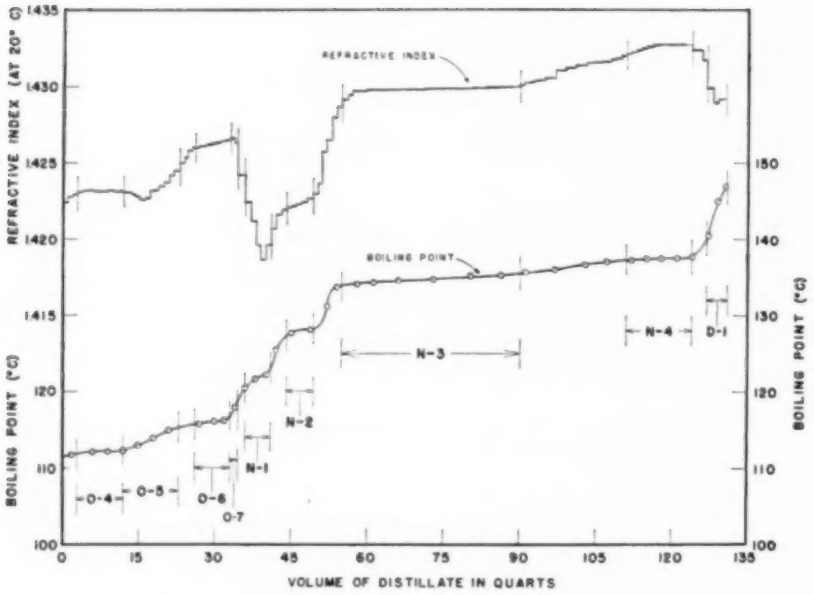

FIGURE 5. *Redistillation of the preliminary nonene cut.*

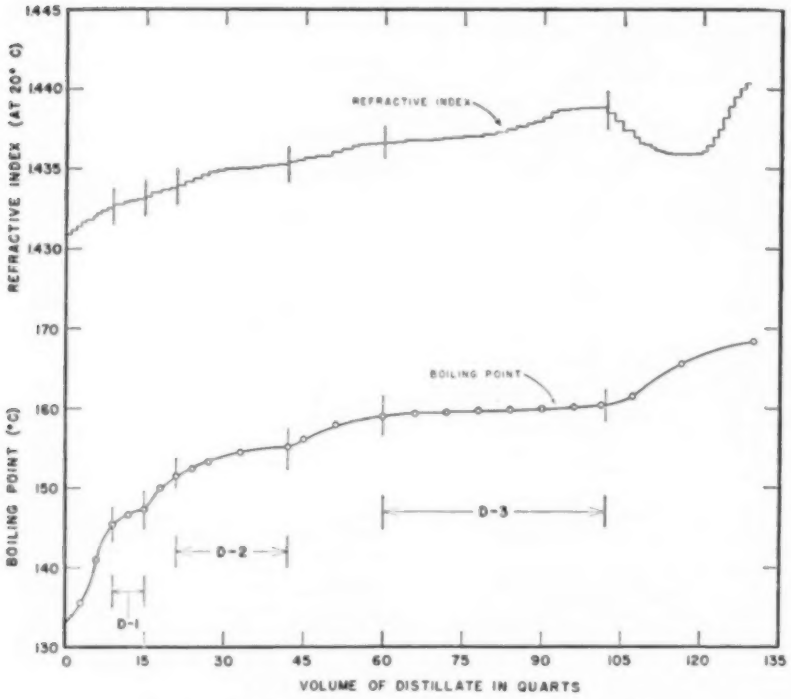

FIGURE 6. *Redistillation of the preliminary decene cut.*

Figure 3 shows the course of one of the redistillations of the heptene portion. This graph, which represents a typical redistillation of this preliminary cut, shows the boiling points and refractive indices (at 20° C) of the distillate, in relation to the volume distilled.

In a similar fashion, figure 4 shows data obtained from redistillation of a part of the octene portion in still 12. Again, this is a typical redistillation of the octenes and shows most of the components present in the octene range. Because of the relatively large hold-up of still 12 and the large pot capacity with the resulting large residue, some of the higher boiling octene components are not shown in figure 4. However, the residue from the distillations represented by figure 4 was added to the charge of nonenes and the combined charge distilled. Figure 5 shows the distillation of a part of the preliminary nonene fraction. Because of the system of amplified distillation used, the octene components not shown in figure 4 are presented in this graph. Similarly, figure 6 shows the redistillation of a portion of the decenes.

Analyses were performed on each of the cuts listed in table 2 and shown in figures 3 to 6, inclusive. If the plateau represented a reasonably pure compound with well-known physical constants, the identification of the cut was made by comparison of the measured physical properties with the literature values. Where the plateau was a mixture, or a compound with literature values not clearly established, hydrogenation and/or ozonolysis were used to establish the identity of the components. Moreover, wherever a reasonably pure compound was obtained, a "heart cut" was redistilled in column 17 to obtain a sample for the measurement of physical constants.

The analysis of the triptene residue, which is shown in table 3, was based primarily on distillation date and is only approximate. For complex fractions, analytical distillation of the hydrogenated cuts was used. Ozonolysis data can be relied on only for qualitative information, inasmuch as several cuts were markedly resistant to ozonization.

TABLE 3. *Analysis of triptene residue*

Cut	Boiling range	Percentage of triptene residue	Compounds in cut [a]	Percent of compounds in cut [b]
	°C			
Heptenes	75 to 100	34	2,3,3-Trimethyl-1-butene	5
			2,3-Dimethyl-1-pentene*	5
			3,4-Dimethyl-1-pentene*	40
			3,4-Dimethyl-2-pentene	
			3-Ethyl-2-pentene	5
			2,3-Dimethyl-2-pentene	45
Octenes	100 to 118	40	3,3-Dimethyl-2-ethyl-1-butene*	10
			2,3,3-Trimethyl-1-pentene	45
			4,5-Dimethyl-2-hexene	2
			3,4,4-Trimethyl-2-pentene	35
			2,3,4-Trimethyl-2-pentene	6
			2-Methyl-3-ethyl-2-pentene*	2
Nonenes	118 to 143	4	3,3-Dimethyl-2-isopropyl-1-butene	5
			2,3,4,4-Tetramethyl-1-pentene*	10
			2,3,3,4-Tetramethyl-1-pentene	45
			3,4,5-Trimethyl-2-hexene*	10
			4,4-Dimethyl-3-ethyl-2-pentene	
			3,4,4-Trimethyl-2-hexene	30
Decenes	143 to 163	5	2,4,4-Trimethyl-3-ethyl-2-pentene*	5
			3,4,5,5-Tetramethyl-2-hexene*	35
			3,5,5-Trimethyl-2-heptene	50
			2,3,4,4-Tetramethyl-2-hexene	5
			3,4,4,5-Tetramethyl-2-hexene	4
			3,4-Dimethyl-3-isopropyl-1-pentene	1
Undecenes and higher boiling substances.	>163	17		

[a] The asterisks indicate the presence of small amounts of unknown component.

[b] This analysis is an estimate and is based on distillation analysis and hydrogenation data.

3. Hydrogenations

The hydrogenation reactions were accomplished in rocking-autoclaves of the type described by Adkins [1]. These were of 1-, 3-, and 20-liter capacity. The catalyst used was a commercial nickel-on-kieselguhr. The hydrogenations were carried out at 1,000 to 2,000 lb/in.^{2} pressure and at a temperature of 140° to 190° C. Several of the cuts contained chlorides in small amounts; and hydrogenation of these proved to be somewhat more difficult than for chloride-free olefins, thus necessitating longer periods for completion. Not infrequently, several treatments were necessary to obtain a saturated product. Hydrogenated cuts were passed through silica gel and distilled in column 11 or 17 for analysis.

4. Ozonolyses

The apparatus used for the several ozonolyses was essentially equivalent to that described by Whitmore and Church [32]. Generally, ozonizations were performed on 0.5-mole samples. The solvent used was petroleum ether that had been washed successively with concentrated sulfuric acid, water, sodium bicarbonate, dried over calcium chloride, and distilled. The portion boiling between 35° and 40° C was passed through silica gel. Ozonization of 0.5-mole sample in 300 ml of solvent at −5° to −15° C was generally accomplished in 14 to 16 hr, although a few olefins were ozonized in less time. In most cases the solvent was not removed prior to decomposition. The ozonide was decomposed with 40 g of zinc and 500 ml of water containing traces of silver nitrate and hydroquinone.

The water layer from the decomposition was always tested for the presence of formaldehyde and acetone. The formaldehyde in the ozonolyses products was identified as its dimethone derivative (mp 188° to 190° C) [15], the acetone by conversion to its dibenzal derivative (mp 111° to 112° C) [16].

The material obtained in the ether trap was tested for acetaldehyde by reaction with ammonia, with the subsequent formation of the acetaldehyde-ammonia crystalline complex (mp 86° to 88° C) [33].

The oily distillate from the decomposition of the ozonide was dried over sodium sulfate and distilled in column 9. The relatively pure fractions from the latter distillation were converted to the semicarbazone and/or the 2,4-dinitrophenylhydrazone for purposes of identification. Orthodox qualitative tests were performed on selected cuts from the oily layer distillation, prior to reaction with derivative-forming reagents.

Aldehydes and ketones were generally identified either by the melting-point values of two derivatives, or by the melting point of one derivative and absence of any depression of the melting point when the unknown was mixed with an authentic sample of known compound.

The results from the ozonization of some of the lower boiling compounds were semiquantitative, but resistance to ozone of some of the higher boiling, highly branched compounds did not warrant even rough approximation by this method of the relative amounts of isomers in the material ozonized.

Ozonolysis of cut H–2, the second concentrate of the heptene fraction is typical and is described as an example. This cut boiled in the range 79.5° to 88.0° C and was a rather complex mixture of heptenes boiling above triptene (bp 77.8° C) and below 3,4-dimethyl-2-pentene (bp about 90° C):

Treatment of 50 g of the cut H–2 with 8 percent of ozone in oxygen at 12.5 liters/hr was carried out for 12 hr at −15° C. The ozonide in pentane solution was decomposed by dropwise addition to 500 ml of boiling water to which had been added 40 g of zinc dust and traces of silver nitrate and hydroquinone. The decomposition was unusually mild and gave 117 ml of aqueous layer and 138 ml of oil layer (which contained some solvent).

The material dissolved in the ether trap was tested for acetaldehyde by introduction of anhydrous ammonia for 5 min. The test was positive, as evidenced by the formation of the characteristic aldehyde-ammonia compound (mp 86° to 88° C). A sample of the water layer was treated with dimedon (dimethyldihydroresorcinol), which resulted in a voluminous precipitate of formaldehydedimethone (mp 189° to 190° C). A test for acetone by treatment with benzaldehyde [15] failed to produce dibenzalecetone.

The oily layer was fractionated in column 9 to give:

(1) 3-Methyl-2-butanone, bp 92° to 93° C, 2,4-dinitrophenyl-hydrazone, mp 117° to 118° C,

(2) 3,3-Dimethyl-2-butanone, bp 104° to 106° C, 2,4-dinitrophenylhydrazone, mp 126° to 126.5° C,

(3) 3-Methyl-2-pentanone, bp 117° to 118° C, 2,4-dinitrophenylhydrazone, mp 67° to 69° C.

The 2,4-dinitrophenylhydrazones of these compounds were each tested for identity by the "mixed melting-point" technique. No depressions of melting points were observed when these compounds were mixed with authentic specimens.

(4) Beta-chloropropionic acid (?): At 100° C a compound distilled, which solidified to a mush in the condenser. This material was removed, cooled, and filtered to yield a small quantity of white crystals that contained halide (Beilstein's test) and was acidic. These crystals melted at 42° C. This compound is believed to be beta-chloropropionic acid, since this melting point agrees well with that listed by Shriner and Fuson [28]. However, it was not definitely identified.

The identification of 3-methyl-2-butanone and acetaldehyde indicates the presence of 3,4-dimethyl-2-pentene; the formaldehyde and 3,3-dimethyl-2-butanone were formed by splitting of triptene (2,3,3-trimethyl-1-butene); the 3-methyl-2-pentanone and formaldehyde came from 2,3-dimethyl-1-pentene.

No 2,4-dimethyl-2-pentene could be detected, since this compound would yield isobutyaldehyde in the oily layer distillation, and no aldehyde derivative was obtained by dimethone tests on the distillate fractions.

III. Identification and Analyses

1. Heptene, Boiling Range 75° to 100° C

The results of the redistillation of the 75° to 100° C cut are shown in figure 3, and the compounds obtained are enumerated in table 2, in which a summary of the entire analysis is given, including physical constants measured, methods of identification, and ozonolysis data.

Cut H–1, bp 77.6° to 77.8° C n_D^{20} 1.4034 to 1.4030: This concentrate was found to contain triptene (2,3,3-trimethyl-1-butene) and comprises about 2 percent of triptene residue. The small quantity of triptene found is material remaining from the original distillation at the Redford Laboratories. The refractive index is higher than the accepted value, due to this plateau being preceded and followed mainly by material of higher refractive index, and undoubtedly it contains some of these higher refractive materials.

Cut H–2, bp 79.5° to 88.0° C, n_D^{20} 1.4025 to 1.4093: Although this material is intermediate between H–1 and H–3 and contained compounds found in both these cuts, its composition was made even more complex by the presence of other heptenes. A detailed account of the ozonolysis has already been given (section II, 4), in which the cut was found to contain triptene, 3,4-dimethyl-2-pentene, and 2,3-dimethyl-1-pentene. Results are given in table 2.

Cut H–3, bp 89.8° to 91.8° C, n_D^{20} 1.4106 to 1.4133: The components of this fraction were found to be 3,4-dimethyl-2-pentene and probably 3,4-dimethyl-1-pentene. Ozonolysis gave formaldehyde and acetaldehyde in the water and ether layers, respectively. The oily layer gave 3-methyl-2-butanone (see table 2), and an oil boiling 111° to 112° C, which contained small quantities of an aldehyde (as shown by reduction of Schiff's reagent), from which only one derivative, the 2,4-dinitrophenylhydrazone, was obtained. This 2,4-dinitrophenylhydrazone, after several recrystallizations, melted at 119.5° to 121.0° C. The aldehyde must be a hexaldehyde, since the highest-boiling pentaldehyde (normal) boils at 103.7° C, and the compound in question was derived by removal of a fragment from a heptene. A comparison of these data with those of all the hexaldehydes gave

Compound	Boiling point [4]	2,4-Dinitrophenylhydrazone [4]
	° C	° C
n-Hexaldehyde	131	104.
2-Methylpentanal	119 to 121 [30]	103 [23].
3-Methylpentanal		93.5 to 94.5.
4-Methylpentanal	121	99.
2,2-Dimethylbutanal	102 to 104	145.
3,3-Dimethylbutanal	102 to 104	147 to 147.
2,3-Dimethylbutanal	115 to 117	123 to 123.5.
2-Ethylbutanal	117 to 119	94.5 to 95.0.
Aldehyde from H–3	111 to 112	119.5 to 121.0.

[4] Data from Brunner and Farmer [3], unless otherwise noted.

These melting point data indicate that the aldehyde from H–3 is 2,3-dimethylbutanal, which, along with formaldehyde, is presumed to be derived from 3,4-dimethyl-1-pentene. The identification of 3-methyl-2-butanone and acetaldehyde show the presence of 3,4-dimethyl-2-pentene.

A sample of cut H–3, when hydrogenated and

refractionated, gave only 2,3-dimethylpentane (see table 2).

Cut H–4, bp 96.6° to 97.4° C, n_D^{20} 1.4192 to 1.4206: The major portion of this cut was found to be 2,3-dimethyl-2-pentene, with some 3-ethyl-2-pentene. Both components were identified by comparison of their physical properties with those of the pure compounds, and by hydrogentation to the paraffins, followed by a comparison of the paraffins' physical properties with reported values (see table 2). A part of cut H–4 was used to prepare 2,3-dimethylpentane for engine test work. When 9 gal of the cut was hydrogenated and distilled in column 11, 8 gal of high-purity 2,3-dimethylpentane was obtained (see table 2). The residue from this distillation was fractionated in column 17 to give 1,230 ml of 3-ethylpentane with the properties shown in table 2. This 3-ethylpentane must have been derived from 3-ethyl-2-pentene (bp about 95° C) [29], since the only other olefin of this carbon skeleton, 3-ethyl-1-pentene, boils about 10° C lower, at 85° C, with a refractive index of 1.3966 [25].

2. Octenes, Boiling Range 100° to 118° C

The results from the distillation of the octenes are shown in figures 4 and 5, and analytical results are tabulated in tables 2 and 3. Because of the relatively large hold-up in still 12, the higher boiling octene components were distilled with the nonene cut (fig. 5). Seven portions of the octenes were designated as cuts O–1 to O–7, as shown in figures 4 and 5.

Cut O–1, bp 100.4° to 106.0° C, n_D^{20} 1.4158 to 1.4169: This material was found to be a complex mixture from which only the major component, 3,3-dimethyl-2-ethyl-1-butene, was characterized. On ozonolysis of this cut, only formaldehyde and 2,2-dimethyl-3-pentanone could be identified (see table 2).

Cut O–2, bp 108.3° to 108.4° C, n_D^{20} 1.4170 to 1.4172: This narrow-boiling fraction was found to be 2,3,3-trimethyl-1-pentene, as evidenced by a comparison of its physical properties with those of this compound previously reported [14]. The sample from the beginning of the plateau showed a boiling range of 0.12° C (20 to 80% distilled), which indicated the presence of some impurity. A portion was hydrogenated, and distillation analysis of the product gave about 93 percent of 2,3,3-trimethylpentane (see table 2) and about 7 percent of 2,2,3-trimethylpentane (bp 110° C, n_D^{20} 1.4028). The latter paraffin could have been formed by hydrogenation of 3,3-dimethyl-2-ethyl-1-butene, which was identified as a constituent of the preceding cut O–1.

Cut O–3, bp 109.5° to 111.2° C, n_D^{20} 1.4190 to 1.4219: The material collected from several runs with the properties designated for O–3 in figure 4 was combined and redistilled in column 13. The composition of the material was found to be complex, but one plateau represented material that is presumed to be 4,5-dimethyl-2-hexene, since a close agreement exists between the properties of the compound isolated and values reported in the literature [7] for 4,5-dimethyl-2-hexene (see table 2).

Cut O–4, bp 112.2° to 112.3° C, n_D^{20} 1.4232 to 1.4233: This portion of triptene residue was predominantly 3,4,4-trimethyl-2-pentene, as shown by a comparison of its physical properties with those of pure 3,4,4-trimethyl-2-pentene previously obtained [14]. This identification is given additional weight by the fact that when 15 gal of the olefin was oxidized by sodium dichromate-sulfuric acid [14], 3,3-dimethyl-2-butanone was obtained in 30-percent yield, not including a large amount of the same ketone that was recovered as an azeotrope with unreacted olefin.

Cut O–5, bp 112.8° to 115.0° C, n_D^{20} 1.4206 to 1.4253: Ozonolysis of this cut gave acetaldehyde, acetone, 3-methyl-2-butanone, and 3,3-dimethyl-2-butanone. The presence of 3,4,4-trimethyl-2-pentene, which gave acetaldehyde and 3,3-dimethyl-2-butanone, and 2,3,4-trimethyl-2-pentene, from which acetone and 3-methyl-2-butanone came, is shown. The presence of at least one additional compound is indicated by a dip in the refractive index curve. From the ozonolysis, at least two additional carbonyl compounds, one of which was an aldehyde, bp 113° to 115° C (as shown by reduction of Schiff's reagent) were obtained. Neither of these nor their derivatives could be separated and identified. The 2,4-dinitrophenylhydrazone of this fraction came down as an oil, which, after successive crystallizations, melted 101° to 105° C.

Cut O–6, bp 115.9° to 116.2° C, n_D^{20} 1.4262 to 1.4266: This cut was found to be 2,3,4-trimethyl-2-pentene by a comparison of its physical properties with those of pure 2,3,4-trimethyl-2-pentene isolated previously in this laboratory [14] and by

the identification of 3-methyl-2-butanone and acetone found in the intermediate cut O–5.

Cut O–7, bp 116.8° to 119.0° C, n_D^{20} 1.4266 to 1.4262: This fraction was found to contain 2-methyl-3-ethyl-2-pentene as the major component.

A portion of O–7 was redistilled in column 17 to yield a cut boiling 117.0° to 118.5° C. Ozonolysis of a 0.5-mole sample of this yielded formaldehyde and acetone in the water layer and traces of acetaldehyde in the ether layer. The oily layer proved to be mostly 3-pentanone (see table 2) with a small quantity of a compound boiling 116° to 119° C, which gave a 2,4-dinitrophenylhydrazone melting 113° to 116.5° C. The latter was not identified. The identification of acetone and 3-pentanone shows the presence of 2-methyl-3-ethyl-2-pentene.

Hydrogenation of the redistilled portion of O–7 yielded 2-methyl-3-ethylpentane. (See table 2.)

3. Nonenes, Boiling Range 121° to 138° C

The results obtained from a typical redistillation of the 121° to 138° C cut (combined with octene residue) are shown in figure 5.

Cut N–1, bp 121.5° to 123.0° C, n_D^{20} 1.4225 to 1.4186: The major component of this cut was found to be 3,3-dimethyl-2-isopropyl-1-butene, the identification of which was made by a comparison of the physical properties of the olefin and also of the paraffin derived by hydrogenation. The fraction boiling 121.5° to 123.0° C was redistilled in column 17 to give a plateau representing a compound in close agreement in physical properties with those of 3,3-dimethyl-2-isopropyl-1-butene previously prepared in this laboratory (see table 2). A portion of this plateau was hydrogenated and distilled in column 17 to give a paraffin with properties almost identical with those of 2,2,3,4-tetramethylpentane [14]. There are only three olefins of this carbon skeleton:

3,3-Dimethyl-2-isopropyl-1-butene, bp 122.21° C, n_D^{20} 1.4669 [14]

2,3,4,4-Tetramethyl-1-pentene, bp 132° to 133° C, n_D^{20} 1.4275 [34]. (See cut N–2.)

2,3,4,4-Tetramethyl-2-pentene, bp $>$134° C, $n_D^{20}>1.4310$ [33]

It is evident that the paraffin is derived from the first of these olefins.

Cut N–2, bp 127.7° to 128.1° C, n_D^{20} 1.4222 to 1.4227: This portion of the nonenes was found to contain 2,3,4,4-tetramethyl-1-pentene as the major component. A sample was refractionated in column 17 and a "heart cut" used for measurement of physical properties and for ozonolysis. Ozonolysis gave formaldehyde, and only 3,4,4-trimethyl-2-pentanone in the oily layer, which was identified by the preparation of two derivatives (see table 2). When a sample of N–2 was hydrogenated and refractionated, quite pure 2,2,3,4-tetramethylpentane was obtained (see table 2). The residue from redistillation of N–2, when ozonized, gave the same products as the main fraction, and, in addition, a small quantity of aldehyde that boiled at 152° to 158° C was found. The 2,4-dinitrophenylhydrazone of this compound melted, after five recrystallizations, at 174.5° to 176° C. This compound was not identified.

Cut N–3, bp 133.9° to 135.5° C, n_D^{20} 1.4295 to 1.4302: Preliminary work on this cut indicated the presence of a complex mixture. The cut was therefore divided into two portions, designated as N–3–A and N–3–B, respectively. Each of these was ozonized separately.

N–3–A, bp 133.9° to 134.6° C, on ozonolysis gave formaldehyde, acetaldehyde, and two ketones boiling at 125° to 126° C and 152° to 153° C, which proved to be 2,2-dimethyl-3-pentanone and 3,3,4-trimethyl-2-pentanone, respectively (see table 2). The presence of a higher boiling aldehyde was detected in the residue from the ketone distillation. The results are interpreted to indicate the presence of 4,4-dimethyl-3-ethyl-2-pentene and 2,3,3,4-tetramethyl-1-pentene in cut N–3–A. The former would, on ozonalysis, give acetaldehyde and 2,2-dimethyl-3-pentanone; the latter would give formaldehyde and 3,3,4-trimethyl-2-pentanone.

Cut N–3–B, bp 134.6° to 135.6° C was ozonized to give formaldehyde, acetaldehyde, 2,2-dimethyl-3-pentanone (bp 125° to 126° C), 3,3,4-trimethyl-2-pentanone (bp 152° to 153° C), and a small amount of 3,4-dimethyl-2-pentanone (bp 136° to 140° C). (See table 2.) A trace of a higher boiling aldehyde was found in the residue. In addition, a compound boiling 109° to 114° C formed a 2,4-dinitrophenylhydrazone melting 94° to 96° C. A "mixed melting point" of the latter with the derivative of 4-methyl-2-pentanone gave a value of 76.5° to 83° C; a "mixed melting point" with 2-methyl-3-pentanone gave 88° to 94° C. This derivative was not identified.

The 3,4-dimethyl-2-pentanone, and acetaldehyde, show the presence of 3,4,5-trimethyl-2-hexene. The other two ketones found were also present in cut N–3–A, and were shown to result from 4,4-dimethyl-3-ethyl-2-pentene and 2,3,3,4-tetramethyl-1-pentene. The aldehyde trace in the oily layer residue is surmised to be a C_8 aldehyde, due to its higher boiling point, which could result from an olefin with the following structure:

$$C_7H_{15}CH{=}CH_2.$$

When cut N–3–A and cut N–3–B were hydrogenated and distilled, only 2,3,3,4-tetramethylpentane (see table 2) could be obtained in a nearly pure state.

Cut N–4, bp 137.4° to 137.6° C, n_D^{20} 1.4324 to 1.4328: This fraction was found to contain 3,4,4-trimethyl-2-hexene, since ozonolysis yielded only 3,3-dimethyl-2-pentanone and acetaldehyde. (See table 2.) The purity of the compound is indicated by its narrow boiling range, and the absence of complex ozonolysis products. A sample of cut N–4 was hydrogenated to a paraffin, 3,3,4-trimethylhexane, with the physical properties listed in table 2.

4. Decenes, Boiling Range 143° to 163° C

The results of analyses of the decenes are shown in table 2, and data obtained in the distillation are illustrated in figures 5 and 6. The decene portion proved to be quite complex and the majority of the decenes found in the triptene residue appear to have been formed by polymerization of he original isopentenes.

Cut D–1: This concentrate, boiling range 144° to 147° C, n_D^{20} 1.4300 to 1.4290, began to appear as an after run of cut N–4, and was characterized by a drop in the refractive index curve. Since only a small quantity was available, the portion marked D–1 in figures 5 and 6 was redistilled in column 17, and a portion from the middle of the narrow-boiling cut was used for reaction with ozone. This material was extremely resistant to the action of ozone; after 50 hr of treatment, only 10 percent of the material was converted to ozonide. The presence of acetone, formaldehyde, and 2,2-dimethyl-3-pentanone was established in the decomposition products. (See table 2.) The acetone and 2,2-dimethyl-3-pentanone are presumed to have been formed by splitting 2,2,4-trimethyl-3-ethyl-2-pentene. No C_9 product was isolated as a companion for formaldehyde. A portion of the "best" olefin was hydrogenated and upon distillation proved to be mostly one compound. The properties of this paraffin, 2,2,4-trimethyl-3-ethylpentane, are listed in table 2.

Cut D–2, bp 151.5° to 155.2° C, n_D^{20} 1.4340 to 1.4356: Ozonolysis of a sample of this fraction gave formaldehyde, acetaldehyde, butanone-2 (bp 80° to 85° C, 2,4-dinitrophenylhydrazone mp and mixed melting point 108° to 110° C), 3,4,4-trimethyl-2-pentanone (see table 2), and a hexaldehyde (bp 110° to 120° C) which was not completely identified because only a small quantity was present, which was contaminated with some butanone-2. Also present was a trace of an unidentified ketone boiling at 166° to 168° C, which gave a 2,4-dinitrophenylhydrazone melting at 160.5 to 162.0° C, which is presumed to be a C_9 ketone.

The identification of acetaldehyde and 3,4,4-trimethyl-2-pentanone indicate the presence of 3,4,5,5-tetramethyl-2-hexene. The formaldehyde and the unidentified C_9 ketone indicate the presence of a decene with a terminal methylene group attached to a doubly branched carbon. The unidentified hexaldehyde is thought to be 2,2-dimethylbutanal and a companion of butanone-2, which, together, would make up 3,5,5-trimethyl-3-heptene. This presumption is strengthened by hydrogenation studies. Hydrogenation of a sample gave a mixture consisting predominantly of 2,2,3,4-tetramethylhexane with a lesser quantity of 3,3,5-trimethylheptane.

Cut D–3, bp 159.0° to 160.8° C, n_D^{20} 1.4372 to 1.4388: This fraction was a mixture and was found to contain 3,5,5-trimethyl-2-heptene and three other olefins which, on hydrogenation, produced 2,3,3,4-tetramethylhexane, 2,3,4,4-tetramethylhexane, and 2,3,4-trimethyl-3-ethylpentane. (See table 2.)

A 1-gal sample of D–3 was redistilled in column 17 to obtain a purer sample for ozonolysis and hydrogenation. When a portion of the "heart cut" (bp 159° C) of the latter distillation was ozonized, traces of formaldehyde were found in the water layer, and large quantities of acetaldehyde in the ether layer. The majority (about 90%) of the oily layer proved to be 4,4-dimethyl-2-hexanone (see table 2), with very small quantities of other unidentified higher-boiling materials present, including a C_9 aldehyde (as shown by re-

duction of Schiff's reagent). The ketone was identified by the formation of two derivatives. The semicarbazone, mp 170° to 171° C, was formed with great ease, whereas the other semicarbazones made in this work required at least 2 days to crystallize. The 2,4-dinitrophenylhydrazone, mp 75° to 75.5° C, showed the 4,4-dimethyl-2-hexanone to be relatively pure because no extensive recrystallizations of the derivative were needed to reach the final sharp melting point. The melting point for this derivative recorded here agrees with that obtained by Schmerling [27], Laucius [20], and Wheeler (cited by Laucius), but disagrees with that of Drake, Kline, and Rose [8], who obtained a value of 146.5° to 147° C. The identification of acetaldehyde and 4,4-dimethyl-2-hexanone prove the presence of 3,5,5-trimethyl-2-heptene.

A portion from the same "heart cut" of olefin was hydrogenated and distilled in column 17. Over 90 percent of the charge was recovered as distillate, with the properties the same as those listed for 3,3,5-trimethylheptane in table 2.

The rest of D–3 was hydrogenated and refractionated in still 11. The major constituent, 3,3,5-trimethylheptane was formed by hydrogenation of the 3,5,5-trimethyl-2-heptene identified previously. Physical constants were measured on this lot. This compound is believed to be of very high purity; the boiling range (20 to 80 percent distilled) was 0.005° C, the refractive index range of the distillate cut was 0.0001.

The paraffin residues from 3,3,5-trimethylheptane were distilled in column 17 to give three additional plateaus with the properties shown in table 2, which show the presence of 2,3,4,4-tetramethylhexane, 2,3,3,4-tetramethylhexane, and 2,3,4-trimethyl-3-ethylpentane. The identification of these compounds was made by comparisons of their physical properties with those listed by Francis [13], and by Johnson [17] who found them in the hydrogenated products of the decenes formed from *t*-amyl alcohol and from 2-methyl-2-butane. Presumably the isolated paraffins were derived from the hydrogenation of 2,3,4,4-tetramethyl-2-hexene, which is probably a normal methylation product of 3,4,4-trimethyl-2-hexene, of 3,4,4,5-tetramethyl-2-hexene, which may be a normal methylation product of 2,3,3,4-tetramethyl-1-pentene, and of 3,4-dimethyl-3-isopropyl-1-pentene, which is assigned this structure because of the aldehyde found in the ozonolysis fragments of cut D–3.

The structure of the 3,3,5-trimethylheptane isolated in this work has been conclusively proven by hydrogenation and ozonolysis data. The physical constants of the 3,3,5-trimethylheptane reported herein agree well with those listed by Francis [13] and Johnson [17] but disagree with those of Drake and Welsh [10], who seem to have had an impure substance containing 2,3,3,4-tetramethylhexane.

It appears that Drake et al [8] were working with a mixture of olefins. This is borne out by the discordant value of the melting point of the 2,4-dinitrophenylhydrazone of 4,4-dimethyl-2-hexanone. Their value for this derivative, 146.5° to 147° C, corresponds to that of 3,3,4-trimethyl-2-pentanone [11], which would appear as an ozonolysis product of 3,4,4,5-tetramethyl-2-hexene. The latter has been shown to be a normal constituent of isopentene dimer by recent work of Cook and Stehman [6], who found no other decene of this carbon skeleton boiling in the neighborhood of 159° C. This indicates that the 2,3,3,4-tetramethylhexane found in the hydrogenated cut D–3 was derived from 3,4,4,5-tetramethyl-2-hexene. Although this olefin could have been formed by methylation, as previously indicated, it also could be a dimerization product of the original isopentene, as found by Cook.

In the case of the 2,3,4,4-tetramethylhexane, the olefin parent is believed to be 2,3,4,4-tetramethyl-2-hexene. Of the olefins of this carbon structure studied by Cook, only this compound boiled in the neighborhood of 159° C. Cook, however, found 2,3,4,4-tetramethyl-2-hexene to be absent from isopentene dimer, and therefore it is probable that this olefin arose by methylation.

The next higher boiling cut, 165° to 168° C, is believed to contain undecenes. Although quite resistant to ozone, prolonged treatment of a sample of this material gave formaldehyde and a complex mixture of carbonyl compounds and olefins (bp 159° to 165° C), from which no pure materials were separated.

IV. Conclusions

The results obtained in this investigation substantiate the mechanism of olefin methylation as described by Miller and Lovell [22]. While the exact origin of some of the decenes is not clear, it

has been shown that the methylation reaction proceeds through the decene range, as evidenced by the series of compounds: 3,3-dimethyl-2-ethyl-1-butene→4,4-dimethyl-3-ethyl-2-pentene→2,4,4-trimethyl-3-ethyl-2-pentene, and also by: 2,3,3-trimethyl-1-pentene→3,4,4-trimethyl-2-hexene→2,3,4,4-tetramethyl-2-hexene.

It is significant that no 2,3,4,4-tetramethyl-2-pentene was found. This nonene should be a normal methylation product of 3,4,4-trimethyl-2-pentene. It is postulated that this compound is present in an equilibrium mixture with 3,3-dimethyl-2-isopropyl-1-butene, 2,3,4,4-tetramethyl-1-pentene and 2,3,3,4-tetramethyl-1-pentene, and that it occurs as only a small fraction of the equilibrium mixture. The same situation obtains when 2,3,4,4-tetramethyl-3-pentanol is dehydrated [31]. Whitmore and Laughlin [33] found only a trace of the 2-olefin in this mixture of nonenes. It has not been found at all in this laboratory.

The authors acknowledge with appreciation the voluminous prepublication data on the isopentene dimers kindly furnished by Professor Cook at Pennsylvania State College.

V. References

[1] H. Adkins, Reactions of hydrogen, chapter III (Univ. of Wisconsin Press, Madison, Wis., 1937).
[2] D. B. Brooks, F. L. Howard, and H. C. Crafton, Jr., J. Research NBS **24,** 33 (1940) RP1271.
[3] H. Brunner and E. H. Farmer, J. Chem. Soc. 1039 (1937).
[4] E. T. Cline, Ph D thesis (Ohio State University, 1940).
[5] I. J. Colonge and K. Mostafavi, Bul. Soc. Chim. [5] **6,** 335 (1939).
[6] N. C. Cook and C. G. Stehman, Pennsylvania State College, private communication.
[7] Dietrich, Ph D thesis (Ohio State University, 1938).
[8] N. L. Drake, G. M. Kline, and W. G. Rose, J. Am. Chem. Soc. **56,** 2076 (1934).
[9] N. L. Drake and F. P. Veitch, J. Am. Chem. Soc. **57,** 2624 (1935).
[10] N. L. Drake and L. H. Welsh, J. Am. Chem. Soc. **60,** 488 (1938).
[11] C. R. Enyeart, Ph D thesis, p. 51 (Pennsylvania State College, 1942).
[12] A. W. Francis, Ind. Eng. Chem. **35,** 447 (1943).
[13] A. W. Francis, Ind. Eng. Chem. **36,** 256 (1944).
[14] F. L. Howard, T. W. Mears, A. Fookson, P. Pomerantz, and D. B. Brooks, J. Research NBS **38,** 365 (1947) RP1779.
[15] E. H. Huntress and S. P. Mulliken, Identification of pure organic compounds, p. 50 (John Wiley & Sons, New York, N. Y., 1941).
[16] E. H. Huntress and S. P. Mulliken, Identification of pure organic compounds, p. 374 (John Wiley & Sons, New York, N. Y., 1941).
[17] G. C. Johnson, J. Am. Chem. Soc. **69,** 146 (1947).
[18] A. M. Khaletskii, J. Gen. Chem. USSR **8,** 164 (1938).
[19] M. S. Kharasch, E. Sternfeld, and F. R. Mayo, J. Org. Chem. **5,** 375 (1940).
[20] J. F. Laucius, PhD thesis, tabulation, pp. 161 to 165 (Pennsylvania State College, 1940).
[21] J. R. Lewis and J. L. Simonsen, J. Chem. Soc. 736 (1936).
[22] V. A. Miller and W. G. Lovell, Ind. Eng. Chem. **40,** 1138 (1948).
[23] G. T. Morgan and D. V. N. Hardy, Chem. Ind. **52,** 519 (1933).
[24] W. A. Mosher, PhD thesis (Pennsylvania State College, 1940).
[25] C. Prevost and J. Daujat, Bul, Soc. chim. [4] **47,** 590 (1930).
[26] C. H. Ruof, PhD thesis (Pennsylvania State College, (1948).
[27] L. Schmerling, J. Am. Chem. Soc. **68,** 1654 (1946).
[28] R. L. Shriner and R. C. Fuson, The systematic identification of organic compounds, p. 98 (John Wiley & Sons, Inc., New York, N. Y., 1935).
[29] F. J. Soday and C. E. Boord, J. Am. Chem. Soc. **55,** 3296 (1933).
[30] M. Sommelet, Bull. Soc. chim. [4] **1,** 406 (1907).
[31] This laboratory, unpublished work.
[32] F. C. Whitmore and J. M. Church, J. Am. Chem. Soc. **54,** 3710 (1932).
[33] F. C. Whitmore and K. C. Laughlin, J. Am. Chem. Soc. **55,** 3732 (1933).
[34] F. C. Whitmore and W. A. Mosher, J. Am. Chem. Soc. **63,** 1122 (1941).
[35] F. C. Whitmore, C. I. Noll, and V. C. Meunier, J. Am. Chem. Soc. **61,** 684 (1939).
[36] H. D. Zook, PhD thesis (Pennsylvania State College, 1942).

WASHINGTON, October 12, 1948.

INDEX TO VOLUME 42

A

Page

Absolute standard capacitance, RP1970 ... 287
Acetylene, flame spectrum, RP1993 ... 567
Acid-base equilibrium constants in benzene, RP1997 ... 595
Acid-base reactions in organic solvents, RP1997 ... 595
Acid, salt, pickle, and tannage, effect on activation of tendon collagen, RP1947 ... 17
Adsorbents, bone char and other carbon, oxidation, RP1948 ... 33
Adsorption of hydrocarbons, RP1957 ... 139
Adsorption of nitrogen, oxygen, and argon on portland cements, RP1967 ... 257
Aircraft material of sandwich construction, stress distribution, RP1979 ... 397
Aircraft wings, vibration from landing impact, RP1984 ... 437
Alkali and commercial soaps, characterization by electron microscopy, RP1973 ... 343
Alkylcyclopentanes, heats of combustion and isomerization, RP1966 ... 251
Ammonia, dissociation constant and base strength, RP1982 ... 419
Ammonium ion, acidic dissociation constant, RP1982 ... 419
Annealing borosilicate thermometer glasses, expansion effects, RP1960 ... 171
Annealing of optical glass, RP1969 ... 279
Automotive gear lubricants, wear tests, RP1955 ... 125

B

Barium oxide-boric oxide system, RP1956 ... 131
Bates, Roger G., Gladys D. Pinching, The acidic dissociation constant of ammonium ion at 0° to 50° C, and the base strength of ammonia, RP1982 ... 419
Batteries, electric, properties of perchloric-acid solutions in, RP1971 ... 309
Beckett, Charles W., John E. Kilpatrick, Edward J. Prosen, Kenneth S. Pitzer, Frederick D. Rossini, Heats, equilibrium constants, and free energies of formation of the C_3 to C_5 diolefins, styrene, and the methylstyrenes, RP1964 ... 225
Benzene, acid-base reactions in, RP1997 ... 595
Blaine, Raymond L., Harold J. Valis, Surface available to nitrogen in hydrated portland cements, RP1967 ... 257
Bloom, Evelyn G., Fred L. Mohler, Edmund J. Wells, Jr., Jonathan H. Lengel, C. Edward Wise, Doubly charged ion spectra in mass spectra of hydrocarbons, RP1975 ... 369
Bolometer mounts, microwave, efficiency, RP1995 ... 579
Bone char and other carbon adsorbents, oxidation, RP1948 ... 33
Boric oxide-barium oxide system, RP1956 ... 131
Boron, effect on cast iron, RP1987 ... 465
Brenner, Abner, Eugenia Kellogg, An electric gage for measuring the inside diameter of tubes, RP1986 ... 461
—, *Seymour Senderoff*, A spiral contractometer for measuring stress in electrodeposits, RP1953 ... 89
—, —, Calculation of stress in electrodeposits from the curvature of a plated strip, RP1953 ... 105
Brickwedde, Langhorne H., Properties of aqueous solutions in perchloric acid, RP1971 ... 309
Bunsen burners, design of natural-gas laboratory type, RP1991 ... 541
Burners, laboratory type for natural gas, RP1991 ... 541
Butadienes, heat of isomerization, RP1968 ... 269
Butylbenzenes, ultraviolet absorption spectra, RP1996 ... 587

C

Calcium melibionate, preparation, RP1977 ... 383
Capacitance, standard, RP1970 ... 287
Carbon adsorbents, oxidation, RP1948 ... 33
Cassel, James, Joseph R. Kanagy, Studies on the purification of collagen, RP1992 ... 557
Cast iron, effect of boron on properties, RP1987 ... 465
Cement, portland, adsorption of nitrogen, oxygen, and argon on, RP1967 ... 257

Page

Chrzanowski, Peter, Richard K. Cook, Absorption by sound-absorbent spheres, RP1963 ... 219
Collagen, purification, RP1992 ... 557
Collagen, tendon, shrinkage, RP1947 ... 17
Colorblindness, Müller theory, RP1946 ... 1
Columbium, volumetric determination of, RP1980 ... 405
Combustion of carbons, RP1948 ... 33
Combustion, heat of, two butadienes, RP1968 ... 269
Commercial and alkali soaps, characterization by electron microscopy, RP1973 ... 343
Computing, high-speed, rounding-off errors, RP1950 ... 57
Concrete as a protective barrier for gamma-rays from radium, RP1983 ... 431
Conductance, electrical, of solutions of soaps and soapless detergents, RP1974 ... 361
Convection currents in pots of optical glass, effect on distribution of striae, RP1959 ... 153
Cook, Richard K., Peter Chrzanowski, Absorption by sound-absorbent spheres, RP1963 ... 219
Cooter, Irvin L., John Keenan Taylor, Roberta E. Smith, Polarographic limiting currents, RP1978 ... 387
Costrell, Louis, Accurate determination of the deadtime and recovery characteristics of Geiger-Müller counters, RP1965 ... 241
Cottington, Robert L., Robert C. Hardy, Viscosity of deuterium oxide and water in the range 5° to 125° C, RP1994 ... 573
Crean, Lawrence E., Herbert F. Schiefer, John F. Krasny, Improved single-unit Schiefer abrasion testing machine, RP1988 ... 481
Cyclohexene and cyclopentene, heat, equilibrium constant, and free energy of formation, RP1976 ... 379
Cyclopentanes, heats of combustion and isomerization, RP1966 ... 251
Cyclopentene and cyclohexene, heat, equilibrium constant, and free energy of formation, RP1976 ... 379

D

Davis, Marion Maclean, E. Anne McDonald, Acid-base equilibrium constants for the reaction of tribenzylamine with picric acid and with trinitro-*m*-cresol in benzene, from spectrophotometric data, RP1997 ... 595
Deadtime and recovery characteristics of Geiger-Müller counters, RP1965 ... 241
Deitz, Victor R., William V. Loebenstein, Leland F. Gleysteen, Kinetic study of the reaction of carbon adsorbents with oxygen, RP1948 ... 33
Density of aqueous solutions of perchloric acid, RP1971 ... 309
Density of deuterium oxide and water, RP1994 ... 573
Detergents, physical-chemical properties of solutions of, RP1974 ... 361
Deuterium oxide, and water density and viscosity, RP1994 ... 573
Diethylbenzenes, ultraviolet absorption spectra, RP1996 ... 587
Diodes, noise spectrum, RP1952 ... 75
Diolefins, heats, equilibrium constants, and free energies of formation of, RP1964 ... 225
Dissociation constants of ammonia and ammonium ion, RP1982 ... 419
Distillation of hydrocarbons, RP1957 ... 139

E

Eineman, John H., A study of laboratory Bunsen burners for natural gas, RP1991 ... 541
Electrical resistivity at aqueous solutions of perchloric acid, RP1971 ... 309
Electric gage for measuring inside diameter of tubes, RP1986 ... 461
Electrode, dropping-mercury, limiting currents, RP1978 ... 387
Electrodeposits, stress in:
RP1953 ... 89
RP1954 ... 105
Electrolytic oxidation, preparation of calcium melibionate by, RP1977 ... 383
Electronic gating device for determination of deadtime and recovery of Geiger-Müller counters, RP1965 ... 241

Page

Electron microscopy of soaps, RP1973 ... 343
Enamel, procelain, surface texture evaluation, RP1985 ... 449
Enamels, porcelain, weather resistance, RP1949 ... 43
Entropy of cyclopentene and cyclohexenes, RP1976 ... 379
Entropy of diolefins and styrenes, RP1964 ... 225
Epstein, Morton B., Beveridge J. Mair, Charles B. Willingham, Frederick D. Rossini, Separation of the 177° to 300° C fraction of petroleum and the isolation of normal undecane, RP1957 ... 139
—, *Kenneth S. Pitzer, Frederick D. Rossini*, Heats, equilibrium constants, and free energies of formation of cyclopentene and cyclohexene, RP1976 ... 379
Equilibrium constants, heats, and free energies of cyclopentene and cyclohexene, RP1976 ... 379
Equilibrium constants of formation of diolefins and styrenes, RP1964 ... 225
Expansivity of borosilicate thermometer glasses, RP1960 ... 171

F

Fabric abrasion test, RP1988 ... 481
Faick, Conrad A., Arthur E. Williams, Gerald F. Rynders, Effect of convection currents on the distribution of striae in pots of optical glass, RP1959 ... 153
Flame spectrum of acetylene, RP1963 ... 567
Fractionation of hydrocarbons, RP1957 ... 139
Francisco, Allen E., Joseph C. Richmond, The use of plastic replicas in evaluating surface texture of enamels, RP1985 ... 449
Free energies, heats, and equilibrium constants of cyclopentene and cyclohexene, RP1976 ... 379
Free energy of formation of diolefins and styrenes, RP1964 ... 225
Freeman, Jacob J., Noise spectrum of a diode with a retarding field, RP1952 ... 75
Freezing temperatures of perchloric-acid solutions, RP1971 ... 309

G

g-Values and Zeeman effect for nitrogen and oxygen, RP1961 ... 183
Gage, electric, for measuring inside diameter tubes, RP1986 ... 461
Gamma-ray protective barrier, concrete as, RP1983 ... 431
Gas, natural, laboratory Bunsen burner design for, RP1991 ... 541
Gear lubricants, automotive, wear tests, RP1955 ... 125
Geiger-Müller counters, deadtime and recovery characteristics, RP1965 ... 241
Glass, optical, properties and heat treatment, RP1969 ... 279
Glass, optical, striae, RP1959 ... 153
Glasses, borosilicate thermometer, expansion effects of annealing, RP1960 ... 171
Gleysteen, Leland F., William V. Loebenstein, Victor R. Deitz, Kinetic study of the reaction of carbon adsorbents with oxygen, RP1948 ... 33

H

Hardy, Robert C., Robert L. Cottington, Viscosity of deuterium oxide and water in the range 5° to 125° C, RP1994 ... 573
Harrison, William N., Dwight G. Moore, Weather resistance of porcelain enamels exposed for seven years, RP1949 ... 43
Hartree, Douglas R., Harry D. Huskey, On the precision of a certain procedure of numerical integration, RP1950 ... 57
Hattiangdi, Gopal S., Characterization of some commercial soaps by X-ray diffraction, RP1972 ... 331
—, *Max Swerdlow*, Characterization of alkali soaps by electron microscopy, RP1973 ... 343
—, *William W. Walton, James I. Hoffman*, Some physical-chemical properties of aqueous solutions of soaps and soapless detergents, RP1974 ... 361
Heat content and capacity of diolefins and styrenes, RP1964 ... 225
Heat, entropy, and free energy of activation of the shrinkage of tendon collagen, RP1947 ... 17
Heat of formation of butadienes, RP1968 ... 269
Heat of isomerization of hydrocarbons, RP1968 ... 269
Heat treatment of optical glass, RP1969 ... 279
Heats, equilibrium constants, and free energies of formation of cyclopentene and cyclohexene, RP1976 ... 379
Heats of combustion and isomerization of hydrocarbons, RP1966 ... 251
Hoffman, James I., Gopal S. Hattiangdi, William W. Walton, Some physical-chemical properties of aqueous solutions of soaps and soapless detergents, RP1974 ... 361
Howard, Frank L., Philip Pomerantz, Thomas W. Mears, Separation and identification of the major C_7 to C_{10} components of triptene residue, RP1999 ... 617

Page

Humphreys, Curtis J., Earle K. Plyler, Flame spectrum of acetylene from 1 to 5 microns, RP1993 ... 567
Huskey, Harry D., Douglas R. Hartree, On the precision of a certain procedure of numerical integration, RP1950 ... 57
Hydrocarbons, heat of isomerization, RP1968 ... 269
Hydrocarbons, heats of combustion and isomerization, RP1966 ... 251
Hydrocarbons, heats, equilibrium constants, and free energies of formation of, RP1964 ... 225
Hydrocarbons, mass spectra, RP1975 ... 369
Hydrocarbons, synthesis and isolation, RP1999 ... 617
Hydrocarbons, ultraviolet absorption spectra, RP1996 ... 587

I

Index of refraction of optical glass, RP1969 ... 279
International temperature scale of 1948, RP1962 ... 209
Ion spectra in mass spectra of hydrocarbons, RP1975 ... 369
Isbell, Horace S., William W. Walton, The preparation of calcium melibionate, RP1977 ... 383
Isomerization and combustion, heats of six alkylcyclopentanes, RP1966 ... 251
Isomerization, heat of, two butadienes, RP1968 ... 269

J

Johnson, Walter H., Edward J. Prosen, Frederick D. Rossini, Heats of combustion and isomerization of the six C_7H_{14} alkylcyclopentanes, RP1966 ... 251
Judd, Deane B., Response functions for types of vision according to the Müller theory, RP1946 ... 1

K

Kanagy, Joseph R., James Cassel, Studies on the purification of collagen, RP1992 ... 557
Kellogg, Eugenia, Abner Brenner, An electric gage for measuring the inside diameter of tubes, RP1986 ... 461
Kennedy, Robert J., Harold O. Wyckoff, Concrete as a protective barrier for gamma rays from radium, RP1983 ... 431
Kerns, David M., Basis of the application of network equations to waveguide problems, RP1990 ... 515
—, Determination of efficiency of microwave bolometer mounts from impedance data, RP1995 ... 579
Kiess, Carl C., George Shortley, Zeeman effect and g-values for neutral nitrogen and oxygen, RP1961 ... 183
Kilduff, Timothy J., Rene Oehler, Treatment of leather with synthetic resins, RP1951 ... 63
Kilpatrick, John E., Charles W. Beckett, Edward J. Prosen, Kenneth S. Pitzer, Frederick D. Rossini, Heats, equilibrium constants, and free energies of formation of the C_2 to C_8 diolefins, styrene, and the methylstyrenes, RP1964 ... 225
Kinetics of oxidation of bone char, RP1948 ... 33
Knowles, Howard B., G. E. F. Lundell, The volumetric determination of columbium, RP1980 ... 405
Krasny, John F., Herbert F. Schiefer, Lawrence E. Crean, Improved single-unit Schiefer abrasion testing machine, RP1988 ... 481
Krynitsky, Alexander I., Harry Stern, Effect of boron on the structure and some physical properties of plain cast irons, RP1987 ... 465

L

Landing impact, vibration in aircraft wings from, RP1984 ... 437
Lead perchlorate, resistivity of perchloric acid containing, RP1949 ... 309
Leather abrasion test, RP1988 ... 481
Leather, impregnation with resins, RP1951 ... 63
Lengel, Jonathan H., Fred L. Mohler, Evelyn G. Bloom, Edmund J. Wells, Jr., C. Edward Wise, Doubly charged ion spectra in mass spectra of hydrocarbons, RP1975 ... 369
Levin, Ernest M., Howard F. McMurdie, The system $BaO-B_2O_3$, RP1956 ... 131
Levy, Samuel, Frank C. Smith, Stress distribution near reinforced circular hole loaded by pin, RP1979 ... 397
Limiting currents, polarographic, RP1978 ... 387
Loebenstein, William V., Leland F. Gleysteen, Victor R. Dietz, Kinetic study of the reaction of carbon adsorbents with oxygen, RP1948 ... 33
London, Albert, Transmission of reverberant sound through single walls, RP1998 ... 605
Lubricants, gear, wear tests, RP1955 ... 125

Page

Lundell, G. E. F., Howard B. Knowles, The volumetric determination of columbium, RP1980 405

M

Madorsky, Samuel L., Sidney Straus, Dorothy Thompson, Laura Williamson, Pyrolysis of polyisobutene (vistanex), polyisoprene, polybutadiene, GR-S, and polyethylene in a high vacuum, RP1989 499
Mair, Beveridge J., Morton B. Epstein, Charles B. Willingham, Frederick D. Rossini, Separation of the 177° to 200° C fraction of petroleum and the isolation of normal undecane, RP1957 139
Maron, Frances W., Edward J. Prosen, Frederick D. Rossini, Heat of isomerization of the two butadienes, RP1968 269
Mass spectra of hydrocarbons, RP1975 369
McDonald, E. Anne, Marion Maclean Davis, Acid-base equilibrium constants for the reaction of tribenzylamine with picric acid and with trinitro-*m*-cresol in benzene, from spectrophotometric data, RP1997 595
McKee, Samuel A., James F. Swindells, Hobart S. White, Wayne Mountjoy, Laboratory wear tests with automotive gear lubricants, RP1955 125
McMurdie, Howard F., Ernest M. Levin, The system BaO–B_2O_3, RP1956 131
Mears, Thomas W., Philip Pomerantz, Frank L. Howard, Separation and identification of the major C_7 to C_{10} components of triptene residue, RP1999 617
Microscopy, electron, of soaps, RP1973 343
Microwave bolometer mounts, efficiency, RP1995 579
Millibiose, electrolytic oxidation, RP1977 383
Mohler, Fred L., Evelyn G. Bloom, Edmund J. Wells, Jr., Jonathan H. Lengel, C. Edward Wise, Doubly charged ion spectra in mass spectra of hydrocarbons, RP1975 369
Moore, Dwight G., William N. Harrison, Weather resistance of porcelain enamels exposed for seven years, RP1949 43
Mountjoy, Wayne, Samuel A. McKee, James F. Swindells, Hobart S. White, Laboratory wear tests with automotive gear lubricants, RP1955 125
Müller theory of color vision, RP1946 1

N

Natural gas, laboratory Bunsen burner design, RP1991 541
Network equations, application to waveguide problems, RP1990 515
Nitrogen and oxygen, Zeeman effect and *g*-values, RP1961 183
Nitrogen, oxygen, and argon adsorption on portland cements, RP1967 257
Noise spectrum of a diode, RP1952 75
Numerical integration, rounding-off errors in, RP1950 57

O

Oehler, Rene, Timothy J. Kilduff, Treatment of leather with synthetic resins, RP1951 63
Optical glass annealing, heat treatment, refractive index, RP1969 279
Optical glass, effect of convection currents on striae distribution, RP1959 153
Oxidation of bone char and other carbon adsorbents, RP1948 33
Oxygen and nitrogen, Zeeman effect and *g*-values, RP1961 183
Ozone, ultraviolet measurement, RP1958 145

P

Paschen-Back effect of nitrogen and oxygen, RP1961 183
Perchloric-acid solutions, properties, RP1971 309
Petroleum, separation, RP1957 139
Phase diagram of $HClO_4$–H_2O system, RP1971 309
Phase equilibrium of the system BaO–B_2O_3, RP1956 131
Phase identification in soaps by X-ray diffraction, RP1972 331
Photoelectric measurement of total ozone, RP1958 145
Picric acid, association constant with tribenzylamine in benzene, RP1997 595
Pinching, Gladys D., Roger G. Bates, The acidic dissociation constant of ammonium ion at 0° to 50° C, and the base strength of ammonia, RP1982 419
Pitzer, Kenneth S., John E. Kilpatrick, Charles W. Beckett, Edward J. Prosen, Frederick D. Rossini, Heats, Equilibrium constants, and free energies of formation of the C_3 to C_5 diolefins, styrene, and the methylstyrenes, RP1964 225
—, *Morton B. Epstein, Frederick D. Rossini,* Heats, equilibrium constants, and free energies of formation of cyclopentene and cyclohexene, RP1976 379
Plastic abrasion test, RP1988 481
Plastic replicas for evaluating surface texture of enamels, RP1985 449
Plyler, Earle K., Curtis J. Humphreys, Flame spectrum of acetylene from 1 to 5 microns, RP1993 567
Polarographic limiting currents, RP1978 387
Polybutadiene, pyrolysis, RP1989 499
Polyethylene, pyrolysis, RP1989 499
Polyisobutene, pyrolysis, RP1989 499
Polyisoprene, pyrolysis, RP1989 499
Polymers, impregnation of leather, RP1951 63
Pomerantz, Philip, Thomas W. Mears, Frank L. Howard, Separation and identification of the major C_7 to C_{10} components of triptene residue, RP1999 617
Porcelain enamel, evaluating surface texture, RP1985 449
Porcelain enamels, weather resistance, RP1949 43
Portland cements, surface available to nitrogen, oxygen, and argon, RP1967 257
Power loss in microwave bolometer mounts, RP1995 579
Prosen, Edward J., Frances W. Maron, Frederick D. Rossini, Heat of isomerization of the two butadienes, RP1968 269
—, *John E. Kilpatrick, Charles W. Beckett, Kenneth S. Pitzer, Frederick D. Rossini,* Heats, equilibrium constants, and free energies of formation of the C_3 to C_5 diolefins, styrene, and the methylstyrenes, RP1964 225
—, *Walter H. Johnson, Frederick D. Rossini,* Heats of combustion and isomerization of the six C_7H_{14} alkylcyclopentanes, RP1966 251
Pyrolysis of polyisobutene (vistanex), polyisoprene, polybutadiene, GR-S, and polyethylene, RP1989 499

R

Radium protection, concrete as protective barrier, RP1983 431
Ramberg, Walter, Transient vibration in an airplane wing obtained by several methods, RP1984 437
Refractivity of optical glass, RP1969 279
Reinforced circular hole in flat plate, stress distribution near, RP1979 397
Resins, impregnation of leather, RP1951 63
Resistivity, electrical, of aqueous solutions of perchloric acid, RP1971 309
Reverberant sound transmission through single walls, RP1998 605
Richmond, Joseph C., Allen C. Francisco, The use of plastic replicas in evaluating surface texture of enamels, RP1985 449
Rossini, Frederick D., Edward J. Prosen, Frances W. Maron, Heat of isomerization of the two butadienes, RP1968 269
—, *John E. Kilpatrick, Charles W. Beckett, Edward J. Prosen, Kenneth S. Pitzer,* Heats, equilibrium constants, and free energies of formation of the C_3 to C_5 diolefins, styrene, and the methylstyrenes, RP1964 225
—, *Morton B. Epstein, Beveridge J. Mair, Charles B. Willingham,* Separation of the 177° to 200° C fraction of petroleum and the isolation of normal undecane, RP1957 139
—, —, *Kenneth S. Pitzer,* Heats, equilibrium constants, and free energies of formation of cyclopentene and cyclohexene, RP1976 379
—, *Walter H. Johnson, Edward J. Prosen,* Heats of combustion and isomerization of the six C_7H_{14} alkylcyclopentanes, RP1966 251
Rounding-off errors in numerical integration, RP1950 57
Rynders, Gerald F., Conrad A. Faick, Arthur E. Williams, Effect of convection currents on the distribution of striae in pots of optical glass, RP1959 153

S

Saunders, James B., Arthur O. Tool, Expansion effects of annealing borosilicate thermometer glasses, RP1960 171
Schiefer abrasion testing machine, RP1988 481
Schiefer, Herbert F., Lawrence E. Crean, John F. Krasny, Improved single-unit Schiefer abrasion testing machine, RP1988 481
Senderoff, Seymour, Abner Brenner, A spiral contractometer for measuring stress in electrodeposits, RP1953 89
——, ——, Calculation of stress in electrodeposits from the curvature of a plated strip, RP1953 105
Shortley, George, Carl C. Kiess, Zeeman effect and g-values for neutral nitrogen and oxygen, RP1961 183
Shrinkage of tendon collagen, RP1947 17
Simha, Robert, Effect of concentration on the viscosity of dilute solutions, RP1981 409
Smith, Frank C., Samuel Levy, Stress distribution near reinforced circular hole, loaded by pin, RP1979 397
Smith, Roberta E., John Keenan Taylor, Irvin L. Cooter, Polarographic limiting currents, RP1978 387
Snow, Chester, A standard of small capacitance, RP1970 287
Soaps, alkali and commercial, characterization by electron miscroscopy, RP1973 343

Page

Soaps, physical-chemical properties of solutions of, RP1974 ... 361
Soaps, X-ray diffraction, RP1972 ... 331
Solutions, viscosity of, effect of concentration, RP1981 ... 409
Sound-absorbent spheres, absorption by, RP1963 ... 219
Sound transmission through single walls, RP1998 ... 605
Spectra, absorption, of butylbenzenes and diethylbenzenes, RP1906 ... 587
Spectra, mass of hycrocarbons, RP1975 ... 369
Spectrophotometric studies of acid-base reactions in benzene, RP1997 ... 595
Spectrum of acetylene flame, RP1903 ... 567
Spheres, sound-absorbent, absorption by, RP1963 ... 219
Stair, Ralph, Ultraviolet absorption spectra of seven substituted benzenes, RP1906 ... 587
——, Winter measurements of ozone over the Organ Mountains, New Mexico, RP1958 ... 145
Standard capacitance, RP1970 ... 287
Stern, Harry, Alexander I. Krynitsky, Effect of boronon the structure and some physical properties of plain cast irons, RP1987 ... 465
Stimson, H. F., The international temperature scale of 1948, RP1962 ... 309
Striae in optical glass, RP1959 ... 153
Stratosphere, ozone in, over Organ Mountains, New Mexico, RP1958 ... 145
Straus, Sidney, Samuel L. Madorsky, Dorothy Thompson, Laura Williamson, Pyrolysis of polyisobutene (vistanex), ployisoprene, polybutadiene, GR–S, and polyethylene in a high vacuum, RP1989 ... 499
Stress birefringence in optical glass, RP1969 ... 279
Stress distribution near reinforced circular hole in a flat plate, RP1979 ... 397
Stress in electroplated metals:
RP1953 ... 89
RP1954 ... 105
Styrenes, heats, equilibrium constants, and free energies of formation of, RP1964 ... 225
Surface tension of solutions of soaps and soapless detergents, RP1974 ... 361
Swerdlow, Max, Gopal S. Hattiangdi, Characterization of alkali soaps by electron microscopy, RP1973 ... 343
Swindells, James F., Samuel A. McKee, Hobart S. White, Wayne Mountjoy, Laboratory wear tests with automative gear lubricants, RP1955 ... 125

T

Taylor, John Keenan, Roberta E. Smith, Irvin L. Cooter, Polarographic limiting currents, RP1978 ... 387
Temperature scale, international, of 1948, RP1962 ... 309
Temperature uniformity in annealing furnaces, RP1969 ... 279
Tendon collagen, shrinkage, RP1947 ... 17
Textile abrasion test, RP1988 ... 481
Thermodynamic functions for the dissociation of ammonia and ammonium ion, RP1982 ... 419
Thermometer glasses, borosilicate, expansion effects of annealing, RP1960 ... 171
Thompson, Dorothy, Samuel L. Madorsky, Sidney Straus, Laura Williamson, Pyrolysis of polyisobutene (vistanex), polyisoprene, polybutadiene, GR–S, and polyethylene in a high vacuum, RP1989 ... 499
Tilton, Leroy W., Optical glass of interferometer and schlieren quality for wind-tunnel optics, RP1969 ... 279
Tsai, Arthur O., James B. Saunders, Expansion effects of annealing borosilicate thermometer glasses, RP1960 ... 171
Tribenzylamine, relative reactivity with picric acid and trinitro-*m*-cresol in benzene, RP1997 ... 595
Trinitro-*m*-cresol, association constant with tribenzylamine in benzene, RP1997 ... 595
Triptene residue, separation and identification, RP1969 ... 617
Tubes, measurement of inside diameter, RP1986 ... 461

U

Page

Ultraviolet absorption spectra of the butylbenzenes and diethylbenzenes, RP1906 ... 587
Ultraviolet, solar, measurements of ozone, RP1958 ... 145
Undecane, isolation, RP1957 ... 139

V

Valis, Harold J., Raymond L. Blaine, Surface available to nitrogen in hydrated portland cements, RP1967 ... 707
Vibration in aircraft wings, RP1984 ... 437
Viscosity of aqueous solutions of perchloric acid, RP1971 ... 709
Viscosity of deuterium oxide and water, RP1994 ... 73
Viscosity of dilute solutions, effect of concentration, RP1981 ... 409
Vision, tritanopic, of the normal eye, RP1946 ... 1
Volumetric determination of columbium, RP1980 ... 405

W

Walls, transmission of sound through, RP1998 ... 605
Walton, William W., Gopal S. Hattiangdi, James I. Hoffman, Some physical-chemical properties of aqueous solutions of soaps and soapless detergents, RP1974 ... 361
—, *Horace S. Isbell*, The preparation of calcium melibionate, RP1977 ... 383
Water and deuterium oxide, viscosity, RP1994 ... 573
Water, heavy, viscosity and density, RP1994 ... 573
Waveguide, application of network equations to, RP1990 ... 515
Wear testing machine, RP1988 ... 481
Wear tests with automotive lubricants, RP1955 ... 125
Weathering of procelain enamels, RP1949 ... 43
Weir, Charles E., Rate of shrinkage of tendon collagen: Heat, entropy, and free energy of activation of the shrinkage of untreated tendon; Effect of acid, salt, pickle, and tannage on the activation of tendon collagen, RP1947 ... 17
Wells, Jr., Edmund J., Fred L. Mohler, Evelyn G. Bloom, Jonathan H. Lengel, C. Edward Wise, Doubly charged ion spectra in mass spectra of hydrocarbons, RP1975 ... 369
White, Hobart S., Samuel A. McKee, James F. Swindells, Wayne Mountjoy, Laboratory wear tests with automotive gear lubricants, RP1955 ... 125
Williams, Arthur E., Conrad A. Faick, Gerald F. Rynders, Effect of convection currents on the distribution of striae in pots of optical glass, RP1959 ... 153
Williamson, Laura, Samuel L. Madorsky, Sidney Straus, Dorothy Thompson, Pyrolysis of polyisobutene (vistanex), polyisoprene, polybutadiene, GR–S, and polyethylene in a high vacuum, RP1989 ... 499
Willingham, Charles B., Morton B. Epstein, Beveridge J. Mair, Frederick D. Rossini, Separation of the 177° to 200° C fraction of petroleum and the isolation of normal undecane, RP1957 ... 139
Wind tunnels, optical glass for, RP1969 ... 279
Wise, C. Edward, Fred L. Mohler, Evelyn G. Bloom, Edmund J. Wells, Jr., Jonathan H. Lengel, Doubly charged ion spectra in mass spectra of hydrocarbons, RP1975 ... 369
Wyckoff, Harold O., Robert J. Kennedy, Concrete as a protective barrier for gamma rays from radium, RP1983 ... 431

X

X-ray diffraction of soaps, RP1972 ... 331

Z
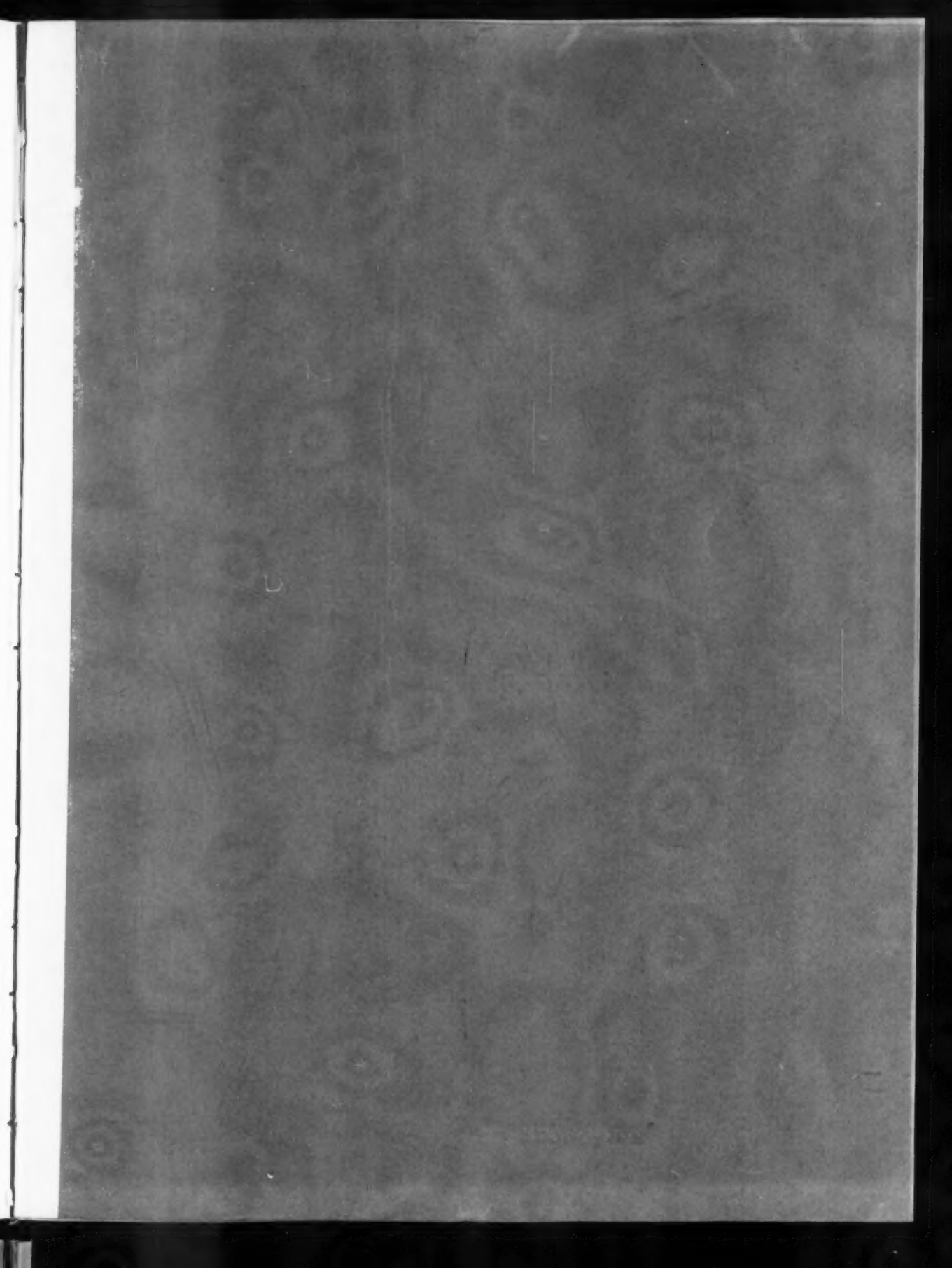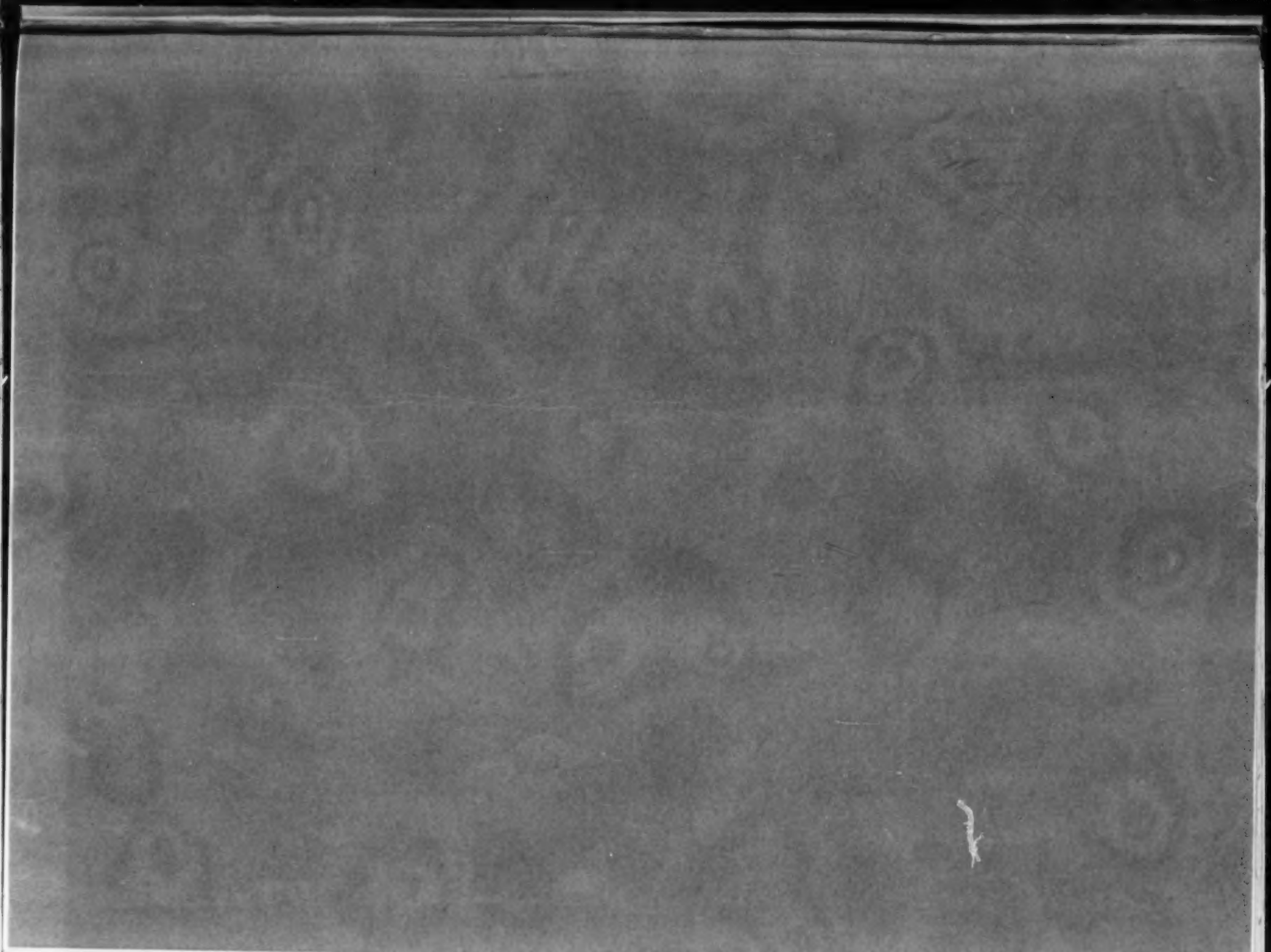
Zeeman effect and g-values for nitrogen and oxygen, RP1961 ... 183